

P  
2.11.74

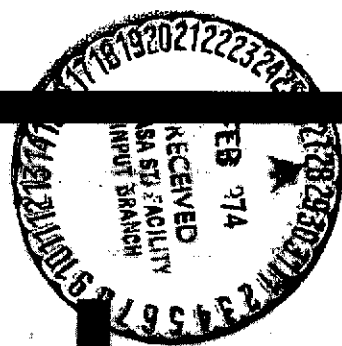
9

(NASA-SP-338) ADVANCED ELECTRO-OPTICAL  
IMAGING TECHNIQUES (NASA) 134 P HC  
\$4.75 128 CSCL 20F

N74-17406  
THRU  
N74-17414  
Unclas  
29877

H1/23

# ADVANCED ELECTRO-OPTICAL IMAGING TECHNIQUES



A symposium held at  
NASA HEADQUARTERS  
Washington, D.C.  
September 22, 1972



NATIONAL AERONAUTICS AND SPACE ADMINISTRATION

# ADVANCED ELECTRO-OPTICAL IMAGING TECHNIQUES

The proceedings of a symposium held at  
NASA Headquarters,  
Physics and Astronomy Programs, Office of Space Sciences,  
September 22, 1972

*Edited by*

Stanley Sobieski  
Goddard Space Flight Center

and

E. Joseph Wampler  
Lick Observatory  
University of California

*Prepared by Goddard Space Flight Center*



*Scientific and Technical Information Office* 1973  
NATIONAL AERONAUTICS AND SPACE ADMINISTRATION  
Washington, D.C.

---

For sale by the National Technical Information Service  
Springfield, Virginia 22151  
Price \$4.50  
*Library of Congress Catalog Card Number 73-600316*

## PREFACE

As the study effort for the Large Space Telescope (LST) program progressed, it became increasingly clear that the sensors are among the most critical elements in the design. Their performance is critical if the full LST potential is to be realized. A large aperture optical system such as the LST, operating at the diffraction limit, imposes stringent requirements on the sensors if the high angular-resolution field of view and the very broad intensity range provided are to be maintained without degradation. Some scientific objectives require that the sensors provide, in addition, high time resolution, very broad dynamic range, and high repeatable accuracy. These requirements must be met with the instruments and sensors configured for remote, automated operation in near-earth orbit.

In recognition of the importance of the sensors a symposium on Advanced Electro-optical Imaging Techniques was convened by the LST Science Steering Group, chaired by Dr. N. G. Roman of NASA Headquarters, on September 22, 1972, with the meeting held at NASA Headquarters.

The purposes of the symposium were to assess the present state of sensors, as may be applicable to the LST, and to acquaint the technical community with the scientific potential and the needs of the LST. With only a limited amount of time available, the in-depth coverage of the sensor field was, of course, impossible. For this reason a number of important techniques which could be utilized were not covered. These included the infrared imaging devices, image dissectors, channel-plate intensifiers, orthicons, and electronographic devices. In keeping with a broad interpretation of the word sensor, the symposium did cover several aspects of sensors, including a discussion of the properties of photocathodes and the operational imaging camera tubes.

CONTENTS

Preface . . . . .	iii
Introductory Comments	
<i>N. G. Roman</i> . . . . .	1
<i>S. Sobieski</i> . . . . .	2
<i>E. J. Wampler</i> . . . . .	3
I. Design of Photoelectronic Optical Image Sensors	
<i>C. B. Johnson</i> . . . . .	5
II. Photocathodes for Use in the Large Space Telescope Program	
<i>W. E. Spicer</i> . . . . .	21
III. Electron-Optic Limitations on Image Resolution	
<i>R. W. Engstrom</i> . . . . .	35
IV. Image Recording Using Charge-Coupled Devices	
<i>C. H. Sequin</i> . . . . .	51
V. The Electrostatic Storage Tube	
<i>R. E. Rutherford, Jr.</i> . . . . .	69
VI. Large Space Telescope Television Sensor Development	
<i>J. L. Lowrance</i> . . . . .	81
VII. Application of Silicon Image Tubes (SIVIT & SIT) to Ground Based Astronomy	
<i>J. A. Westphal</i> . . . . .	93
VIII. Digital Multichannel Photometry with Digicons	
<i>C. E. McIlwain</i> . . . . .	107
Participants . . . . .	125

## INTRODUCTORY COMMENTS

*Nancy G. Roman*  
*Chairman, LST Science Steering Group*

The Large Space Telescope Science Steering Group has been meeting for somewhat over a year to advise NASA on the planning of a 3-m telescope to be launched about 1980 using the facilities of the Space Shuttle but operating in an automated mode most of the time. Because we expect long, unattended stays, it is likely that, for the most part, film is not going to be a useful medium for recording images. Therefore, we have been interested from the beginning in electronic image recording techniques, and we felt, in the course of our deliberations, that it was important to inform the panel on the modern state-of-the-art in electronic imaging techniques. To do this, we asked two members of the steering group, Dr. S. Sobieski and Dr. J. Wampler, to arrange today's Symposium, which will review the present state-of-the-art and, to the extent that people are willing to commit themselves, the state-of-the-art in the foreseeable future.

I feel very happy that so many of you were willing to discuss the work you are doing, and I feel equally happy that so many of the rest of you decided that you were sufficiently interested to come and participate in the discussion.

With this introduction, I will turn the rest of the day's meeting over to Dr. Sobieski, who will act as our chairman.

## INTRODUCTORY COMMENTS

*Stanley Sobieski*  
*Symposium Chairman*

I would like to welcome all participants at this Symposium. According to the ancient Greeks, a symposium is a time for drinking, conversation, and intellectual entertainment. I am sure we will have a bit of each; a free exchange among the invited speakers, guests, and science steering group members is certainly anticipated.

The program has been arranged so that not only subjects bearing directly on instrumentation needs for the Large Space Telescope will be addressed, but also new approaches and future directions will be illuminated. Since the meeting is open and publication of the proceedings is expected, proprietary or classified material should not be presented.

I have asked Dr. Wampler, the Cochairman of this Symposium to begin with a description of the LST for the purpose of establishing background and perspective.

## GENERAL CHARACTERISTICS OF THE LARGE SPACE TELESCOPE

*E. Joseph Wampler*  
*Symposium Cochairman*

Dr. Nancy Roman has given the rough outline of the Large Space Telescope (LST) project. It is a 3-m telescope, and hopefully it will work at the resolution limit of a 3-m telescope. Right now we are thinking in terms of an f:12 focal ratio; if the telescope is resolution limited, star images will be approximately  $5 \mu\text{m}$  in diameter at the focal plane. Since the focal length of the telescope is very long, the focal plane will be nearly flat. For direct imaging, flat-faced tubes will be the preferred configuration. Five- $\mu\text{m}$  images are smaller than any TV target resolution that I know about, so there must be some sort of magnification between the telescope focal plane and the electron image plane in the camera. This magnification could be in the form of an optical relay system in which case one has the disadvantage of a substantial light loss, particularly in the UV portion of the spectrum, or a camera tube incorporating electronic zoom capability could be used. Zoom tubes would probably represent a new development, since I know of no commercially available tubes with flat photocathodes.

It is perhaps also worth mentioning that the telescope should be able to compete with ground-based telescopes. Because the LST is a very expensive instrument, it would be a disappointment if it were launched and would prove to have very poor sensitivity and resolution. This telescope is not intended to be just a very large light bucket in space since in that case the only advantage it would have over ground-based instruments would be its extended UV response. That is not deemed sufficient to justify its expense.

Now, what can one do from the ground? In spectroscopy it turns out that one can reach stars of magnitude of about 22, perhaps a bit fainter if you are ready to expend very large amounts of telescope time. With an efficient spectroscope one gets about ten counts per nanometer wavelength interval from 22nd magnitude stars in 10 min of integration time. It is easy to see that one does not do high-resolution spectroscopy at magnitude 22. At best, the achievable resolution of the instrument is of the order of several tenths of a nanometer. But resolution in the order of 1.0 or 1.5 nm has been obtained at that counting rate. For direct imaging, of course, one doesn't need the spectroscope, and the system efficiencies are a little higher. Perhaps one can obtain 50 to 100 counts/nm in 10 min.

It is hoped that the LST will be able to detect stars of magnitude 27. That is a factor of 100 fainter than magnitude 22 and means that we are talking about very, very low input flux levels. Because the sky background that the telescope will see will be very low, we must have detectors that are extremely quiet so that their background noise does not add to the shot noise of the signal. In addition to being quiet, the background noise of the detector should

be stochastically distributed in time and space. One shouldn't have ion spots, bursts of electrons, and so forth.

We have invited you all here so that we could be better informed on the state-of-the-art. I think our speakers are quite capable of describing new developments; and, for this reason, I have tried only to outline some of the limitations we have and the type of sensitivity that we are trying to achieve.

## I. DESIGN OF PHOTOELECTRONIC OPTICAL IMAGE SENSORS

*C. B. Johnson  
Bendix Research Laboratory  
Southfield, Michigan*

I would like to present the results of a general design study of photoelectronic optical image sensors for the Large Space Telescope (LST). This work is sponsored by the Goddard Space Flight Center, and the technical supervisor is Dr. Kenneth L. Hallam.

The main performance goals are as follows:

- Number of picture elements (pixels) –  $10^7$  to  $10^8$
- Minimum irradiance sensitivity – 0.01 incident photon/s/pixel
- Dynamic range –  $10^4$

The sensor itself has been given a package size of about 15 cm (6 in.) diameter by 60 cm (24 in.) long, a power requirement of approximately 30 W and a weight of approximately 14 kg (30 lb).

A typical astronomical scene has also been established, and out of the  $10^7$  picture elements in the scene, it has been assumed that  $10^4$  will be stellar sources. There will also be nebular sources in the scene. A single stellar image will occupy approximately the area of one picture element.

Let me carry this a step further. Note that this definition, which is being used to determine sensor performance, is arbitrary. One percent of these stellar objects are in an adjacent pixel, 5 percent are spaced two pixels apart, 10 percent are three pixels apart, and the remainder are distributed at random. The faintest stars would have an input flux density of 0.01 photon/s/pixel.

As to the nebulosity, 50 percent of the active format is covered by a nebular source. The remaining 50 percent is dark or contains stars, and the nebulosity intensity varies from 0.03 to 300 photon/s/pixel.

Now, the question is, "What type of sensor (if any) satisfies these very demanding requirements?"

In principle, the sensor parameters are used to make this decision. However, each image sensor has a large number of parameters associated with it, and furthermore, these parameters are not, in general, constants. Examples of some of the sensor parameters are dark current, modulation transfer function, spectral quantum efficiency, and the mechanical

parameters. Options such as electronic shutter capability and electronic zoom must also be considered.

It is difficult to weigh all the sensor parameters and come up with a specific design to be used. We decided to lay out the design possibilities in very general terms and to eliminate possibilities which cannot be used. These design possibilities are presented in diagrammatic form in Figure I-1.

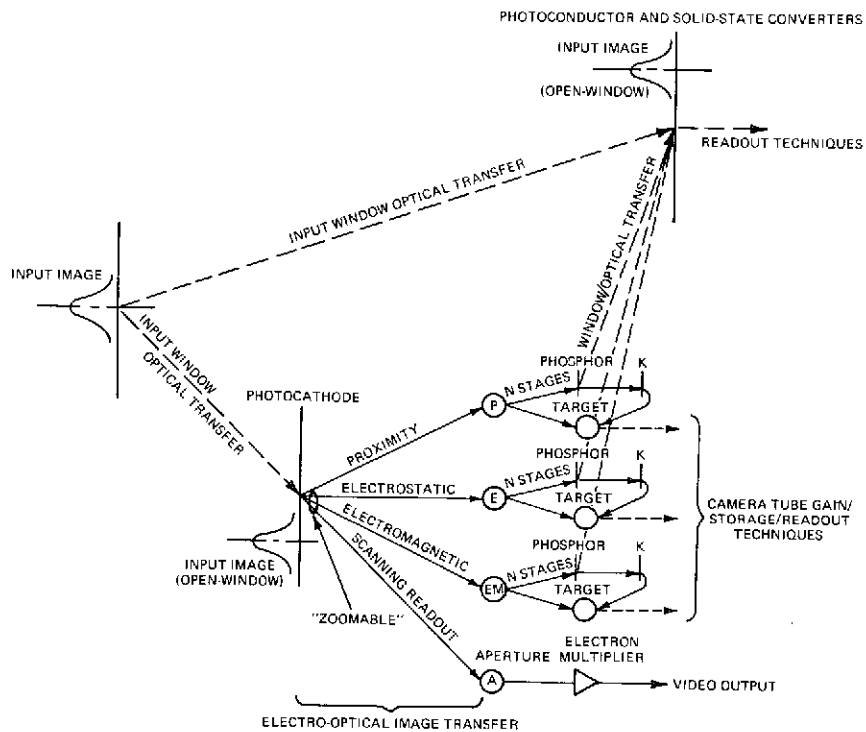


Figure I-1. Image sensor structural analysis.

In general, an object can be considered to consist of bright emitting points that are imaged by the telescope as point-spread functions.

For a visible wavelength sensitive system, an input window must be used, and the window causes some degradation of the optical characteristics. A photoconductor, a solid-state type of readout device, or a photocathode can be used as a primary detector surface. If a photocathode is employed, free electrons must be focused onto a gain or storage surface, and there are three ways to do that. Proximity, electrostatic, or electromagnetic focusing can be used. In addition to focusing onto some kind of target surface, a direct kind of readout is possible in which the photocathode is electron-optically scanned, and the electrons from a small part of the photocathode are amplified by an electron multiplier (the

familiar image dissector approach). The photocathode route was chosen for detailed analysis because it allows a very sensitive, high-quantum-efficiency sensor to be designed.

If electron-optical characteristics are considered, it is found that the electromagnetic lens has the highest information throughput, the highest modulation transfer function (MTF). The trade-off is that it is heavier than the electrostatic lens.

The next step in the design is to decide what kind of target to use. High gain, high MTF, and low dark current are desirable target characteristics. At the same time, the target should not be mechanically, thermally, or electronically fragile. The two types of targets that are being considered are the silicon-diode array target and the microchannel plate with a storage surface on the output.

The next functional element of the image sensor is the readout section. The return-beam readout mode has been developed to a very great extent by RCA. It gives a very high information throughput, and it is also a very sensitive method of readout. As a result of this design study, two basic designs have been established. Each design uses one vacuum envelope, a photocathode on the input window, electromagnetic focusing between the photocathode and the target, and high-resolution return-beam readout. The schematic design of the camera tube employing a silicon target is shown in Figure I-2.

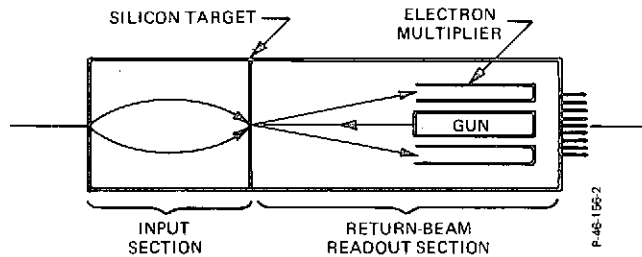


Figure I-2. Schematic design of an intensifier/silicon target/return-beam vidicon.

A microchannel plate with a storage surface can be employed in place of the silicon target. This is not an engineering design by any means, but shows in somewhat more detail what the functional elements might actually look like.

From the photon input to the video output we have the following components: a photocathode, the electrodes required for the electromagnetic focusing, an element for providing the alkali metal vapor generators to make the photocathode, a silicon-diode array target or a microchannel plate/storage target, and finally a high-resolution return-beam readout section.

In Table I-1, I have listed some of the goals and characteristics of the two types of devices. One should note that the somewhat smaller MTF of the silicon-diode array target requires

Table I-1  
 Characteristics of Candidate Image  
 Sensors for the Large Space Telescope

	Goal	I/SIT/RBV	I/MCP/RBV
Minimum Irradiance (quanta/s/pixel)	$10^{-2}$	$10^{-2}$	$10^{-2}$
“Resolution” Element Size ( $\mu$ ); MTF = 0.50	16 → 4	22	14
Resolution Elements (number)	$10^7 \rightarrow 10^8$	$10^7$	$10^7$
Active Diameter and Format Size (mm, mm X mm)	50 → 150	96, 68X68	62, 44X44
Field Divisions (points, lines)	4, 2	0, 2	0, 0
Cosmetic Quality (spots)	$300 \rightarrow 10^3$		
Spectral Sensitivity (Minimum $Q_e$ )		S20	S20
$\lambda = 300$ nm	0.03	0.02	0.02
$300 \text{ nm} < \lambda(\text{peak}) < 750$ nm	0.30	0.25	0.25
$\lambda = 750$ nm	0.03	0.01	0.01
Uniformity (%)	$\pm 5$	$\pm 10$	$\pm 10$

that it be larger than the microchannel plate/storage target assembly. In this regard, there may be a problem of obtaining large diameter single-piece silicon-diode array targets, because of the availability of large diameter single crystal silicon. However, it may be possible to build a silicon-diode array target mosaic having the required total area to produce  $10^7$ , 50 percent MTF pixels. Another characteristic shown in this table is the spectral response. The required response in the visible range is closely approached by the S-20 characteristic. For other wavelength ranges, other photocathodes and input windows could be used to attain sensitivity in the near infrared and the near ultraviolet ranges.

At the present time, we are looking at the target characteristics. A demountable camera tube having return-beam readout is being constructed. We plan to look at both silicon-diode array targets and the microchannel plate/storage target assemblies to determine their readout properties, beam landing properties, dark current, and so on. We are concentrating on establishing a set of target specifications and in general are studying theoretically the optical information throughput of the optical-image sensor to determine which elements or components in the tube should be modified or replaced.

Let me end by discussing one type of electron optic that came out of this study.

We realize—and Dr. Hallam has stressed this particular point—that if an opaque photocathode could somehow be used as the primary image sensor, you could gain, as a rule, a factor of three or five times the quantum efficiency of a semitransparent alkali-halide photocathode. In addition, the output image contrast of a tube with an opaque photocathode is expected to be significantly improved. The chance for scattered light to strike the photocathode should be reduced, so veiling glare or signal induced background in

the tube should be decreased. An opaque photocathode is, of course, an absolute necessity for work in the vacuum ultraviolet region.

We therefore considered the possibilities of using an electron lens with opaque photocathodes and arrived at one solution which looks very attractive. A patent disclosure has been applied for; it was described at the Conference on Developments in Electronic Imaging Techniques held in San Francisco, Oct. 16-17, 1972. I can tell you we have successfully checked the operation of this electron lens in the laboratory. It is possible to use opaque photocathodes in large active diameters; flat input and output image surfaces are also possible. In fact, this is what we checked in the laboratory.

## DISCUSSION

*S. SOBIESKI:*

Thank you very much. You have certainly whetted our technological appetite with your final remarks. The possible application, vis-a-vis the new III-V cathodes, comes to mind immediately.

*J. L. LOWRANCE:*

With a microchannel plate, what sort of storage target do you anticipate?

*C. B. JOHNSON:*

You can use the image-orthicon types of targets: glass or magnesium oxide. You can also use aluminum triple oxide.

*J. L. LOWRANCE:*

What do you plan to use?

*C. B. JOHNSON:*

Probably aluminum triple oxide to begin with.

*J. L. LOWRANCE:*

At what voltage will the electrons strike aluminum oxide?

*C. B. JOHNSON:*

Under normal operating conditions, electrons leave the microchannel plate with a range of electron energies as broad as a few hundred electron volts. Microchannel plate/storage target assemblies have been made at the Bendix Research Laboratories and also at RCA.

*J. L. LOWRANCE:*

What is the yield of the aluminum oxide at these voltages?

*C. B. JOHNSON:*

Approximately three.

*J. L. LOWRANCE:*

How thick is the target? I am concerned about its self-supporting capability.

*C. B. JOHNSON:*

A few hundred angstroms. At this thickness it is self-supporting. In fact, there are three ways to support the storage target. You can mount the storage target on a ring, and then bring the microchannel plate into proximity to it, or you can actually place the two surfaces in contact. The other type employs a storage surface that is formed directly on the output surface of the microchannel plate.

*J. L. LOWRANCE:*

The resolution that you talk about is quite high. What is the transmission efficiency of the channel plate at this resolution? In other words, how many photoelectrons are actually collected?

*C. B. JOHNSON:*

The open area ratio, or transmission efficiency, is about 50 percent.

*E. DENNISON:*

I just want to make sure I understand. In going from the microchannel plate to storage target, some sort of an accelerating voltage is needed, is that right?

*C. B. JOHNSON:*

An accelerating voltage is not required because the electrons coming out of the microchannel plate have an energy distribution, and the most probable energy is approximately 100 eV. These output electrons give rise to secondary emission off the gain/storage surface, and the secondary electrons are collected on the output electrode of the microchannel plate.

The electrons from the microchannel plate have enough energy to provide secondary emission at the storage surface.

*E. DENNISON:*

Have tubes of this type been built?

*C. B. JOHNSON:*

Yes.

*G. GILBERT:*

I would like to ask about noise properties of the channel plate. Do you have problems with ion feedback?

*C. B. JOHNSON:*

Yes, there is a problem with this, of course, but techniques of using microchannel plates have been improved greatly. This has been more of a problem in the past than it will be in the future. We have obtained dark count rates of 10 counts/cm<sup>2</sup>/s in special microchannel plates, so when you consider all the channels in a square centimeter, the count rate per channel is very low.

*W. E. SPICER:*

What initial velocity for the photoelectrons did you use in calculating the resolution?

*C. B. JOHNSON:*

For the silicon-diode array targets, the photoelectrons will strike the target with an energy in excess of 10,000 eV. We would like gains of a couple of thousand in the silicon. In the microchannel plate version, the gain is not a strong function of the input electron energy, so we would be talking about 200 V there, I suppose.

*W. E. SPICER:*

If the photoelectrons were ejected with say 5 eV initial energy from the photocathode, would this disturb your resolution?

*C. B. JOHNSON:*

Yes. The higher that energy distribution is, the worse off the resolution is. Normally, one assumes an initial energy of about 1 eV for visible sensitive photocathodes, for the purpose of making calculations. You have to assume something before making an electron-optic calculation. It is easiest to choose a monoenergetic emission energy but still allow different angles of emission. This usually gives results that agree well with measurements. The best test is to make measurements on the actual device to determine its image transfer properties. We know pretty well from experience what to expect from different types of electron-lens and photocathode combinations.

*W. E. SPICER:*

Have you ever used photocathodes that have high initial electron energy like UV photocathodes?

*C. B. JOHNSON:*

Yes. The resolution, of course, does get considerably worse as the input photon energy increases. However, something else to keep in mind is that when the incoming photons have enough energy to release two photoelectrons, the initial energy of the electrons may be reduced, and the resolution may improve.

*H. M. JOHNSON:*

Have you studied the expected resolution as a function of difference of magnitude of adjacent stars, say a bright and faint one rather than two equally faint ones?

*C. B. JOHNSON:*

We haven't considered that for specific cases, but we have looked at the general problem from a theoretical standpoint. If the system MTF is known, then the edge-response function, the line-response function, and the point-spread function can be calculated. You can then go back and say what the point-spread functions are at the input of the device. These point-spread functions, weighted in intensity by the relative star brightnesses, are then used to determine the actual modulation that can be expected. This modulation will decrease as the objects are moved closer together and as the brightness ratio of the objects increases. But, as I said, solutions for specific object ratios and device MTFs have not been worked out.

*N. G. ROMAN:*

Does that really work for the problems that he was asking about – where you may have an overexposed image?

*C. B. JOHNSON:*

For an overexposed image, the same general procedure can be used to analyze the image pattern; but, the limiting resolution will also depend upon the saturation characteristics of the sensor. Therefore, the image-transfer properties of the gain/storage target as a function of signal intensity must be specified. For large input signals, the microchannel plate output saturates, but the saturated area does not spread or bloom because each channel is physically isolated from its neighbor. However, present day silicon-diode array targets do not have physical barriers between adjacent p-n junctions, and bright-point inputs produce relatively large diameter outputs, and for low input signals the output diameter grows as the square root of the input signal.

*K. HALLAM:*

The modulation transfer functions that Dr. Johnson has derived allow the possibility of accounting for prevalent glare, which is apropos to Dr. Hugh Johnson's question. One merely has to have the information for the various types of targets available in order to predict what you should be able to do in any particular design.

*J. L. LOWRANCE:*

Can you tell us the time constant of this aluminum storage target? How long can you expose before you have to read out?

*C. B. JOHNSON:*

The maximum measured storage time of aluminum oxide storage targets mounted directly on the output surface of a microchannel plate is on the order of tens of seconds.

*N. G. ROMAN:*

So it is not a storage tube at all.

*C. B. JOHNSON:*

That is correct; it is not a storage tube.

*N. G. ROMAN:*

That leads us to a communications problem.

*J. A. WESTPHAL:*

What is your mode of operation? Are you going to let the light fall on the tube for a long period of time and then read it out?

*C. B. JOHNSON:*

We anticipate a dual mode of operation. In the high-sensitivity photon counting mode, the  $10^7$  picture elements are readout in a 1-s period, and if an electron has arrived in a picture element then, using a threshold setting, we either do or do not detect a signal at each picture element. A 1 or a zero is stored in a memory location, and we continue doing this until enough statistical information is obtained to cover about three orders of magnitude. For higher intensity input signals, an analog readout mode will be employed.

*J. A. WESTPHAL:*

Will you obtain a readout every second regardless of the mode of operation?

*C. B. JOHNSON:*

Yes. The silicon-diode array target, I should say, also has to be cooled, and this may be a significant limitation because the target dark current is on the order of  $10 \text{ nA/cm}^2$  at room temperature. This dark current is approximately halved with every 8-degree Kelvin reduction in temperature. The microchannel plate does not have to be cooled.

*H. M. JOHNSON:*

Is your tube capable of doing photometry on pulsars which might have a frequency up to 30 Hz? I refer to photometry at various phases of the cycle – not to the integrated or averaged brightness.

*J. A. WESTPHAL:*

Your frame time would have to get shorter.

*C. B. JOHNSON:*

Yes, the problem is to be able to handle the bandwidth, unless you underscan the target.

*C. E. MCILWAIN:*

To what extent does the performance depend upon past history? If you had a bright pulse, for example, can you in the next millisecond obtain the kind of performance you were shooting for?

*C. B. JOHNSON:*

If you had actual bursts of light coming in?

*C. E. MCILWAIN:*

Yes. But what is the time response? How long do you have to wait in order to achieve the kind of performance you want after a bright flash? Can you give an approximate time?

*C. B. JOHNSON:*

I would expect that charges produced by a bright flash can be adequately erased after the target has been read out about three times. Certainly much less than an hour will be needed.

*M. GREEN:*

I wonder if you could explain exactly how the storage target works.

*C. B. JOHNSON:*

In the microchannel plate?

*M. GREEN:*

No, not the microchannel plate. You talked about secondary electrons being produced by the electrons coming from the microchannel plate after they hit the aluminum oxide. Where do these secondaries go?

*C. B. JOHNSON:*

They go back to the microchannel plate output electrode. The storage surface is stabilized at the readout electron cathode potential, and the electrons coming out of the microchannel plate have energies of about 100 eV. These give rise to secondary electrons which leave a positive charge on the storage surface. The secondary electrons go to the microchannel-plate output electrode.

*E. EBERHARDT:*

Dr. Johnson, can I make a comment on that? One must remember that these films, which go on the backside of the channel plate, are very thin. They are only on the order of 10 nm thick. That means the charge transfers through these films not because of the emission energy of the secondary electrons but essentially because of a field breakdown effect in the film. You put the charge on the channel-plate side, and it transfers through the film to the readout side.

*M. GREEN:*

You do not have any gain then.

*E. EBERHARDT:*

All I am saying is that the charge transfer mechanism is by field breakdown. You see, as the signal propagates down the channel, you get a very large number of secondaries and primaries. Finally, one obtains a big charge burst that deposits on the back side of this auxiliary film.

*C. B. JOHNSON:*

Consider a single channel in the microchannel plate. A primary photoelectron that enters the channel will produce on the order of 1000 output electrons which have an average energy of about 100 eV when they strike the storage surface. When the beam from the electron gun scans the storage surface, the storage surface is lowered to the potential of the hot cathode in the electron gun, for example, zero volts. The secondary electrons from the channel strike this storage surface with an energy of 100 eV. These electrons from the storage surface are collected by the microchannel-plate output electrode.

*M. GREEN:*

Doesn't that have to be 100 V negative?

*C. B. JOHNSON:*

No. The microchannel-plate output-electrode potential will be only a few volts positive.

*E. DENNISON:*

I just wanted to make sure I understood you. You said the crossover point between the pulse-counting and analog modes was at  $10^3$  electrons/channel?

*C. B. JOHNSON:*

We cover a range of 1000 in the photon-counting mode.

*E. DENNISON:*

That means you are not digitizing.

*C. B. JOHNSON:*

At the maximum sensitivity, we are looking for  $10^{-2}$  photon/s/pixel with a quantum efficiency of approximately 10 percent, so the signal is about  $10^{-3}$  photoelectron/pixel/s.

*E. DENNISON:*

It is  $10^{-2}$  photoelectron/pixel at the crossover.

*P. ZUCCHINO:*

What is the fate of primary electrons that hit the closed area of the entrance to the channel plate?

*C. B. JOHNSON:*

Those primary electrons can produce secondaries which scatter into adjacent channels. They won't be fed back into the electron-lens section.

*P. ZUCCHINO:*

Will any be lost?

*C. B. JOHNSON:*

Yes.

*P. ZUCCHINO:*

Of the input photoelectron flux, what fraction successfully enters the channels?

*C. B. JOHNSON:*

Approximately 50 percent.

*T. KELSALL:*

The microchannel plate seems to have many overriding virtues. What are its defects? Second, just a general question: What effect will low-energy cosmic rays have on all these systems? The device description is premised on the absence of external perturbations.

*C. B. JOHNSON:*

Let me speak to the second part first.

The microchannel plate can be used as a soft X-ray converter and amplifier. However, the gain and dark-current characteristics of microchannel plates are relatively insensitive to high-energy radiation. They can also be used as detectors in the UV for wavelengths shorter than about 150 nm, again as primary detectors. For longer wavelengths, you have to use photocathodes to provide the photoelectrons. It is also conceivable that a photocathode can be formed on the inside of the front section of the channels, but this option has not been seriously considered in this study. An increase in the dark current in silicon-diode array targets due to high energy radiation is expected, and this may limit their usefulness in some space applications. The problems with microchannel plates are mainly ones of control at each stage of manufacture, storage, and use. You start out with a particular type of glass for the center-to-center spacing required for the application. When the glass is reduced, the proper strip current density and gain results in the channels. In essence, the type of glass used to make microchannel plates is tailored to the application. After the plates are made, they must be stored in a dry and inert atmosphere. If the microchannel plate is vacuum baked along with the rest of the tube, and if the microchannel plate is also "electron scrubbed," then stable and predictable electrical characteristics can be expected. In other words, if careful tube building procedures are used, good results can be expected from tubes employing microchannel plates.

It should be emphasized that the two designs that have been singled out for detailed analysis make use of existing technology. Silicon-diode array targets having the required diameter are not presently available, but it should be possible to develop large enough targets in the near future. However, microchannel plates as large as 75-mm active diameter have already been made.

The technology is here. It is the devices we have not seen yet.

*J. B. OKE:*

Could you give us some measure of the uniformity of response of the channel plates?

*C. B. JOHNSON:*

The nominal uniformity of gain across a microchannel plate is about 10 percent, but this gain variation can be calibrated out once the device is made.

*K. HALLAM:*

In the photon counting mode, the gain differences are not that important.

*C. B. JOHNSON:*

Yes, in the most sensitive photon counting mode, the effects of this gain variation can be eliminated.

*J. A. WESTPHAL:*

Are you concerning yourself about how to take care of the flat-field problem, that is, gain calibration, in space or are you depending on the localized gain of the target to be forever constant?

*C. B. JOHNSON:*

It may be necessary to provide for a method of periodically recalibrating the instrument (the image sensor) in space, because these surfaces can degrade due to radiation.

*J. A. WESTPHAL:*

You have not thought how to do it?

*C. B. JOHNSON:*

No, we have not looked at that.

*S. SOBIESKI:*

I think that this has been an informative discussion. To summarize, the needs for computers, cooling, and calibration were clearly established.

*N. G. ROMAN:*

And the need for shielding.

*S. SOBIESKI:*

Shielding, definitely. The remainder of the papers are not as directly LST oriented and will address state-of-the-art developments. The important input interface, the photocathode, will now be discussed by W. Spicer.

PRECEDING PAGE BLANK NOT FILMED

## II. PHOTOCATHODES FOR USE IN THE LARGE SPACE TELESCOPE PROGRAM

*W. E. Spicer*

*Stanford University*

*Stanford, California*

My purpose in this paper is to bring to your attention the photocathode materials that are presently available and, in particular, to emphasize the new materials that are becoming available. These new materials present tremendous potential advantage to astronomical users but are not yet available to the astronomical community. Figure II-1 shows a collection of response curves indicating the available and potentially available photocathodes. In Figures II-2 through II-5, additional curves are shown presenting more restricted spectral regions. I have not attempted to present curves for all presently available (commercially) photocathodes because these curves are in most cases readily available to the reader, and because in some cases, data are lacking for the ultraviolet regions.

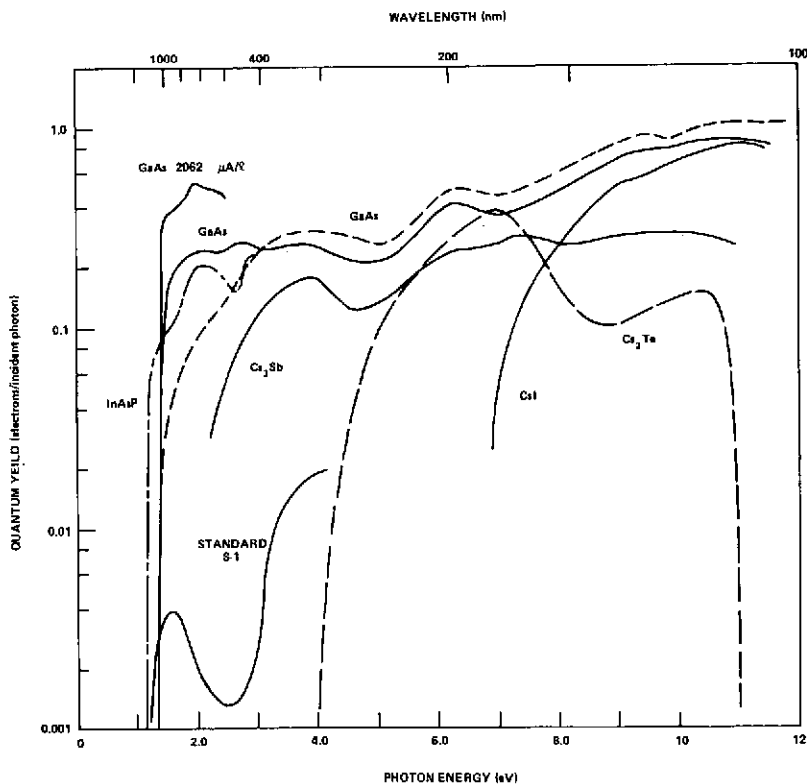


Figure II-1. Representative photocathode response curves.

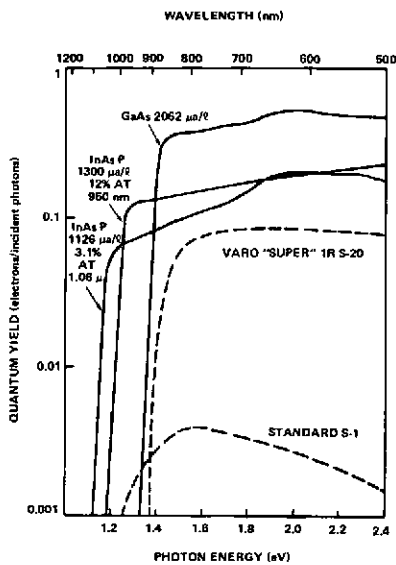


Figure II-2. Photocathode response curves in the infrared.

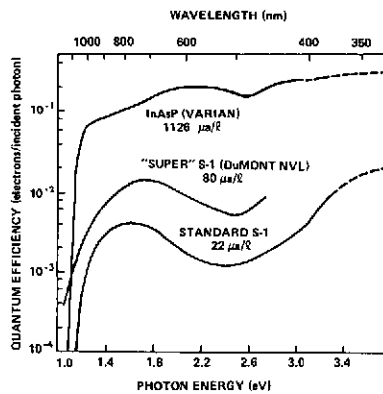


Figure II-3. Response curves of the red sensitive photocathodes.

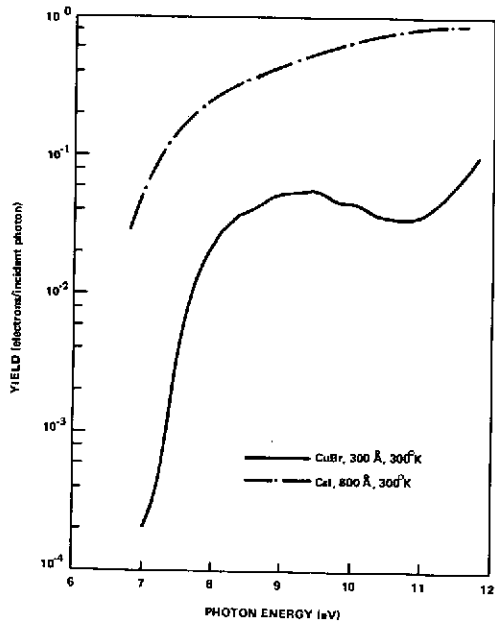


Figure II-4. Response curves for solar blind photocathodes.

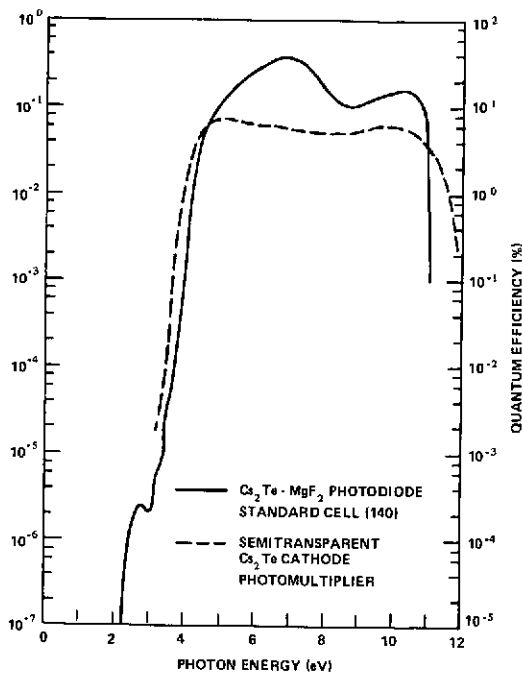


Figure II-5. Response curves for devices with  $\text{Cs}_2\text{Te}$  photocathodes.

It can be seen from these curves that a new class of photocathodes has been developed that is potentially available for the LST. These cathodes have responses equal to or much better than commercially available photocathodes over a very wide spectral range. For example, if one examines the solid gallium arsenide curve in Figure II-1, one sees that it has an increased efficiency over the S-1 in the infrared region of almost two orders of magnitude. Furthermore, throughout the visible, and much of the ultraviolet, it has a sensitivity of 50 to 100 percent more than the presently commercially available tubes. It thus has the advantage of having a high quantum yield over a very large spectral range. This is important in many astronomical observations. Energy distribution curves are available for most of the cathode materials presented in our figures. I will not attempt to reproduce these data here. However, I will point out to the designer of any image tube the importance in the relationship between the initial energy distribution and the resolution that can be obtained from a given device. I should also point out that the energy distributions are a strong function of photon energy but not necessarily simple functions. One must understand the physics of the photocathode in order to understand and predict the energy distributions. To give one example, near 11 eV, the spectral responses of the gallium-arsenide and the cesium-iodide photocathodes are comparable. However, the average energy of the electrons from the gallium-arsenide cathode is about 1 eV, whereas it is approximately 4 eV for the cesium-iodide photocathode. If the designer of image tubes is not aware of these effects, he may get into significant difficulties, particularly in regard to resolution capability.

The III-V photocathodes are a recent development and are still being developed and improved. They have one difficulty that is likely to make astronomical and military tubes using these cathodes different. This is that it is very difficult to make a semi-transparent III-V cathode having a spectral response over a wide wavelength range. This has to do with the necessity of making excellent single crystals. Details are given in the literature. The Department of Defense (DOD) is now funding almost all of the research and development work on these photocathodes. The emphasis in the DOD work is on semi-transparent cathodes with a limited spectral range. If the astronomical community is interested in having such cathodes, which are useful over a large spectral range, then it will be necessary for reflectronic tubes to be developed in which an opaque rather than a semi-transparent photocathode is used. If this is done, then the wide spectral response shown in Figure II-1 can be realized from these photocathodes. It should be noted that if one is willing to restrict the use of the photocathode to a fairly small spectral range near the threshold of response, then the semi-transparent cathodes can be used.

As is typical, in the development of new cathodes with increased sensitivity there have been problems with the life of the cathode and such things as uniformity and blemishes. It appears that steady improvements are being made in overcoming these difficulties, and there is not yet any indication that these give basic limitations to the photocathode. The severest problems were with lifetime for the cathodes whose response extends furthest into the infrared such as, the InAsP cathode shown in Figures II-1, II-2, and II-3. Even if one has a reduction of yield of an order of magnitude due to these problems, it should be noted that

the infrared response would still be approximately an order of magnitude better at  $1.06 \mu\text{m}$  than the tubes presently available commercially. For the III-V cathodes with sensitivity cutoff at shorter wavelengths for example the gallium-arsenide cathode, then these effects are already under better control.

The thermionic emission, and thus dark current from the III-V photocathodes, is in general much less than that from a conventional cathode with a comparable threshold of response. Details on the thermionic emission are available in the literature.

Figures II-4 and II-5 show data on cathodes which have special usefulness since they are not sensitive to the thermal radiation from the sun but are quite sensitive to ultraviolet radiation. In the first curve, I show responses of the CsI and CuBr. Cesium iodide is clearly more sensitive. Its only problem is a high resistivity (this can be counteracted by thin metallic underlay) and a susceptibility to damage through the long ultraviolet exposure. The damage is manifest in an increased response beyond 6 eV, extending into the visible. It is important to be sure that such effects will not bother the performance of the system.

In Figure II-5, we show spectral response curves for one of the alkali-telluride photocathodes,  $\text{Cs}_2\text{Te}$ . This surface is particularly useful when response is desired between 4 and 6 eV. It was recently found that optimizing the activation process gives promise of increasing the quantum yield in photon energies above 4 eV by factors from 2 to 4. In addition, it may be possible to further reduce the response below 4 eV. This reduction is desirable in order to minimize the response to the visible radiation from the sun. It has proven possible to make cathodes of this type with extreme uniformity. Once again, if this cathode is of practical interest to NASA, it appears that substantial gains may be found in sensitivity by optimum activation in practical tubes.

In the accompanying table, Table II-1, I have attempted to describe the principal photocathodes and list some of the important characteristics of these. In studying this table, it is important to realize that the quality of the cathodes can be expected to improve as more experience is obtained in activating them. This is particularly true of the newer cathodes such as the III-Vs. Further information on this cathode can be found in the review article by Spicer and Bell.\*

If stability is of concern, one can use a copper-bromide photocathode but at a loss of gain of a factor of 10 or so compared to CsI.

There is one cathode that is missing in the compilation because I didn't have a wide range of spectral response data for it. It is the multi-alkali cathode. People are now able to make these with a threshold almost identical to that for gallium arsenide in the semi-transparent mode. It has a yield a little under 10 percent, and it is fairly flat with wavelength. We don't know what its characteristics are in the ultraviolet, but it still should be at least, I would

---

\*"The III-V Photocathode: A Major Detector Development." *Publications of the Astron. Soc. of the Pacific*. 84. 1972. p. 110.

Table II-1  
Properties of Various Photoemitters

Cathode Material	Geometry	Spectral Range		Approximate Quantum Yield el/ph	Approximate 10 percent Maximum Electron Energy	Stability	Thermionic Emission Amp/cm <sup>2</sup>	
		Threshold 10 <sup>-3</sup> el/ph (eV)	High h $\nu$ Cutoff				Room Temperature	250°C
GaAs(CsO)	Opaque Semi-transparent	1.35(0.9 $\mu$ m)	*W ~ 1.6 (0.77 $\mu$ m)	0.3 at 0.8 $\mu$ m/1.0 at 0.12 $\mu$ m 0.3 at 0.8 $\mu$ m	4.5 eV at 0.21 $\mu$ m ~ 1/40 eV	can be problem	10 <sup>-16</sup>	10 <sup>-20</sup>
InAsP(CsO) 1.06 $\mu$ m	Opaque Semi-transparent	1.1(1.1 $\mu$ m) 1.1(1.1 $\mu$ m)	*W ~ 1.4 (0.9 $\mu$ m)	0.2 at 0.6 $\mu$ m No $\mu$ mV Data $\leq$ 0.08 at 1 $\mu$ m	~ 4.5 eV at 0.21 $\mu$ m ~ 1/40 eV	can be problem	10 <sup>-14</sup>	10 <sup>-17</sup>
III-V Alloy	Opaque Semi-transparent	Adjustable 1.1 to 1.35 (1.1 at 0.9 $\mu$ m)	*W substrate	Varies between GaAs(CsO) and 1.06 $\mu$ m InAsP (CsO) as alloy content is changed.				
S-20 Varo-Super	Semi-transparent	1.35(0.9 $\mu$ m)	*W	0.09 at 0.7 $\mu$ m No $\mu$ mV Data (Cs <sub>3</sub> Sb ~ 0.12) at 0.18 $\mu$ m)	Estimate ~ 2 eV at 0.3 $\mu$ m	O.K.	No Data Estimate ~ 10 <sup>-15</sup>	No Data
S-1 (Standard)	Either mode	1.2(1.0 $\mu$ m)	*W	5 x 10 <sup>-3</sup> at 0.78 $\mu$ m	1 eV at 0.6 $\mu$ m 3 eV at 0.4 $\mu$ m	can be problem	10 <sup>-11</sup>	5 x 10 <sup>-15</sup>
Cs <sub>2</sub> Te	Either mode	4(0.3 $\mu$ m)	*W	0.4 at 0.18 $\mu$ m 0.09 at 2.4 $\mu$ m	~ 4 eV at 0.15 $\mu$ m ~ 4 eV at 0.15(?)	O.K.	O.K.	O.K.
CsI	Either mode	6.5(0.19 $\mu$ m)	*W	0.9 at 0.11 $\mu$ m 0.5 at 0.11 $\mu$ m	5 eV at 0.1 $\mu$ m Bad EDC	Should be checked	O.K.	O.K.
Cu Halides	Either mode	7.4(0.17 $\mu$ m)	*W	0.06 at 0.14 $\mu$ m	~ 4 eV at 0.11 $\mu$ m	O.K.	O.K.	O.K.

\*W = Window sets high h $\nu$  cutoff.

hope, 10 percent. The advantage of the multi-alkali cathode is that there is a large amount of experience in making them, and the problems of stability and uniformity, as far as I can find now, are not severe. In particular, the stability seems adequate.

I should say that it is difficult to make multi-alkali cathodes with a threshold in the infrared, but if one wants to give up some red response one can probably get better UV response as well as better red response than with the cesium-antimonide cathode. If one were to choose a single cathode to span the widest wavelength region, it may be a very good choice. Cooling may still be necessary, but this is not certain. I do not have any data on the newer extended red response tubes.

## DISCUSSION

*E. J. WAMPLER:*

I have two questions. One, what do you mean by good or not good uniformity?

*W. E. SPICER:*

What I mean by good is that I know of cases where the cathode can and has been made in a fairly routine fashion with good uniformity.

*E. J. WAMPLER:*

Does that mean plus or minus 10 or 20 percent?

*W. E. SPICER:*

About 10 percent, approximately.

For GaAs, as with most new photocathodes, early cathodes have uniformity problems. However, these problems are disappearing as more experience is gained in making them.

*E. J. WAMPLER:*

Now, would you consider poor uniformity to be plus or minus 50 percent?

*W. E. SPICER:*

Like that, yes.

*E. J. WAMPLER:*

The other question I had regards cost. I suppose one might estimate the cost of the spacecraft will go as the collecting area or the square of the aperture. In the case of the LST, we are talking about a very large sum of money. If we can double the quantum efficiency for cathodes then one should compare the cost of doing that with the cost of making the

actual telescope larger by a factor of 1.4, which would approximately double the cost of the spacecraft. What sort of sums would it take to bring these cathodes into good, solid, reliable tubes?

*W. E. SPICER:*

Let me summarize my remarks on the III-V cathode by emphasizing the increase in sensitivity that can be gained if the astronomical community, including NASA, is willing to pay a fairly modest cost for the development of tubes appropriate for astronomical use. The cost is very small considering the price that would be paid for increasing the sensitivity through larger telescopes. It also seems to me that it would pay for itself by the economy of data acquisition with existing equipment. It would also make possible observations that are not presently possible. This is particularly true in the infrared region.

It might be argued that no money should be spent on developing improved instrumentation of this type, but rather that NASA should wait for the military or other agencies to pay for the development of the necessary hardware. In my opinion, this is a mistaken philosophy. First of all, the requirements of the astronomer and of the military are different. Thus, the equipment developed by the military may be much less than optimum for astronomical use. I have indicated some of the reasons for this in the above discussion. Second, there is just the question of time. If a relatively modest expenditure by NASA would assure early accessibility of the improved tubes, the lack of wasted time and effort could pay for the cost of development many times over. A very favorable comparison would be made in comparing the cost of developing tubes that would increase the sensitivity by a factor of two with the cost of building a telescope where this improvement would be achieved through light gathering.

In answer to your direct question, it depends greatly on the details of the objective. Amounts between \$50,000 and \$500,000 should produce useful tubes if spent judiciously.

*E. J. WAMPLER:*

So \$10 million would do it?

*W. E. SPICER:*

Do you want me to sign the contract right now? (Laughter)

*E. J. WAMPLER:*

Seriously, that would represent only somewhat more than two percent of the satellite cost while affording a doubling of the efficiency.

*J. B. OKE:*

Do you get multiplication at the higher rates, and what is the real quantum efficiency?

*W. E. SPICER:*

That is an important point. The question concerns the fact that at high photon energies one obtains electron multiplication in GaAs. The quantum yield increases, but this may not be advantageous if pulse counting techniques are employed. Even at the highest yields shown for GaAs, counting techniques would give a sensitivity of about 0.7 output pulses per incident photon. GaAs should be superior in sensitivity to all other materials, with the exception of CsI, in the 10 to 12 eV range.

*S. DUCKETT:*

How does the quantum efficiency of the gallium arsenide change at low temperatures? The thermionic emission goes down, but how does this affect the sensitivity?

*W. E. SPICER:*

The threshold is set by the band gap. At lower temperatures the band gap increases, the threshold wavelength decreases a bit, but the yield well away from the threshold will tend to increase. Trapping effects are not a problem for those cathodes that have true "negative electron affinity." But for operation at wavelengths longer than 1.06  $\mu\text{m}$ , one begins to encounter again a barrier and sensitivity problems related to temperature that can become important.

*C. B. JOHNSON:*

In making electron-optic calculations, one must know the energy and direction of electron emission. You mentioned some values for the energies of the electrons. Do you have information on the emission angle distribution function? In particular, is there any directed emission from negative electron affinity photocathodes?

*W. E. SPICER:*

In III-V materials, near the threshold, electrons are emitted in the forward direction. In all other cases, something like a cosine distribution is obtained. More work is needed, however, because very few measurements have been made.

*J. L. LOWRANCE:*

Does the gallium photocathode have a more crystalline structure? In turn, will it be more affected by energetic trapped radiation in terms of long term effects?

*W. E. SPICER:*

It will have the sort of sensitivity as that which you get in a solar cell. In other words, if it is caught in a radiation belt you are in trouble. But it is not supersensitive.

*J. L. LOWRANCE:*

But is it a cumulative effect? Does it gradually deteriorate?

*W. E. SPICER:*

Yes. However, these materials start out being rather heavily doped so that you are starting from less than the most perfect situation. The sensitivity to damage is accordingly reduced.

*J. L. LOWRANCE:*

Can you estimate any order of magnitude? Does that increase the dark current: lower the gain?

*W. E. SPICER:*

I would guess that the sensitivity to radiation damage would be less than for solar cells. I would not expect any overwhelming increase in dark current.

*J. L. LOWRANCE:*

If we are guessing, can you give us an order of magnitude on the dose that lowers it by a factor of two?

*W. E. SPICER:*

Perhaps, and it is just a guess, something like  $10^{17}$  damage-induced lattice defects.

*J. L. LOWRANCE:*

Are you equipped to make a measurement like this?

*W. E. SPICER:*

No, I am not presently, but I think the measurement could be made fairly easily.

*J. L. LOWRANCE:*

This is obviously a very attractive material. It is new. I think that this sort of investigation is very important to LST applications, and someone should find the money to make that measurement.

*W. E. SPICER:*

That is certainly a good point.

*J. F. MCNALL:*

When you say cesium iodide picks up a red response when you expose it to large amounts of ultraviolet, what do you mean by large amounts?

*W. E. SPICER:*

Again, this isn't well documented. For example, we use a McPherson monochromator, which has at the output typically something like  $10^{10}$  photons/s/cm<sup>2</sup>. Over periods of hours we start seeing changes. There is a lot of old literature on this by Apker and Taft, written in the 1950s.

*J. F. MCNALL:*

Does it recover?

*W. E. SPICER:*

In cesium iodide, yes, but I suspect without positive proof, that once you damage the cathode it is more susceptible to damage the second time.

*J. F. MCNALL:*

Is the problem boiling off the cesium?

*W. E. SPICER:*

It appears to be a matter of producing F-centers, that is, lattice defects.

*S. DUCKETT:*

That hasn't been my experience—that the cathodes become more susceptible to damage. Maybe a little, but the F-centers do bleach and are not nearly as bad as in KI.

*W. E. SPICER:*

Just because they bleach easier.

*S. DUCKETT:*

I think it is a little harder to make F-centers in cesium chloride lattice and cesium iodide than in the sodium chloride lattice.

*W. E. SPICER:*

Duckett knows more about this than I do so I defer to him.

*S. DUCKETT:*

It should be recognized that this certainly is a problem. Usually what happens, however, is that if you are in a situation where you get so much UV energy that you would damage the cathode, you would be outside your normal measurement; you would be in a glare situation where the white light tends to bleach out the damage anyway. There is a bit of help there. It is not so bad.

*C. E. MC ILWAIN:*

I have a question regarding stability and uniformity, but first I preface it with a question to the committee and the audience: Isn't the sole objective of having a high-quantum efficiency that of achieving the highest accuracy within a given observation time? Is there any objective other than improving the accuracy?

*E. J. WAMPLER:*

There is another advantage in our application. Because you are orbiting the earth, you may lose the object. If you are only able to observe for a short period during each orbit, it would be very advantageous to achieve the desired accuracy during that period because one would not have to reacquire the object on subsequent orbits.

*C. E. MC ILWAIN:*

Thus, for a given observation time, you want to be able to get the best accuracy possible.

*E. J. WAMPLER:*

The observation time tends to be quantitized.

*C. E. MC ILWAIN:*

Again, it is not the quantum efficiency, but rather the accuracy that is obtained with the whole system operating. So now to the question for the speaker.

Any errors in calibration will obviously produce inaccuracies. If the photocathode uniformity is such that there is a microstructure, calibration becomes difficult. For example, if the relative response depends upon the exact registration between the sensor and the photocathode, errors will be introduced if the registration changes with time. In fact, errors will tend to be increased if there are any changes in the system response within an observation period of approximately an hour, regardless of what causes the changes. Either the error in calibration must be accepted or the observation time must be reduced to increase the number of calibrations. I think that right along with the quantum efficiency, we need to have the stability and uniformity questions answered.

*W. E. SPICER:*

Yes. Let me try to answer these, and then I will ask Dr. Hughes to comment also.

I think that with the gallium arsenide, the problems are less severe. The uniformity problems particularly with the new high yield photocathodes are just beginning to be tackled, and the results are encouraging. The concensus of opinion seems to be that the uniformity problems are tractable. As far as changes over a period of approximately an hour, I think that one doesn't have to be concerned.

*F. R. HUGHES:*

In regard to the sensitivity, we have obtained sensitivities (at RCA) in excess of half of the high values given in Table II-1 and uniform over several square centimeters.

*W. E. SPICER:*

Did you have any experience with stability in regard to ion feedback on these cathodes?

*F. R. HUGHES:*

With the reflection-mode cathode, unless the cathodes are subjected to very high illumination levels, stability is not a problem. But if you have an optic system wide open, obviously pointed directly at the sun, you are in trouble because of the surface film of cesium and oxygen; our opinion is that heating leads to a loss of the cesium oxide.

*C.E. MC ILWAIN:*

I would like to ask also about the temperature stability. What is the temperature dependence?

*W. E. SPICER:*

I think with a few degrees to 10 degrees, I wouldn't expect much variation. If it is more than that, one would obtain measurable variations.

*B. RUBIN:*

I just want to make a comment about the materials problems for the III-V compounds.

First, these are relatively new materials. I think research and development was started in 1968 or 1969.

*W. E. SPICER:*

Not quite. As photocathodes, yes, but not as materials.

*B. RUBIN:*

These cathodes must be made as single crystals, which presents a formidable problem in their utilization. Another point is that the Department of Defense in many of its branches, for example, the Night Vision Laboratory, is supporting activities for the development of these III-V compound semiconductors so that investment of additional development funds should be done only after careful consideration.

*W. E. SPICER:*

Yes. I think that what you say makes sense except that what DOD is emphasizing is a semi-transparent cathode, which has a different set of constraints. Their efforts will not be directly applicable to the needs of space astronomy in all cases. I would be very surprised if one does not want to use them in the opaque mode, which is not emphasized in the DOD work.

The semi-transparent mode is a much harder problem to treat. If, for example, one had put all the money spent in researching that mode into researching the opaque mode I think most of the questions being asked would have been well answered by now.

*J. A. WESTPHAL:*

What is the sensitivity of these surfaces to polarized light. Does it make any difference what the polarization is?

*W. E. SPICER:*

It is a cubic crystal so there is no optical axis.

*J. A. WESTPHAL:*

Could you explain why you need an opaque mode?

*W. E. SPICER:*

The basic problem with the semi-transparent photocathode is obtaining simple crystal material of sufficient quality and still keeping it sufficiently transparent to the incident radiation. Normally, a thin layer of the III-V cathode material is grown epitaxially on a second material; however, in order to obtain an epitaxial layer of sufficient quality, it is necessary to have its crystal lattice match almost exactly that of the cathode. This limits the substrate materials to those with band gaps near that of the photocathode material.

For mechanical strength, the substrate material must be relatively thick. As a result, the radiation with  $h\nu$  greater than the substrate band gap will be absorbed in the substrate and thus will not be available to produce photoelectrons in the cathode material. The net result is that the spectral response of the semi-transparent cathode drops to a very low value

within about 0.5 eV or 1.0 eV of the threshold of response. Thus, the wide spectral response shown in Figure II-1 is lost.

### III. ELECTRON-OPTIC LIMITATIONS ON IMAGE RESOLUTION

R. W. Engstrom  
 RCA  
 Lancaster, Pennsylvania

A simple, electrostatic lens is shown in Figure III-1. The dashed lines indicate equipotential

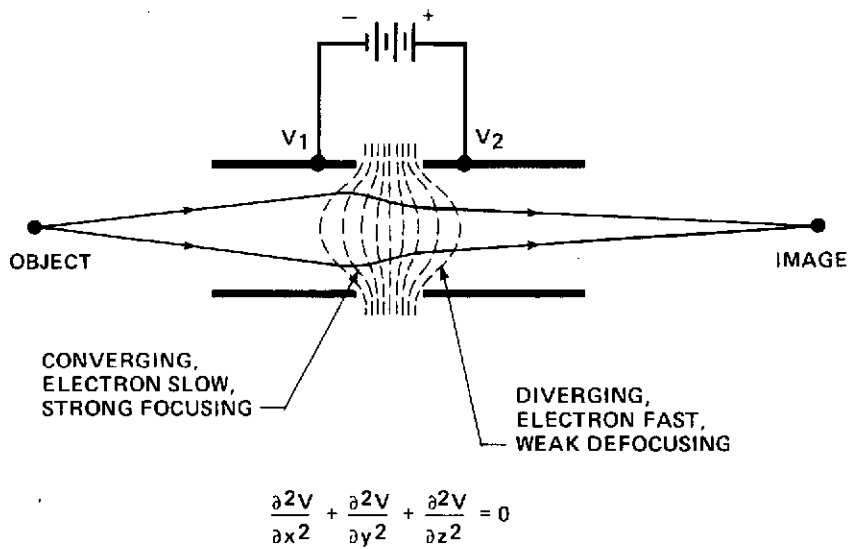


Figure III-1. Electrostatic lens composed of two coaxial cylinders.

surfaces formed in the space between the coaxial cylinders, which are operated at a different electric potentials. Note how the electron paths are shaped in much the same manner as light is by a lens. An early form of electrostatic imaging was described by Peter Schagen<sup>1</sup> and is shown in Figure III-2. It uses a spherical arrangement in which the photocathode is part of a large sphere, and the anode is a small sphere having a hole through which the electrons are directed. The arrangement is such that the electrons come into focus behind the anode sphere in an image plane as illustrated.

It is also possible to provide electron imaging by superimposing uniform electric and magnetic fields, both in the same direction as illustrated in Figure III-3. The equation for the force on an electron is shown in the figure as is the radius of the spiral path.

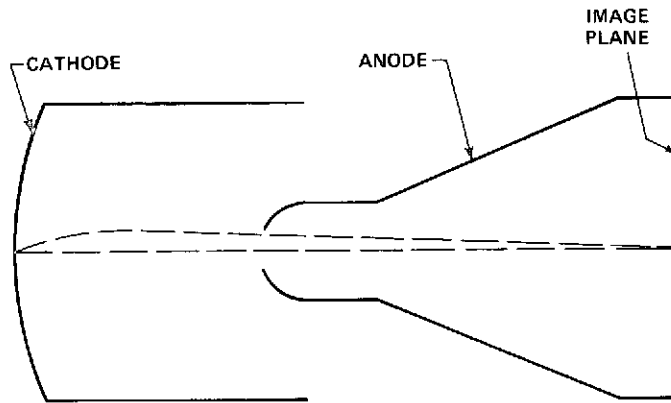


Figure III-2. Concentric sphere image system of Schagen.

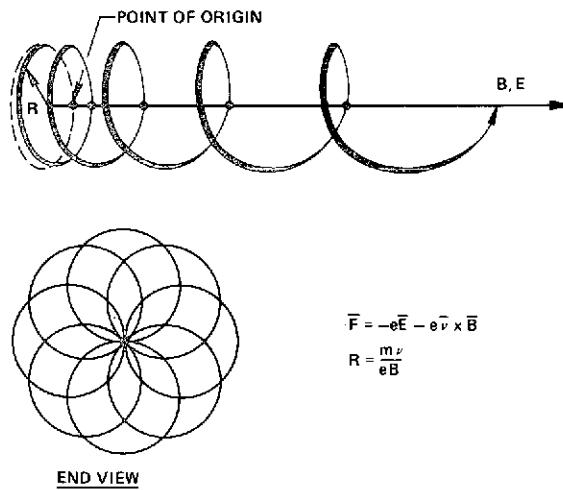


Figure III-3. Path of electron in superposed uniform electric and magnetic fields with the same direction.

There are several possible approaches to the solution of the electron-optical problem of designing an image tube configuration: analytical, experimental, analogue, and computer. The analytical technique involves solving Laplace's equation,

$$\frac{\partial^2 V}{\partial x^2} + \frac{\partial^2 V}{\partial y^2} + \frac{\partial^2 V}{\partial z^2} = 0$$

to obtain the equipotential distribution and then tracing the electron trajectories by using the force equation. Only a few special geometric situations can be solved completely by analytical techniques.

One practical image-tube design technique is to build a series of experimental image tubes with minor variations to approach a desired solution. Special demountable vacuum systems can also be utilized in which the spacings and voltages between electrodes can be varied. One clever experimental arrangement provides an image tube with the phosphor screen placed at a slight angle away from the normal to the axis of the tube. Thus, in a single tube, one has a means of studying the variation of the cathode-to-screen separation.

For many years, analogue techniques were widely utilized in the solution of electron-optical problems. One such analogue is the resistance network. A regular rectangular array of points is established in a plane. Resistances are connected between the points in lines parallel to the  $x$ -axis and also between points in lines parallel to the  $y$ -axis. By suitably choosing the values of the connecting resistances, the matrix can be made to represent either cylindrical or plane symmetry. In using the network, points are connected together to form the shape of the desired electrodes. Each such group of points is tied to a particular electrical potential. Equipotential lines may now be established by sampling the potentials of the junction points between the electrodes establishing the tube configuration. The electron paths are traced by solving the force equation between equipotential lines. Although the method is somewhat tedious, it can be quite accurate if the resistance network has a sufficient number of points in the matrix.

Another analogue is the rubber membrane, which is useful in the solution of problems having plane symmetry. In the rubber-membrane analogue, gravitational potential takes the place of electrostatic potential. Special electrodes are fabricated to hold the rubber membrane at heights proportional to the applied voltage. Electron paths are determined by allowing small steel balls to roll down the incline. The rubber membrane is very useful in obtaining a quick, though not very accurate, first solution.

Finally, electrolytic tanks may be used to trace equipotential surfaces. The technique, however, is very cumbersome and essentially obsolete today.

The most useful technique today for developing electron-optic image sections is to use digital computers with relaxation techniques to solve Laplace's equation for a specified

electrode configuration. Once the equipotentials have been established, a relatively simple computer program provides trajectory information.

Just as in optical designs, there are problems in electron optics of minimizing distortions. One type of distortion is spherical aberration which results because the outer electrons of a ray bundle tend to have a shorter focal length. In image-tube electron optics, spherical aberration is usually negligible because the high voltages used minimize the diameter of the ray pencils. Coma, which is a form of off-axis distortion resulting in the typical comet tail, is also essentially negligible in image tube configurations.

Chromatic aberration, which results from the difference in initial electron velocities, is also essentially negligible because of the high voltages used in image tubes.

A major problem in the design of an image tube is to minimize field curvature. Usually, it is desirable that the image plane be a flat surface. The simplest configurations usually lead to an image plane that is concave toward the lens. Another related problem is that the tangential and sagittal surfaces tend to differ, resulting in an astigmatism problem. Geometrical distortion in which the image of a square tends to be of pincushion shape or, on occasion, barrel shaped, is a second major problem in image-tube design.

As an illustration of the method of computer design of image-tube sections, I will describe some of the problems encountered in the design of an 80-mm image tube with a zoom capability of 3:1, which was recently designed on a Navy contract with RCA (Contract No. N00039-70-C-0550). For the first design of the 80-mm tube, an existing 40-mm tube was scaled up to size. The 40-mm tube did not have zoom capability, but it provided a front-end design, which we thought would be suitable for initial studies. Figure III-4 shows the outline of the initial design, some of the equipotentials, and some of the electron-ray bundles. The design incorporated four electrodes: a photocathode that was operated at 0 V, a focus electrode that was operated at 100 V, a zoom electrode that was operated at 1000 V, and the anode or screen that was operated at 12 kV. The symbolic resistance lines at the periphery of the envelope were programmed into the computer to have a uniform potential gradient between the pair of electrodes as indicated.

This first computer run attempted to see how the proposed design would work in the zoom mode. Although the tube did demagnify by 4:1, numerous problems were apparent. Some of the ray bundles were obstructed by the zoom electrode, as illustrated. Also observed was a large image distortion, which apparently resulted from the rather long trajectory in the nearly field-free region inside the zoom electrode.

In approaching the final solution, it was realized that although the two lenses in the tube were not independent in their operation on the electron trajectories, the lens in the front of the tube between the cathode and the first two focusing electrodes was most important relative to the unity magnification case, while the second lens between the zoom electrode and the anode was most useful in contributing to the proper operation in the zoom condition.

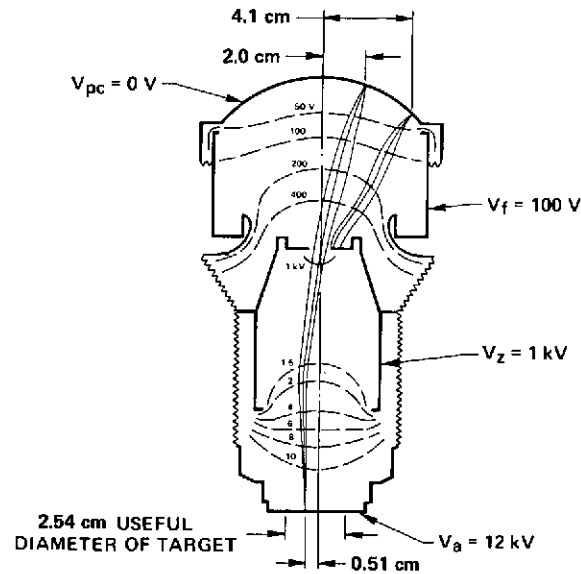


Figure III-4. Computer-calculated trajectories and equipotentials for initial 80-mm image section design.

Before achieving the final solution, about a dozen variations were run through the computer program. These variations included voltage changes as well as dimensional changes.

The final solution is shown in Figure III-5 for the unity magnification case and in Figure III-6 for the demagnification case. Note that the aperture in the zoom electrode has been opened up and that the positioning of the focus electrode has been changed. The zoom electrode was also shortened, which puts the second electron optical lens in a more favorable location. The equipotential surfaces in the cathode end of the tube are now much more favorable, as can be seen in Figure III-6. Note also that there is no problem of electron bundles striking the zoom electrode.

The final configuration did achieve the objective of the design program. Characteristics of the magnification and focus voltage as a function of the zoom voltage are shown in Figure III-7. The image plane was quite flat. The integral distortion was less than 2 percent at 25-mm, and the resolution was remarkably good. A picture of the final 80-mm zoom-image tube is shown in Figure III-8.

Three types of an electron-optical configuration are next examined for the electron-optical limitations to resolution: the proximity image tube, in which there is reasonably good resolution because cathode and image plane are spaced very close together; the magnetic-type image tube having uniform electric and magnetic fields; and the electrostatic-type image tube such as the 80-mm zoom tube just discussed.

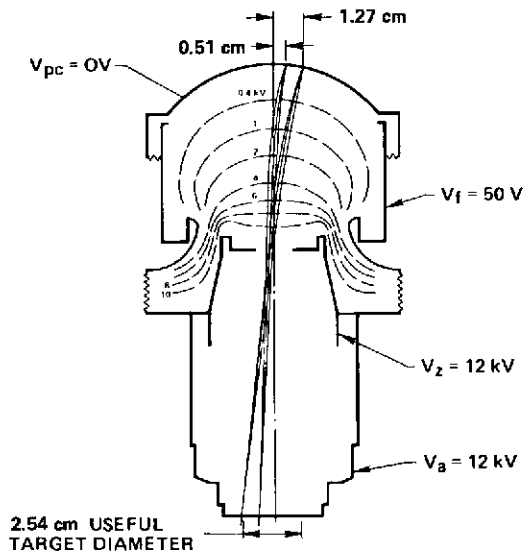


Figure III-5. Electron trajectories and equipotentials for unity magnification; 80-mm image section, final configuration.

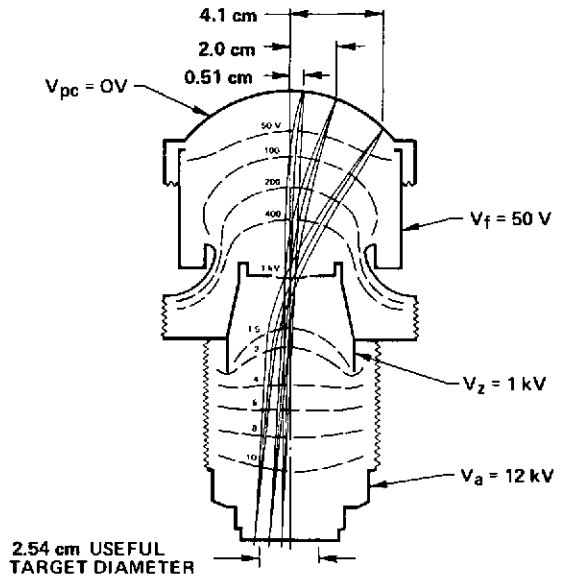


Figure III-6. Electron trajectories and equipotentials for 80:25 operation; 80-mm image section, final configuration, magnification = 0.34.

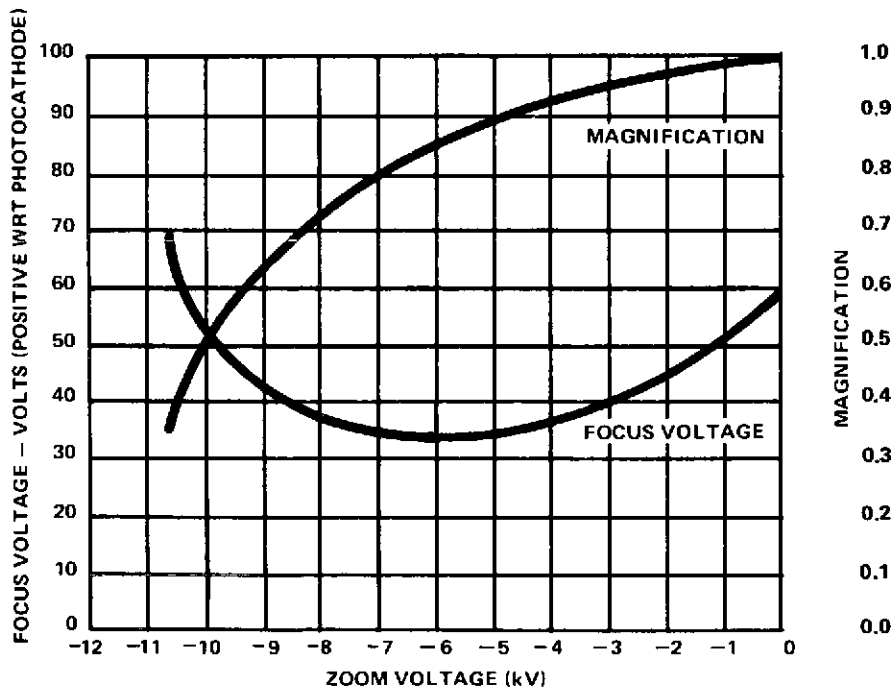


Figure III-7. Magnification and focus voltage as functions of zoom voltage for RCA developmental 80-mm zoom image tube, developmental Type No. C33114; anode voltage of 12 kV.

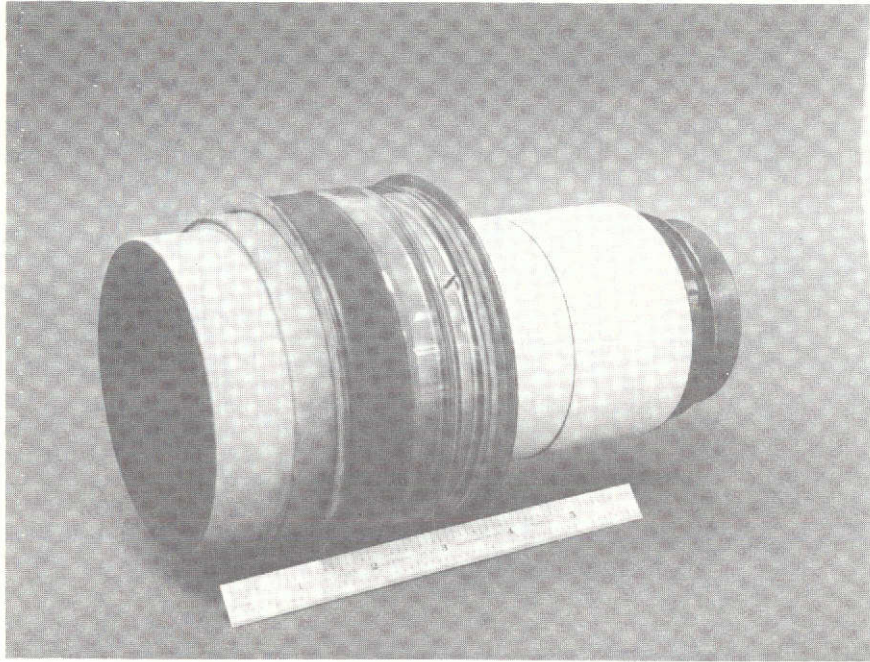


Figure III-8. RCA developmental Type No. C33114, 80-mm zoom image tube.

Figure III-9 shows the parabolic electron path in a proximity section. In this case, the size of the smallest resolvable spot is proportional to the separation of the parallel planes and inversely proportional to the square root of the applied voltage, as indicated by the formula shown in Figure III-9. It is, of course, the radial component of the electron emission velocity that causes the loss in resolution.

A wide-spaced, proximity-type image tube (actually, a magnetic-type image tube without applied magnetic field) was used to verify theoretical calculations of the modulation transfer function (MTF). The model for the MTF calculations assumed Lambertian monoenergetic emission. The experimental data permitted an evaluation of the magnitude of the emission energies of the photoelectrons.

The experimental MTF data are plotted in Figure III-10 for various wavelengths of the exciting radiation. The plot is made on a log-log scale of the MTF versus a log scale of the spatial frequency. This was done after the manner of C. Bruce Johnson<sup>2</sup> because many types of MTF curves, when so plotted, result in straight lines. The calculated MTF is also shown in Figure III-10 for an arbitrary value of the emission energy. An effective emission energy may be arrived at by measuring the shift between the theoretical MTF and the experimental curve.

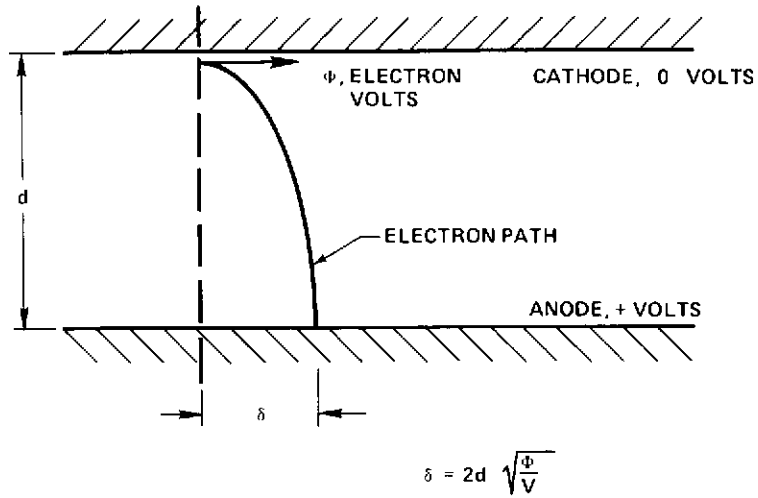


Figure III-9. Electron trajectories in a proximity section.

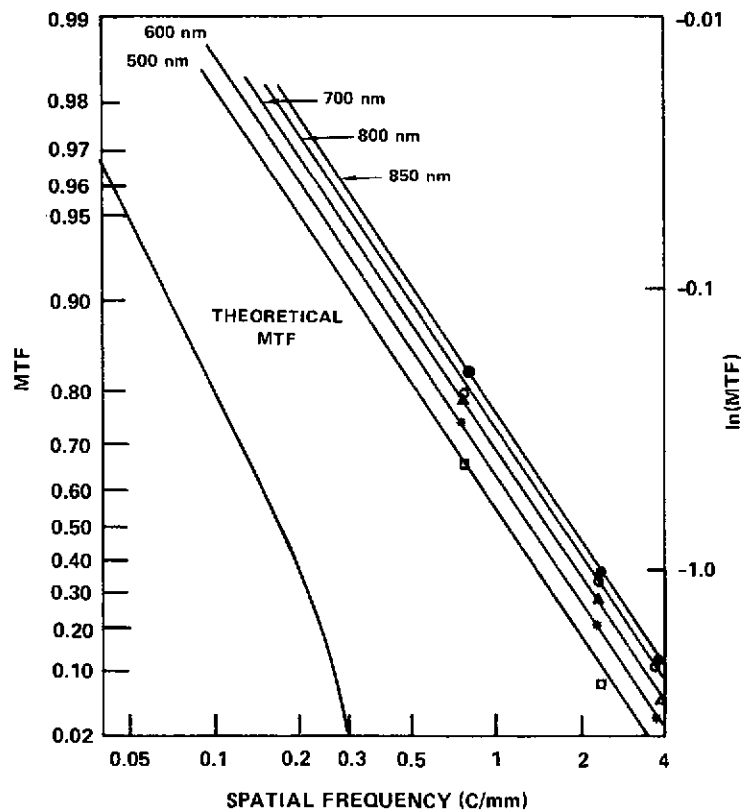


Figure III-10. MTF as a function of spatial frequency for the RCA C7002HA as a function of incident radiant energy at various wavelengths. The theoretical MTF curve is used to evaluate  $\Phi_e$ , the effective electron emission energy.

Figure III-11 shows the effective emission energy, as obtained from Figure III-10, as a function of the incident photon energy. The effective emission energy is surprisingly small even for high-energy incident photons. The limiting resolution, therefore, for a proximity-type image tube with a multi-alkali photocathode is somewhat better than anticipated.

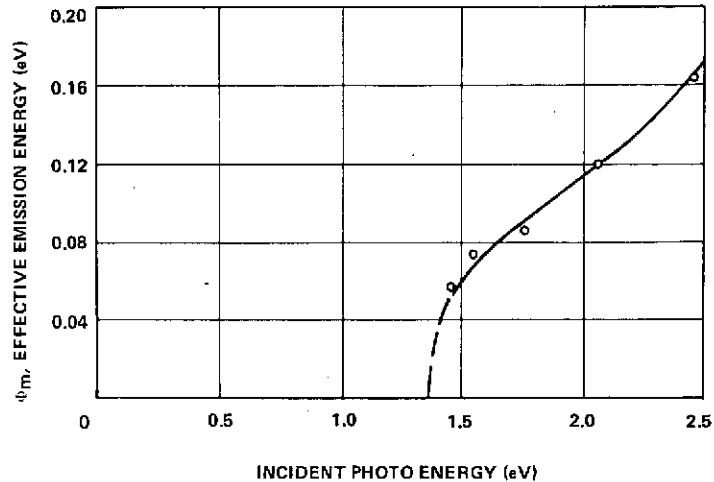


Figure III-11. Data on the maximum of the emission energy for a multi-alkali photocathode as a function of incident photo energy.

Figure III-12 shows an experimental verification of the prediction that the limiting spatial frequency in a proximity-type image tube varies inversely as the square root of the electron emission energy. The data were obtained from Figure III-10 taking a particular value of MTF of 0.3. (The result would be similar for a lower value of MTF.)

Measurements and theoretical estimates of the MTF for a proximity-focused image tube having an experimental GaAs photocathode are compared in Figure III-13. The lower theoretical curve was drawn assuming the emission energy to be 0.2 eV with Lambertian angular distribution. There is some reason to believe that for a negative-electron-affinity photocathode such as GaAs, the emission may be more forward-directed than a Lambertian distribution. Therefore, a fit to the experimental data was made assuming 0.2 eV and a 39-degree cone of emission.

The experimental data shown in Figure III-13 were obtained by correcting the resulted MTF measurement in a tube for both the MTF losses in the phosphor screen and in the fiber-optic element. The particular data used for this correction are shown in Figure III-14.

It is interesting that the MTF of a phosphor screen has been found to vary with the energy of the incident photoelectrons. This variation is shown in Figure III-15. The data were

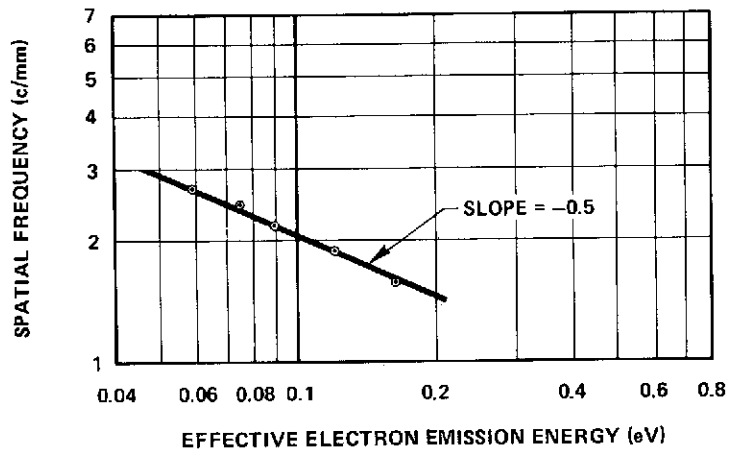


Figure III-12. Spatial frequency as a function of effective energy for an MTF of 0.3. Data from a C70021A used as a proximity-focused image tube.

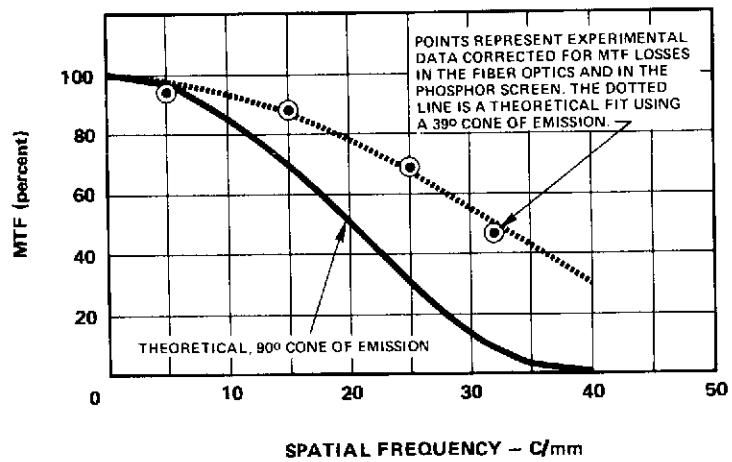


Figure III-13. MTF for a proximity-focused image section; 6 kV, 1.5-mm spacing; experimental GaAs photocathode.

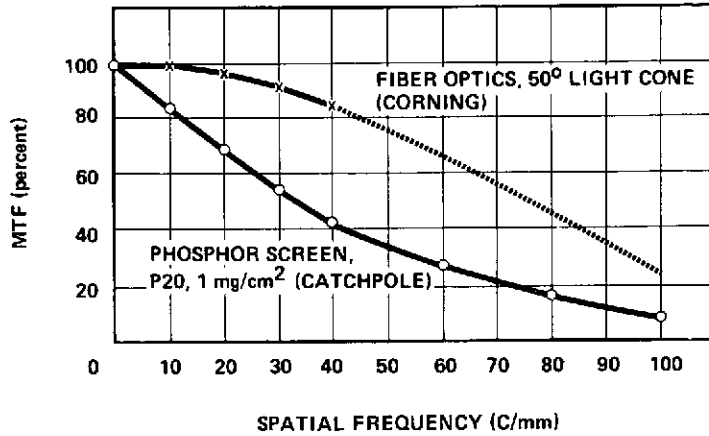


Figure III-14. MTF data for Corning fiber-optics and for a phosphor screen. (These were used in obtaining the data shown in Figure III-13.)

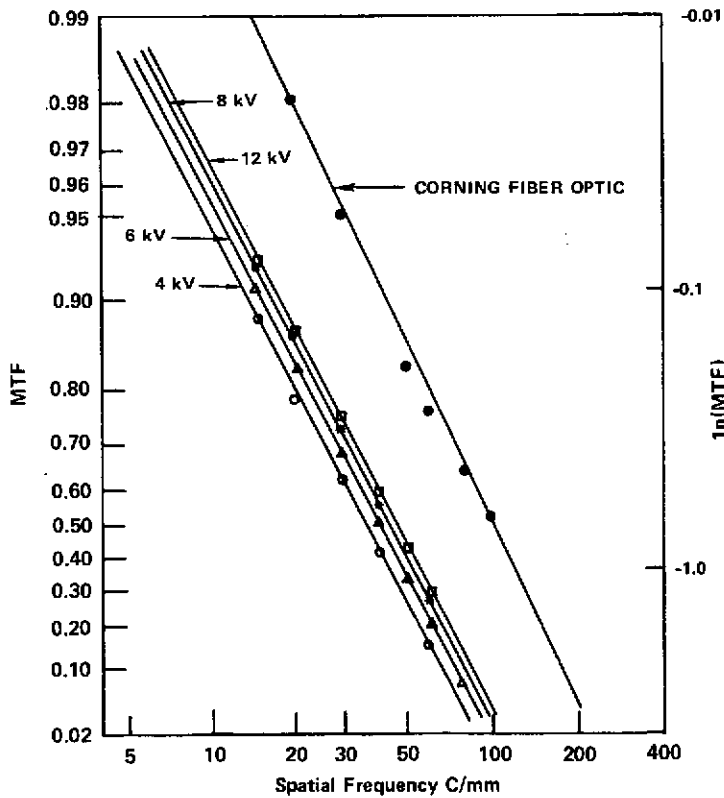


Figure III-15. MTFs of a Corning fiber-optic faceplate and a phosphor screen at various anode voltages.

obtained by fabricating a special experimental image tube having a thin nickel foil with a 2.5- $\mu\text{m}$  slit overlaying the phosphor screen.

For magnetically-focused image tubes, the electron optics do not appreciably limit the spatial response of the device. It can be shown<sup>3</sup> that the image of a point has a diameter of  $4 \phi/E$ , where  $E$  is the electric field strength, and  $\phi$  is the electron emission energy equivalent in volts. In a case of a magnetically-focused tube, the axial emission velocity causes the aberration. Because the limiting resolution is inversely proportional to the image spot diameter for a typical 200-V/mm case, the electron-optic limitation is of the order of 180 line pairs/mm. The limiting resolution of a magnetic image tube is generally set by the phosphor to about 80 line pairs/mm. For a 25-cm (10-in.) tube, which is about the largest that could be built today, the limiting resolution would be the equivalent of 40,000 TV lines.

In an electrostatic tube, the point image diameter is given by  $2 \phi/E$ , where the symbols have the same significance as discussed for the magnetic tube case. In the electrostatic case, both the axial and the radial emission velocities enter into the aberration. Again, it is only in special tubes that the electron optics are truly a limit to resolution. Usually it is the fiber optic and the phosphor screen that limit the resolution of an electrostatic image tube. However, for very large tubes or for the case of relatively low applied voltage, the electron-optic limitation can be significant. There can also be a limitation due to a mismatch of the phosphor and the electron-optic image surfaces.

To illustrate the limiting resolution caused by electron optics, the RCA Developmental Type C33114, the 80-mm zoom tube described above, was operated in the 1:1 mode at relatively low voltages. Limiting resolutions were measured as a function of voltage and are plotted in Figure III-16. It was found that the data were quite closely fitted by the expression given in the figure. This expression assumes that the resolution limitation is the quadrature sum of the combined fiber-optic and phosphor-screen limitation given in the first term and the electron-optic limitation given in the second term. Comparing this empirical relationship with the expression for minimum image point diameter indicates that the effective electron emission energy for the multi-alkali photocathode is of the order of 0.07 eV. (For the 80-mm tube operating at 12 kV, the electrostatic field at the photocathode was found to be 20 V/mm.) This value of  $\phi$  is not at odds with that shown in Figure III-11, especially considering that the radiation source was a tungsten lamp operating at a moderate temperature.

It is of interest that the limiting resolution of the 80-mm tube, as measured at the phosphor screen, was essentially the same at normal operating voltages when operated in the zoom mode (3:1 magnification) as in the 1:1 mode. Again, the limitation was principally that of the phosphor screen and the fiber-optic faceplate.

Most image tubes are not fundamentally limited in resolution by electron optics. The reason is that the variation in emission energies is very small compared to the electron energy

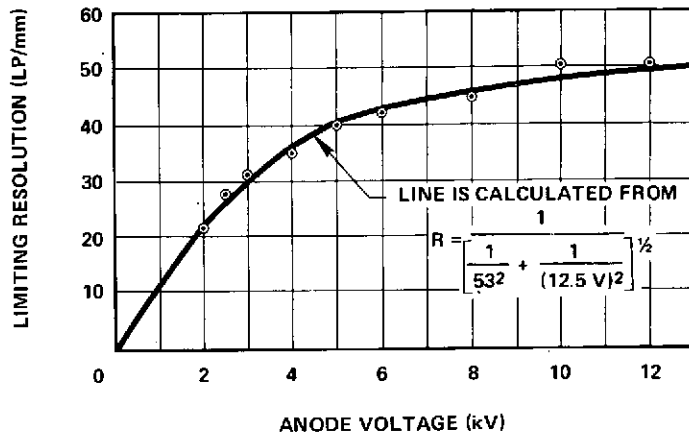


Figure III-16. Limiting resolution of 80-mm Type C33114, 1:1 magnification.

resulting from the applied voltage. Nonideal solutions to electron imaging can, of course, result in poor resolution due to field curvature and other distortions. Fiber-optic elements and phosphor screens are generally the principal limitations to resolution.

The exceptions to these conclusions are for "proximity-focused" image tubes and for focused-type image tubes operated at low voltages where the initial emission velocities of the electrons do, indeed, limit resolution.

I should like to make a plea for proper nomenclature with respect to various camera tubes. The name "vidicon" is now used by the entire industry, although at one time it was an RCA trade name. The defining feature that characterizes a tube as a vidicon is that it has a photoconductive target sensor. It may or may not have a target readout feature; the return-beam vidicon does not. An SEC tube is not a vidicon; it should be called an SEC camera tube. An SIT camera tube does have a target readout; it is not a vidicon.

## DISCUSSION

*W. E. SPICER:*

Was the multi-alkali photocathode, referred to in Figure III-11, an extended-red type?

*R. W. ENGSTROM:*

I cannot answer this question because spectral response measurements were not made. The tube was experimental and, although no attempt was made to process it for extended-red response, it could have had a nontypical S-20 response.

*S. GILBERT:*

Because of the potential for a compact detector package, a flat photocathode with an electrostatically focused detector package would be of great utility in astronomy. Has any progress been made in this area?

*R. W. ENGSTROM:*

My recommendation for obtaining a flat cathode with high resolution is to use an electromagnetic-type image tube. Plano-convex fiber-optic elements are usually used in electrostatic-type image tubes to present a flat field to the optical input and still provide the desired curved electron-optical surface for the photocathode surface. Many attempts have been made to provide a flat photocathode surface by electron-optical solution. I do not know of a good solution. Using a number of extra focus electrodes, some success has been achieved at the expense of distortions, which result in loss of resolution. I doubt that a really good solution to the problem can be found that will provide zoom capability in a relatively short tube.

*A. MEINEL:*

In Figure III-16, what is the modulation equivalent to "limiting resolution?"

*R. W. ENGSTROM:*

There is no standard value. Limiting resolution refers to the limit that can be perceived visually using a presentation such as with the standard Air Force tri-bar test pattern.

*M. GREEN:*

I was puzzled by your comments on the zoom tube. You said that whether it was operated in narrow angle or wide angle, the resolution at the output screen was essentially the same. In Figure III-6, where the zoom electrode is operated at only 1 kV compared with 12 kV in the 1:1 mode (Figure III-5), one would expect much poorer resolution.

*R. W. ENGSTROM:*

Two considerations apply here. In the first place, the 1:1 mode is primarily limited by the phosphor and the fiber optics, not by the electron optics. Secondly, in the demagnification mode, the second lens comes into play reducing the image size and, proportionally, the aberration diameter. (Post-Symposium comment: At lower applied voltages, where the phosphor and fiber optics are not the dominant factors, there is a loss in resolution in the demagnification mode as expected.)

*J. A. WESTPHAL:*

It is deceptive that RCA data sheets for Silicon Intensifier Target (SIT) tubes show standard S-20 spectral response characteristics, when actually the tubes have fiber-optic faceplates that severely limit the short-wavelength response.

*R. W. ENGSTROM:*

I will call this to the attention of our Application Engineering group. (Post-Symposium comment: The problem had been recognized already; the latest data sheets reflect the proper spectral response.)

## REFERENCES

1. P. Schagen, H. Bruining, and J. C. Francken. "A Simple Electrostatic Electron-Optical System with Only One Voltage." *Philips Res. Rept.* 7, 1952. p. 119.
2. C. B. Johnson. "A Method for Characterizing Electro-Optical Device Modulation Transfer Functions." *Photographic Science and Engineering.* 14. No 6. November-December 1970.
3. O. Klemperer. *Electron Optics.* Cambridge. 1971.

#### IV. IMAGE RECORDING USING CHARGE-COUPLED DEVICES

*C. H. Sequin  
Bell Laboratories  
Holmdel, New Jersey*

The type of imaging detector I am going to talk about is still very new. Charge-coupled devices (CCDs) were invented only about three years ago,<sup>1</sup> but since then they have shown tremendous growth, and the momentum of that development will eventually carry these devices a long way beyond what has been achieved to date. I would like to begin with a review of the principle of charge coupling and discuss some performance limitations. I will then show the results obtained on a practical device before leading over to a discussion, with some extrapolations, about the future of charge-coupled devices.

The basic element of a charge-coupled device as shown in Figure IV-1 is the MIS capacitor.

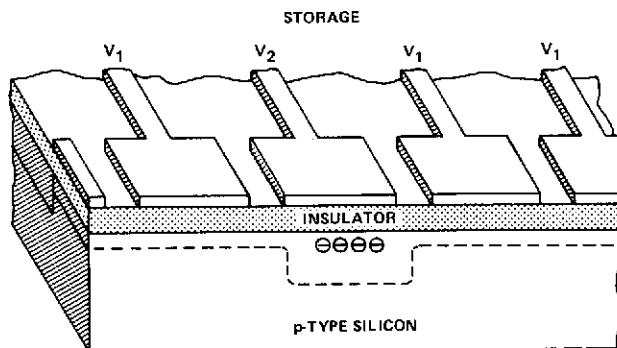


Figure IV-1. CCD: Storage mode.

It consists of a metal electrode and a thin insulator on top of a semiconductor crystal. In the Bell Laboratories' devices, we have typically used p-type silicon, 150 nm of oxide, and, for instance, tungsten electrodes. If a positive voltage is applied to the metal electrode, a potential well is formed underneath in the silicon, which is at first depleted of charge carriers. This, however, is not a stable situation. Thermally generated electrons will be swept towards the surface and eventually fill up the whole potential well.

The time it takes to reach that thermal equilibrium is called the storage time or thermal relaxation time. In a good MIS system this can take more than 10 s. For short time intervals, compared to this relaxation time, such an arrangement can serve as a memory cell for analog information, in which the information is represented by the charge contained in the potential well. The charge can be injected electrically or it can be generated by light.

A CCD now consists of a whole row of such MIS capacitors. They are so closely spaced that the potential wells underneath overlap as shown in Figure IV-2. Typically the gaps are on the order of a few microns.

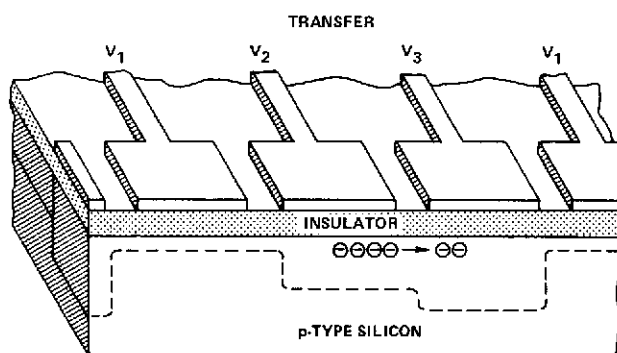


Figure IV-2. CCD: Transfer mode.

Such an arrangement can transfer charge along the insulator-semiconductor interface. To transfer a charge packet one step to the right we apply an even higher voltage to the next electrode. This creates an even deeper potential well underneath, into which the charge starts to flow. The voltage on the first electrode is then reduced to restore the original condition. To continue the motion of the charge packet along the surface, the transfer electrodes are interconnected into three independent electrode systems. Figure IV-3 illustrates such a configuration. There are three electrode systems,  $P_1$ ,  $P_2$ ,  $P_3$ . At least three independent systems are needed if we use these simple electrodes in order to define the directionality of the charge transfer. There are some other schemes which use only two electrode systems, but they have the directionality built into each potential well<sup>2</sup> either by means of a step in the oxide thickness or by a localized ion-implanted barrier. But today, I restrict myself to three-phase structures.

In Figure IV-3, electrodes  $P_2$  are biased to create a potential well underneath that can store a packet of charge. If we pulse these three sets of electrodes properly then these potential

wells will move to the right and carry along with them the charge that is contained in them. To detect these charge packets, an  $n^+$  diffusion has been used. This output diode is reversed biased by an external resistor. The arriving charge packets generate a current through this resistor, and voltage pulses at the output. Normally, an additional gate electrode is introduced to serve as an electrostatic shield and thereby reduce the pickup from the pulsed electrodes by the output diode. The same kind of arrangement can also serve as an electrical input on the other end of the device and one would then have an analog shift register.<sup>3</sup>

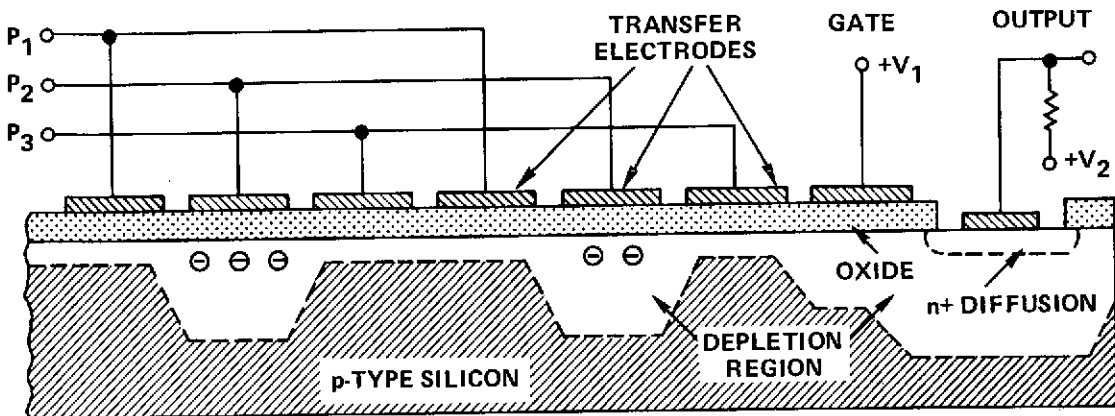
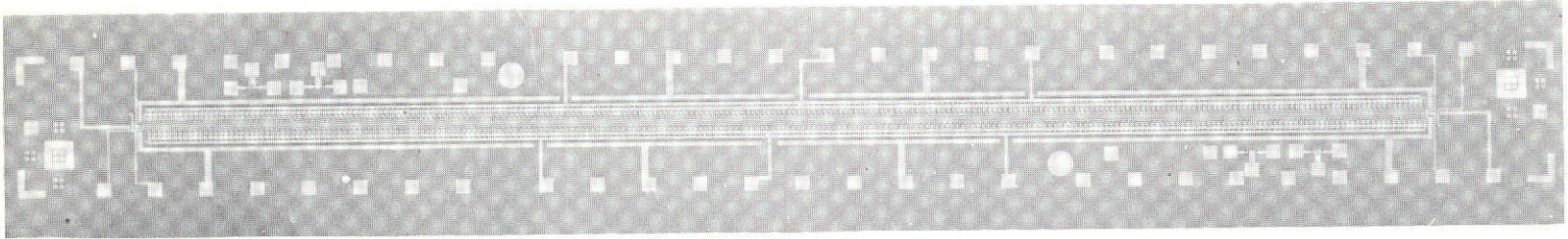


Figure IV-3. Schematic operation of a CCD.

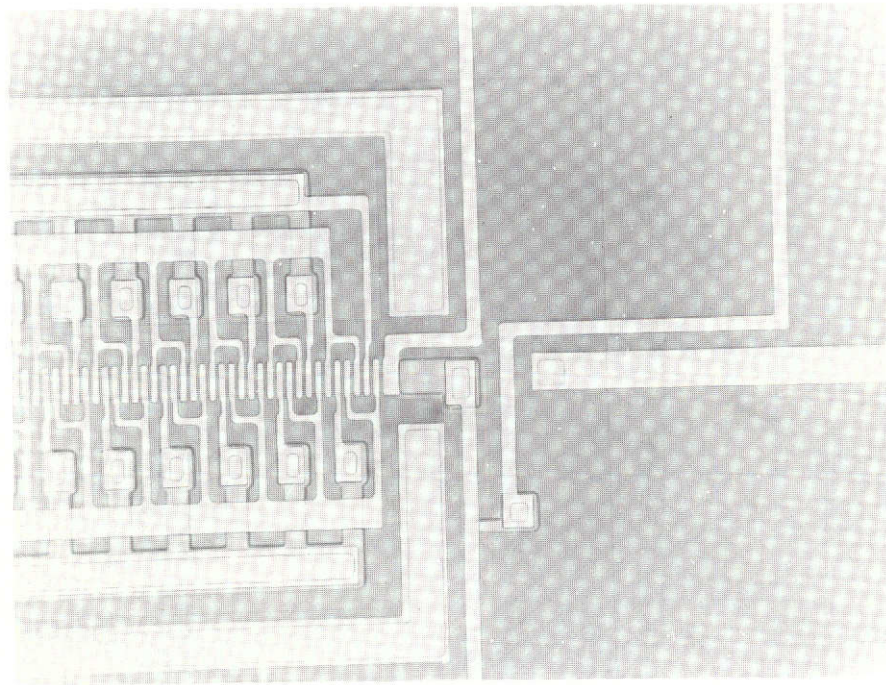
Because we are interested in imaging, let us consider an optical input. Light coming in from either the front side through the gaps between the electrodes or from the back side of the thinned Si-substrate creates hole-electron pairs in the silicon. The holes recombine in the p-type silicon bulk. The electrons travel to the nearest potential well. After a suitable integration time, a charge pattern is formed that represents the image focused onto the device. Pulsing the electrodes initiates readout of the information in serial form.

An actual CCD is shown in Figure IV-4a. It is a linear structure with 1500 electrodes.<sup>4</sup> The transfer electrodes are 3- $\mu\text{m}$  gaps. The complete cell shown in Figure IV-4b comprising three electrodes is 18- $\mu\text{m}$  long. The whole device is about 1 cm long, and it indeed transfers charge from one end to the other.

We have operated that device as an analog shift register<sup>3</sup> as well as a line imaging device.<sup>4</sup> In both modes some signal degradation due to transfer inefficiency was found. Each time a charge packet is transferred from one potential well to the next, a little bit of charge is left behind. This effect is cumulative, so it can lead to substantial signal degradation.



(a)



(b)

Figure IV-4. Actual CCD: (a) linear structure and (b) complete cell.

Figure IV-5 illustrates what happens to a single charge package as it travels down CCDs of varying performance. Each rectangular frame represents the output from a charge-coupled device with a different performance, as, for instance, that seen on an oscilloscope. The first box represents the ideal case. A single-charge packet comes out in a single time slot after the

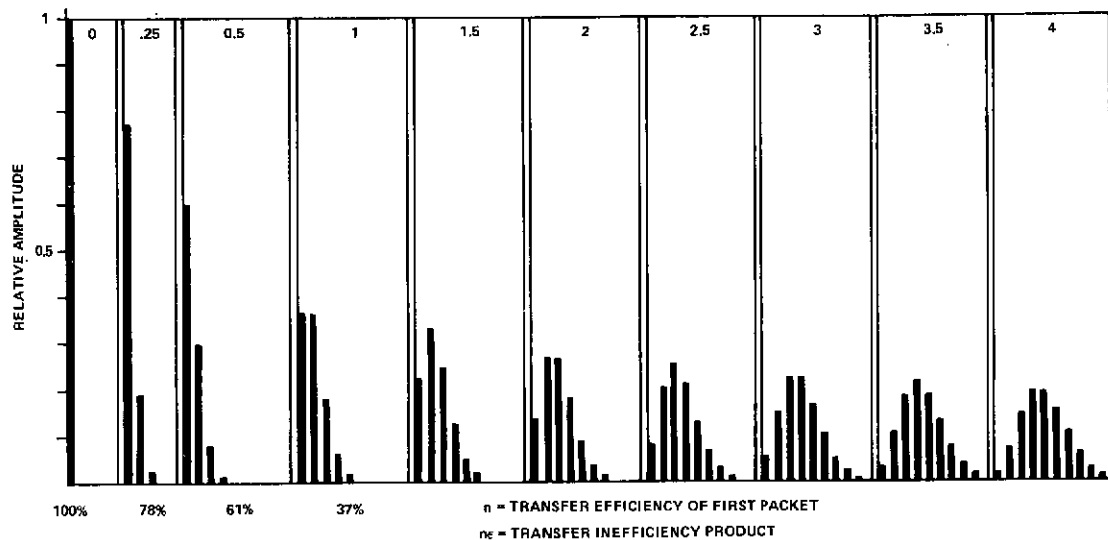


Figure IV-5. Signal redistribution as a function of transfer inefficiency.

proper delay, given by the number of transfers and the clock frequency. In real devices, however, not all the charge reaches the output at the prescribed time. The rest of the charge lags behind and comes out in the following time slots.

Originally, the fraction of charge in the leading station was used to define an overall transfer efficiency.<sup>5</sup> However, in long devices the degradation can be so strong that the leading station no longer carries the maximum amount of charge. It is then more practical to define an inefficiency product,  $ne$ , in which  $n$  denotes the number of transfers and  $\epsilon$  the fractional loss of charge in each transfer.<sup>6</sup> This expression has no limitations, and it increases linearly with the length of a uniform device.

Figure IV-6 shows the degradation experienced by sine waves. The sine wave signal frequency is normalized with respect to the spatial period of the elements of our CCD. A CCD carries the charge along in a discrete number of potential wells. It is therefore a sampling system. From Nyquist's theorem we know that a sampling system can handle only frequencies up to half the sampling rate.<sup>7</sup> That is why the  $x$ -axis ends at a value of 0.5.

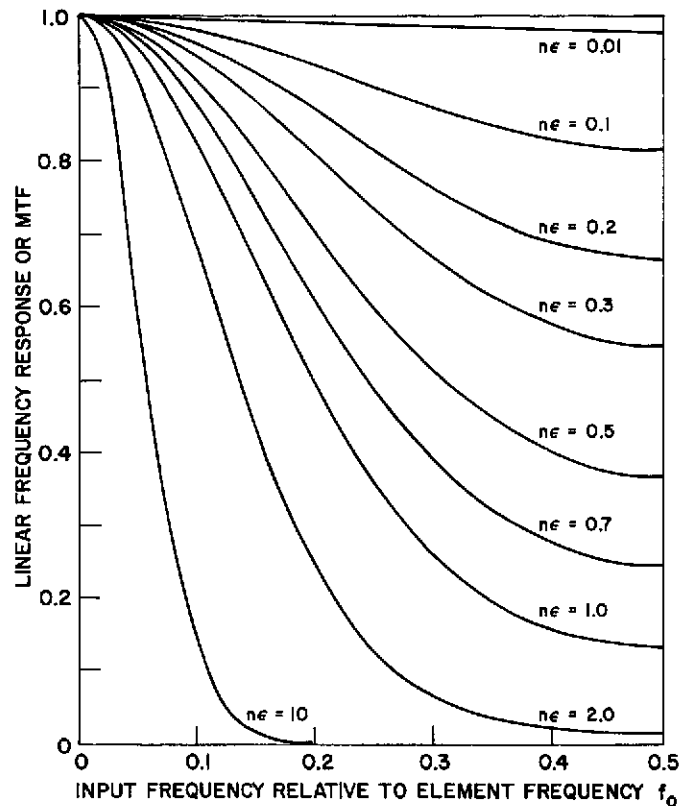


Figure IV-6. Frequency response or MTF of a CCD with an overall transfer inefficiency of  $n\epsilon$ .

The curves in Figure IV-6 show the attenuation of sine waves as a function of frequency for different inefficiency products. I would like to point out as a reference value, that, for an inefficiency product of 0.3, the strongest degradation of the modulation transfer function is about 50 percent. This is about the limit of acceptable performance.

Where does this transfer inefficiency come from? A variety of mechanisms exist. I will only talk about one of them: the capture of charge by interface states.<sup>8</sup> Along the oxide-semiconductor interface there are states that capture an electron as soon as they come in contact with one of the charge packets. If in Figure IV-7 a charge packet resides in the potential well, all the interface states underneath the third electrode would be immediately filled. As the charge packet moves along, the electrons are released again but at much slower rates. In the previous time slot, the charge packet has been underneath the second electrode; so, all the interface states there have been filled and are now releasing their charge again. If the carriers are released early enough, then they will still join their proper charge packet. However, if they are released more than a time slot later, as the arrows under the first electrode of Figure IV-7 indicate, then they can join the next packet. This represents a direct loss of charge from one charge packet to the next one. Fortunately, each packet also gets a contribution from the previous charge packet. But if the previous potential well has been emptied completely, then the interface states have no chance to get filled in the previous time slot, and the contribution from there would be zero.

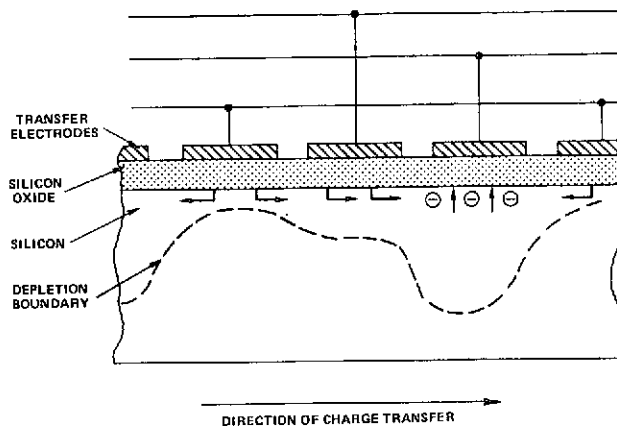


Figure IV-7. Schematic representation of charge loss due to captures in interface states.

This brings us to the concept of “background charge” or “fat zero”.<sup>5</sup> The CCD should never be operated with a completely empty potential well; at least about 20 percent of charge should be kept in each well so that the interface states will get filled. Then loss and gain in each transfer can cancel out in first order. The difference between the two contributions that can be achieved with that method is a fraction on the order of  $10^{-4}$  of a full potential well. That corresponds to the measured  $\epsilon$  value. However, the absolute magnitude of each contribution is on the order of  $10^{-3}$ , and since it is a statistical amount, it will fluctuate and thus represent a possible noise source.<sup>9</sup>

These are some of the basic facts we have to live with. Now I examine how to make an actual imaging device.

Figure IV-8 shows the basic principle we have used to make a two-dimensional charge-coupled imaging device. It is essentially a gigantic linear CCD running in the vertical direction. However, its transfer region is subdivided with stripes of a channel stopping diffusion into several parallel lanes running in the vertical direction. All these lanes are driven by the same electrodes running horizontally across the whole structure. At the lower end of this array lies a single-channel CCD running in the horizontal direction and ending in the output diode.

In our application for live TV pictures, only half of this device is used as an actual image sensor. The picture is projected on the top half only and is integrated there. Then the whole charge pattern is transferred quickly to the lower half of the device. One must do that in order to avoid optical smearing. If a frame is read too slowly, then the continuously incident light would superimpose a smeared picture.

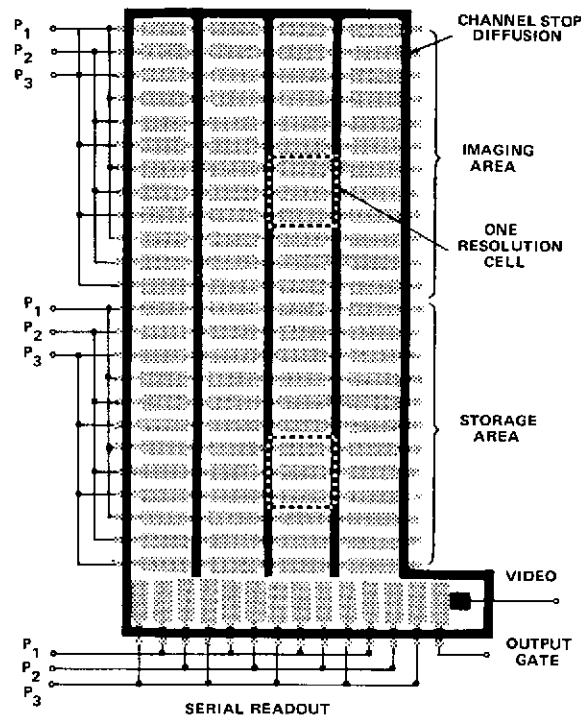


Figure IV-8. Charge-coupled area imaging device frame transfer principle.

In applications where one can live with low frame rates and where the integration time can be made much longer than the readout time, the full array can be used. In a space telescope the picture would be projected onto the whole array. One of the electrode systems, for example,  $P_2$ , would be held at the high voltage. This creates the potential wells in which the incident light generates a representative charge pattern. When sufficient charge has been accumulated, we pulse the entire array and shift the whole charge pattern down one line. The lowest line then enters the readout register. A clock pulses the serial readout register

and readout of this line occurs in serial form. The process is repeated. The next line is shifted into the readout register and read out, and so on, until the whole array is read out.

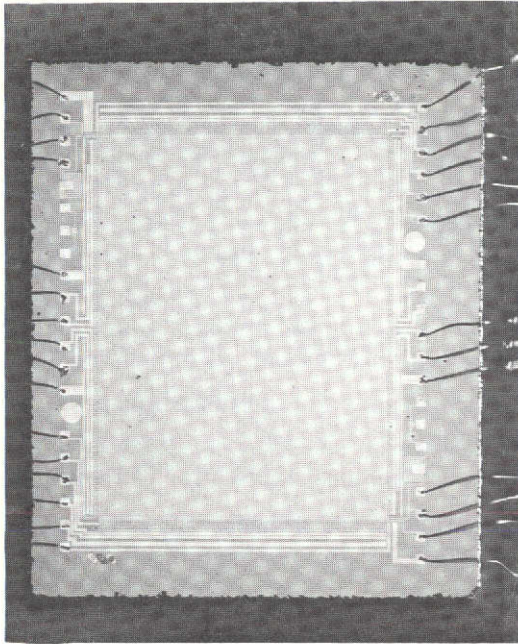
There are several possible approaches to make a two-dimensional charge-coupled area-imaging device. We have chosen this "frame transfer" approach because it has a very simple resolution cell.<sup>5</sup> It needs only a little amount of peripheral logic to drive the device. It has a very small output diode, with a very small output capacitance, and it promises good signal-to-noise ratio. Furthermore, the pickup from the pulsed electrodes at the output diode is very uniform so that it can easily be filtered out or subtracted. Figure IV-9a shows our latest device of this type.<sup>10</sup> Here there are actually 106 vertical columns at a spatial pitch of 30  $\mu\text{m}$ . In the vertical directions there are 128 triplets of electrodes. Each electrode is 9  $\mu\text{m}$  long and separated from the next one by a 2- $\mu\text{m}$  gap. The metalization pattern is very critical. For example, as illustrated in Figure IV-9b there are over 41,000 transfer pads in the device. The total length of narrow gaps in between is more than 1 m and there must not be a single short in that pattern, because it would make the device inoperable. In our case, we have used a tungsten metalization. With about 150 nm of tungsten, we have obtained good results in pattern definition and metal etching. The main problem was to get a defect-free set of photolithographic masks. Figure IV-9c shows the actual device. It is a small chip of silicon of about 3.5 by 5 mm, which is mounted on a ceramic substrate for easy handling. Not all the 30 leads are really used to operate the device in the imaging mode. Some of them are redundant, and some are for test purposes only.

The described device can produce a picture of the quality shown in Figure IV-10. This picture was taken at an element readout rate of 1 MHz and at 15 frames/s.<sup>10</sup> The integration-to-readout duty cycle was only three to one, but still, you cannot see optical smearing.

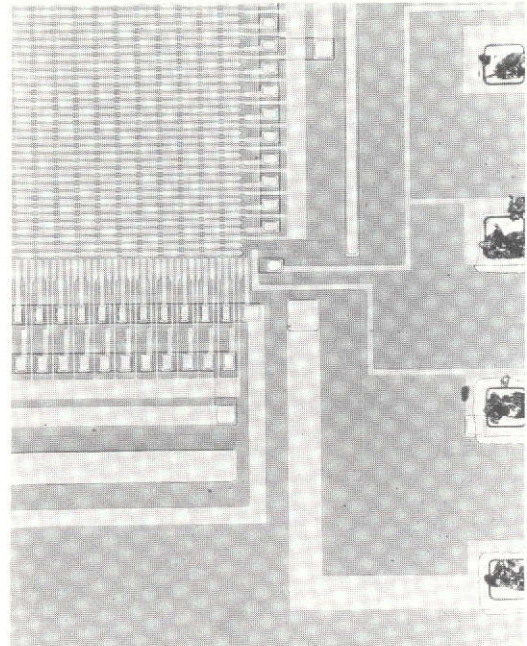
The uniform part of the dark current is on the order of 10-nA-cm<sup>-2</sup>. However, there are some localized current sources that are much stronger. These white video defects are nothing new. They are well known from the construction of the silicon-diode array target.<sup>11</sup> Gettering procedures have been developed that have essentially eliminated these defects from the diode array target, and we are pretty confident that the same gettering procedures will also eliminate the white video defects from charge-coupled devices.

However, there are some types of defects to worry about. One is the black bar seen at the bottom of Figure IV-10. It is produced by a blockage in one of the vertical-transfer channels.<sup>10</sup> Since no charge from behind that blockage can reach the output, which with respect to Figure IV-10 is in the upper lefthand corner, the area behind appears black.

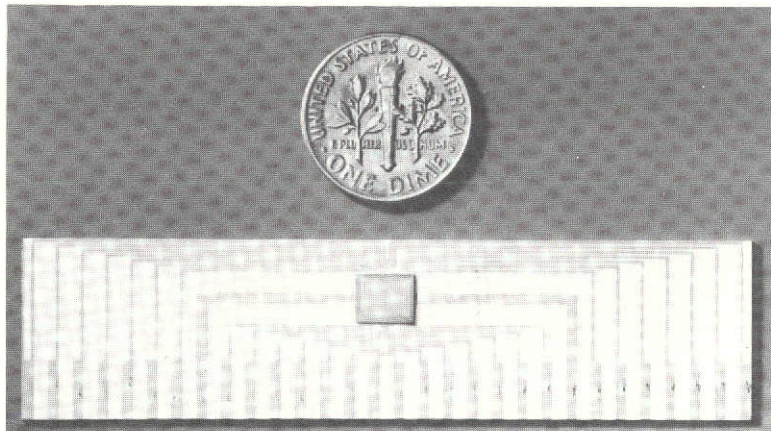
A second problem is transfer inefficiency. The picture looks blurred due to loss of resolution. A reasonable goal is that the inefficiency products,  $\eta_e$ , in the vertical direction and in the readout register be independently less than 0.3. On the other hand, one does not have to worry about lag. In these structures, all the charge from the imaging area is completely read out in each frame.



(a)



(b)



(c)

Figure IV-9. Two-dimensional charge-coupled area imaging device: (a) resolution cell; (b) transfer pads; and (c) actual device.



Figure IV-10. Picture produced by the two-dimensional charge-coupled area imaging device.

I would like to conclude this presentation by extrapolating the current results into the future. I would like to consider the question: Is it possible to build a device with 1000 by 1000 elements?

First of all, can one obtain the required transfer efficiency? Fractional losses of about  $10^{-4}$  per transfer have been achieved already. In a three-phase structure with 1000 elements, this would lead to an inefficiency product of 0.3; this is just sufficient for acceptable performance.

For how long can we integrate a picture? The storage time of a single MIS capacitor can be made greater than 10 s. Even longer storage times can be achieved if the device is cooled. This applies also to the storage time of an actual CCD. The experiment has been performed, and the dark current has been seen to be reduced by about a factor of two for every 9 degrees when the device is cooled. Extrapolation then tells us that for a device at about 200 K, we can expect storage times of more than an hour.

The single-resolution cell of such a CCD is on the order of  $30\ \mu\text{m}$  by  $30\ \mu\text{m}$ . This size cannot be reduced very much because one would lose resolution due to the diffusion of the carriers

in the bulk silicon. This means that a device with 1000 by 1000 elements actually covers 9 cm<sup>2</sup> of active area, and this is a very large-scale integrated circuit!

The question is: Can such a device ever be made? I make a very optimistic projection here: Using a defect density of only one defect per cm<sup>2</sup>, which can just about be achieved in thermally growing a simple layer of silicon dioxide, and assuming the same low defect count in all four major photolithographic levels required to make the simplest version of such a device, we would get a projected yield of only 2.8 percent.

Nevertheless, our latest device has 13,000 elements already. And as an average over the last two years, the number of elements has increased by a factor of 10 in every 10 months. Obviously, this trend has to slow down! But, we have found no basic limitations that would rule out the construction of a charge-coupled area-image sensor with 1000 by 1000 elements. These extrapolations are:

Achieved	Projected
$\epsilon < 10^{-4}$	→ $N \epsilon \approx 0.3$ for 1000 Elements
$\tau_s > 10$ s	→ $\tau_s > 1$ h at 200 K
$30\mu\text{m} \times 30\mu\text{m}$	→ 9-cm <sup>2</sup> Active Area
1 Defect/cm <sup>2</sup>	→ Yield: 2.8 percent
106 × 128 Elements	→ 1000 × 1000 Possible in the Future

## DISCUSSION

*E. J. WAMPLER:*

Can the CCDs be operated in a mode to detect electrons as well as photons, and if so, can single electrons be detected?

*C. H. SEQUIN:*

Yes, to the first part, and it depends upon on how many carriers are generated per electron for the second part.

*E. J. WESTPHAL:*

Twenty-eight hundred carries per 10 kV electron in silicon.

*C. H. SEQUIN:*

Then, I think, you could detect even the single electron.

*S. DUCKETT:*

I would like to review this. According to what you said before, it was advantageous to have a small number of carriers in each well, a loading of 10 percent or so, and it is a fluctuation of this number that limits you to the smallest charge pulse of electrons that can be detected. Are you now saying that  $2800^{0.5}$ , is that number of electrons?

*C. H. SEQUIN:*

I'm sorry, I am not a specialist in low-light-level applications, so I don't really know what the limit is here. CCDs are very advantageous because the output diode is only a small localized diffusion and the capacitance of that diode can be on the order of tenths of a pF, especially if one would integrate the amplifier right at the output of the device. If you compare that with the capacitance of a diode array target, which may be on the order of 25 pF, you gain more than a factor of 100 in capacitance and that promises, directly, a gain of more than a factor of 10 in signal-to-noise ratio. From that point of view, CCDs look advantageous, and the number of electrons you can detect should be more than a factor of 10 smaller as compared to a silicon-diode array target.

*A. MEINEL:*

I have a few questions here. One is: Can you clarify what is the light-sensitive area if you talk about the gap and the electrode? Is the gap the sensitive area, the electrode, or both? We are concerned about the loss of photons in a non-operating area of the image.

*C. H. SEQUIN:*

In our present device, we have a tungsten metalization, and we shine the light onto the front surface. Since we have narrow gaps, they are the only place where the light enters. The electrodes are on the front surface, and we shine the light onto the electrode side. Only the part of the light that goes through the gaps into the silicon is actually active.

*A. MEINEL:*

Then, only two-ninths of the photons are used?

*C. H. SEQUIN:*

Yes. We throw three-quarters of our light away. It is clear that we cannot live with that, not even for TV applications. There are two ways around it. Either we use transparent electrodes, a possible contender is poly-silicon, or bring in the light from the backside. We then have to thin down our device just the way we do it in the silicon-diode array target. To keep good resolution in the visible, we thin the substrate down to about 20  $\mu\text{m}$ . Shining the light onto the backside, we can get a quantum efficiency that is very close to one. And that's the way to go in the future. Technologically, it is a little more difficult, so we haven't yet tried it.

*A. MEINEL:*

The second question is: Aren't we into some bandwidth problems in trying to reach 1000 by 1000 elements? What's your recycle time, in other words? In some applications 13,000 elements may be needed.

*C. H. SEQUIN:*

We normally read out our devices at a rate of 1 MHz. So 13,000 elements would be read out in 12 ms, a value that would be compatible with the 16-ms frame time of commercial TV. These devices can easily be designed so that they can operate up to about 4 MHz. To readout 1000 by 1000 elements would then take a fourth of a second.

*A. MEINEL:*

The third area is the sensitivity to defects that is reflected as sensitivity to cosmic rays especially. Can you comment about the sensitivity of the CCD to such problems.

*C. H. SEQUIN:*

The kind of damage that a high-energy particle creates is not a killing defect. Instead, they create interface states. The more interface states you get, the more the described capture of carriers will play a significant role. My thesis was a study of the interface states in MOS transistors, which are introduced by gamma radiation. From that work I remember some numbers: A dose of  $10^{16}$  1 MeV photons  $\text{cm}^{-2}$  increased the interface state density from  $10^{10}$  to  $10^{12}$   $\text{cm}^{-2}$ . And I am pretty convinced that a CCD with an interface state density of  $10^{12}$   $\text{cm}^{-2}$  would not work properly. From that I would assume that  $10^{16}$  high-speed electrons/ $\text{cm}^2$  would kill the device. Neutrons and other heavy particles might be even more damaging since they seem to produce defect clusters.

*B. RUBIN:*

In this discussion you had limited yourself to visible imaging. Is there any hope of extending the use of the CCDs into the IR using this technology or this technique?

*C. H. SEQUIN:*

The CCDs so far have all been made of silicon, and thus they have the absorption properties of Si. There are some studies going on with GaAs, but that does not improve the situation for IR radiation.

Let me add one more thing. One could think of making a CCD in a material that has a smaller energy gap. But the problem is that a CCD needs a very good interface between the insulator and the semiconductor. So far, that has only been achieved reliably in the system Si-SiO<sub>2</sub>.

*C. B. JOHNSON:*

If the possibility of using high-energy photoelectrons to produce hole-electron pairs in CCDs can be developed, then the range can be extended well into the vacuum ultraviolet and somewhat into the near infrared (to about 1100 nm).

*W. E. SPICER:*

In the photon detection mode, how many photons would be required per element to produce a usable signal? Would it be like  $10^2$  or  $10^5$ ?

*C. H. SEQUIN:*

The linear structure shown in Figure IV-3 had about  $10^5$  electrons in a full bucket, and this number was very easy to detect. We used an amplifier made of discrete components, and we had no problem detecting that signal with many gray levels. I would say we had at least 20 gray levels. From that I estimate that a packet of 1000 electrons can be detected. I do not dare to extrapolate how much further down this limit can be pushed.

*M. GREEN:*

I wonder if you could convert your transfer efficiency that you have given,  $\epsilon = 0.3$ , into a modulation transfer for 1000-element devices?

*C. H. SEQUIN:*

I would like to refer back to Figure IV-6, which shows a group of MTF curves. The value of 0.3 for the inefficiency product causes a modulation transfer function that starts at 100 percent for a dc value, then drops monotonically and ends at a value of 50 percent for the highest signal frequency corresponding to the Nyquist limit. At the highest signal frequency the signal amplitude for the elements farthest away from the output diode would be reduced to 50 percent.

*N. G. ROMAN:*

Was that for one 1000 elements squared or 1000 elements total?

*C. H. SEQUIN:*

The inefficiency product represents the overall performance of the device, regardless of how it is achieved. You can either have 1000 very good elements or 10 very bad elements. The MTF curves shown are normalized to that overall inefficiency product.

*N. G. ROMAN:*

How long do you think it will be before such a device with 50 percent recording of the highest frequency and 1000 elements can be built?

*C. H. SEQUIN:*

I expected that question. I worried a long time about what I should say. If we extrapolate our growth curves we would have it next year, but I can assure you we will *not* have it next year! I estimate that if somebody really puts his will to it—and the money—about 4 years from now you could have your device.

*J. L. LOWRANCE:*

Do you expect to have the 128- by 406-element device in operation by next year and not just as a laboratory device?

*C. H. SEQUIN:*

Well, Bell Laboratories does not sell semiconductor devices, so we will not produce this device and sell it. But we are continuing our studies. We are working on a device that is twice as large. The momentum is carrying on.

*E. EBERHARDT:*

You just gave a number of  $10^5$  electrons per full bucket. How is this to dynamic range?

*C. H. SEQUIN:*

That is another area where I lack experience. The dynamic range depends not only on the performance of the pre-amplifier but also on the stability of the background charge. If you could inject exactly the same amount of charge into each potential well, it would only control the dc level without impairing the dynamic range. A lot depends therefore, on your input/output circuitry, and I cannot make a prediction of the ultimate limit.

For an application in the space telescope, the goal would be to make your system so perfect that the fluctuations are finally determined by the shot noise of the incident photons.

*A. MEINEL:*

Is not the smallest charge per bucket that can be measured approximately  $10^3$  electrons? That would indicate a rather small dynamic range of approximately  $10^2$  if it is  $10^5$  for the full bucket.

*C. H. SEQUIN:*

The number  $10^5$  applies to a device that has a relatively small bucket. The electrodes in our linear device were only  $3\ \mu\text{m}$  long, and the channel was  $15\ \mu\text{m}$  wide. In our latest devices the electrodes are longer, and the insulator is thinner. This produces buckets that can handle an order of magnitude more charge. The sensitivity limit would essentially be given by the output circuitry, so it would be an absolute value.

*A. MEINEL:*

The problem will be whether one can generate on the order of 1000 electrons per single photon event. The number may be closer to 20.

*K. HALLAM:*

This assumes that a photocathode precedes the CCD.

*C. H. SEQUIN:*

Charge-coupled devices are more sensitive than the diode array target; but, they are not that much more sensitive that you could use them directly and get the full range, starting at the detection of single photons. For that, amplification by a photocathode is required.

*S. DUCKETT:*

Part of the reason that the resolution deteriorates has to do with the phase lag, in that the electrons don't all go into the same bucket. They are three or four buckets behind. It seems to me that, if one were to consider a spot image or perhaps a single photon where a photoelectron from the cathode is accelerated into the CCD array producing approximately  $10^4$  electrons, the resolution would in real fact be greater than you say. By interrogating the buckets as they went by, one could get some idea where the particle, this pulse, actually hit the target. The ability to pinpoint the origin of an incoming particle is better than that which you could calculate from your resolution or transfer function.

*C. H. SEQUIN:*

There are two things to say here. For an inefficiency product of 0.3, the second box in Figure IV-5, showing the degradation experienced by a single charge packet, applies. One obtains about 78 percent of the charge in the leading station, maybe 15 percent in the second, and the rest in the following stations. If you just ask a yes/no question, it is easy to discriminate, and you could actually tolerate an inefficiency product up to approximately 0.5. As long as the leading station still carries more than 50 percent, it is easy to get the proper discrimination.

If you know you have a bad device, you could use more sophisticated techniques to reconstruct the original image. If you know what the inefficiency product is, you could feed the output signal through an analog circuit or even a little computer that reshapes the original signal form, using the calculated functional degradation shown in Figure IV-5. Then you could discriminate for binary information even with inefficiency products of two or three.

## REFERENCES

1. W.S. Boyle and G.E. Smith. "Charge Coupled Semiconductor Devices." *Bell System Tech. J.* **49**. 1970. pp. 587-593
2. D. Kahng and E.H. Nicollian. U.S. Patent No. 3651349.
3. M.F. Tompsett and E.J. Zimany. "Use of Charge-Coupled Devices for Analog Delay." *ISSCC Digest 1972*. 1972. pp. 136-137.
4. W. J. Bertram, D.A. Sealer, C.H. Sequin, M.F. Tompsett, and R.R. Buckley. "Recent Advances in Charge Coupled Imaging Devices." *INTERCON Digest 1972*. 1972. pp. 292-293.
5. M.F. Tompsett, G.F. Amelio, W.J. Bertram, R.R. Buckley, W.J. McNamara, J.C. Mikkelsen and D. A. Sealer. "Charge Coupled Imaging Devices: Experimental Results." *IEEE Trans. Electron Devices*. **ED-18**. 1971. pp. 992-996.
6. W.B. Joyce and W.J. Bertram. "Linearized Dispersion Relation and Green's Function for Discrete-Charge-Transfer Devices with Incomplete Transfer." *Bell System Tech. J.* **50**. 1971. pp. 1741-1759.
7. R. Bracewell. *The Fourier Transform and Its Applications*. McGraw-Hill, 1965.
8. M.F. Tompsett. "The Quantitative Effects of Interface States on the Performance of CCDs." to be published by *IEEE Trans. Electron Devices*.
9. K.K. Thornber and M.F. Tompsett. "Spectral Density of Noise Generated in Charge Transfer Devices." to be published by *IEEE Trans. Electron Devices*.
10. C.H. Sequin, D.A. Sealer, W.J. Bertram, M.F. Tompsett, R.R. Buckley, T.A. Shankoff, and W. J. McNamara. "A Charge Coupled Area Image Sensor and Frame Store." to be published by *IEEE Trans. Electron Devices*.
11. A.J.R. de Kock. "Vacancy Clusters in Dislocation-Free Silicon." *Applied Phys. Lett.* **16**. 1970. pp. 100-102.

## V. THE ELECTROSTATIC STORAGE TUBE

*R. E. Rutherford, Jr.  
CBS Laboratories  
Stamford, Connecticut*

At CBS Laboratories, we have been working on a system called an electrostatic camera, which is based on the electrostatic storage tube. It is a video system based on a photoelectric image storing dielectric target device with secondary emission readout. The device being developed is based on a study of the limitations of the existing camera devices of the general type used for television.

The study led to a series of experiments with materials and techniques that indicated the practical feasibility of a device that offers significantly improved performance over the currently available devices. The device could approach the ultimate response limit for specialized scientific applications.

The approach to the high-performance camera that is being followed in this development is to convert the input image to an electron image at low loss, to apply a low noise gain process, and to store the resulting charge pattern in a low-loss target. The charge pattern is read out by an electron beam that senses the target surface potential by producing a secondary electron emission beam whose potential in turn is demodulated yielding video. The video then can be transmitted to a recorder from which a film image can be produced for viewing or to a digitizer and processor for automatic analysis and sundry uses. The functions of erasure, exposure, storage, and readout are separate in this approach, which results in elimination of image retention and in an uncompromised performance in the readout function.

The basic processes involved in the electrostatic storage tube are shown in Figure V-1. The target (T) is prepared for exposure by charging the thin dielectric film to a low negative potential relative to the backing electrode. The target as shown in the exposure part of Figure V-1 is charged prior to exposure. The photoemitter (PE), which is chosen for its high-quantum efficiency in respect to the wavelength range of interest, generates an electron image in response to the radiant input image.

The electron image is accelerated and focused on the charged target by the action of the electromagnetic fields, discharging it by bombardment-induced conductivity. This results in a charge pattern on the target surface corresponding to the input image.

The electron bombardment-induced conductivity (EBIC) offers a prestorage gain process applicable to a high-resistivity thin-film target and useful nonlinearity in which the gain is highest for the weakest signals. Used in this manner, the target enables one to achieve high sensitivity, high resolution, long exposure and storage times, and a wide dynamic range. The

target in turn is read out by scanning the surface, as shown in the readout part of Figure V-1, with a primary beam (generated from an electron gun using a thermionic emitter). The primary beam lands on the surface at about 100 V and generates a secondary emission electron beam. This secondary beam returns on the same path as the primary beam through the deflection-focusing structure.

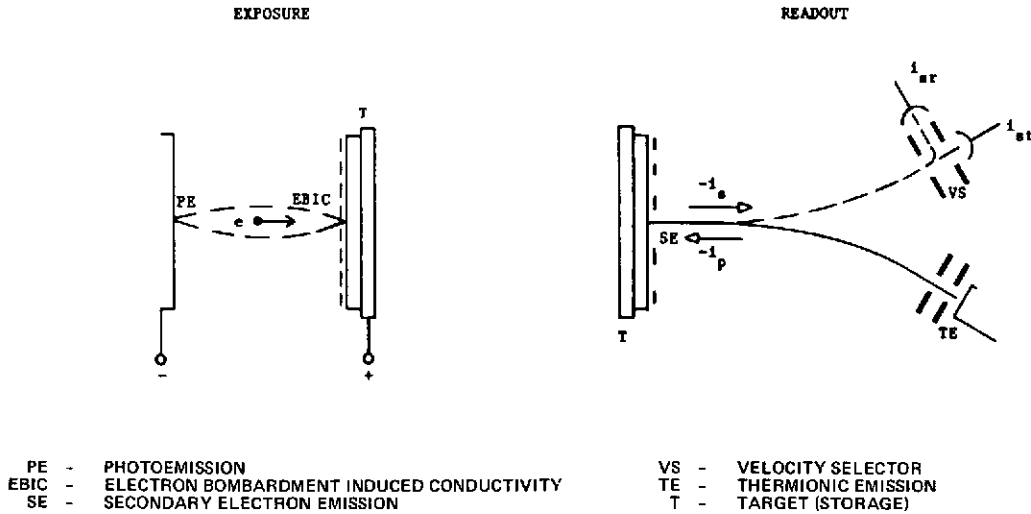


Figure V-1. Basic processes of the electrostatic image storage tube.

The secondary beam is separated from the primary beam by a weak magnetic field. It is passed into a velocity selector such that the potential of the target surface from which the secondary beam originated determines what fraction of the secondary beam enters an electron multiplier, resulting in video output.

Since the readout beam has not significantly changed the relative charge distribution on the target surface, it is not destructive, and the readout beam current need only be sufficient to avoid shot noise at the upper frequency of interest. Further, the target can be re-readout without significant degradation.

The combined basic elements of the electrostatic storage tube are shown schematically in Figure V-2. The radiant image (I) of the object field (O) is produced on a photocathode (PC) by the lens (L). The electron image bombards the target (T), and the potential image is stored there. The target is then turned in this particular configuration to the readout side, presenting a recharged surface to the imaging side, and is read out by the process described.

The primary readout beam is generated by the electron gun (EG) and is focused, scanned, and decelerated by the readout electrode structure (RES). It lands on the target surface,

generating the secondary readout beam. The secondary beam is separated by the separator field (SF) and is passed into the potential selector (PS). A fraction of the secondary electron beam depends on the target potential entering the electron multiplier (EM) and produces the video.

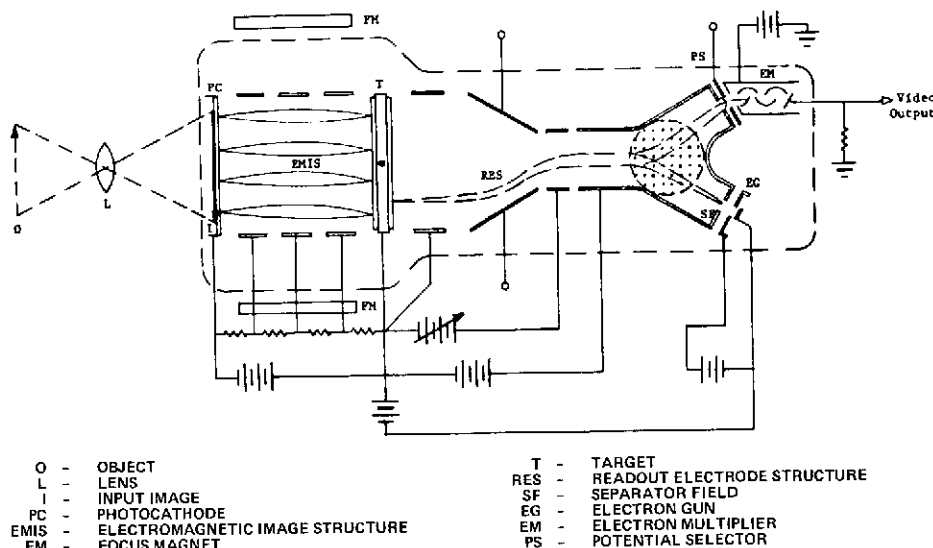


Figure V-2. Basic elements of the electrostatic image storage tube.

Significant advantages of this readout method are the avoidance of a decelerator mesh in the electrode structure and the landing at high energy, both of which avoid the loss of resolution by beam spread and scattering as well as the introduction of noise.

Camera operating characteristics are indicated by the graphs shown on Figure V-3. We have considered a rather conservative photocathode that for daylight-type operations would have a quantum efficiency of only 6 percent. It is reasonable to expect cathode-quantum efficiency to be in the order of 20 to 30 percent even with current technology. Better performance can be expected in the future.

For a given exposure, the input is converted to photoelectrons per element that land on the image storage surface, discharging the surface. The change in surface voltage is then read out, producing the image signal (video) which is recorded in the density variation of the film by, for example, an electron beam recorder. This particular readout characteristic is that of a constant selector potential. We can use that output voltage as an error signal to adjust the selector potential and thereby get a very wide dynamic range.

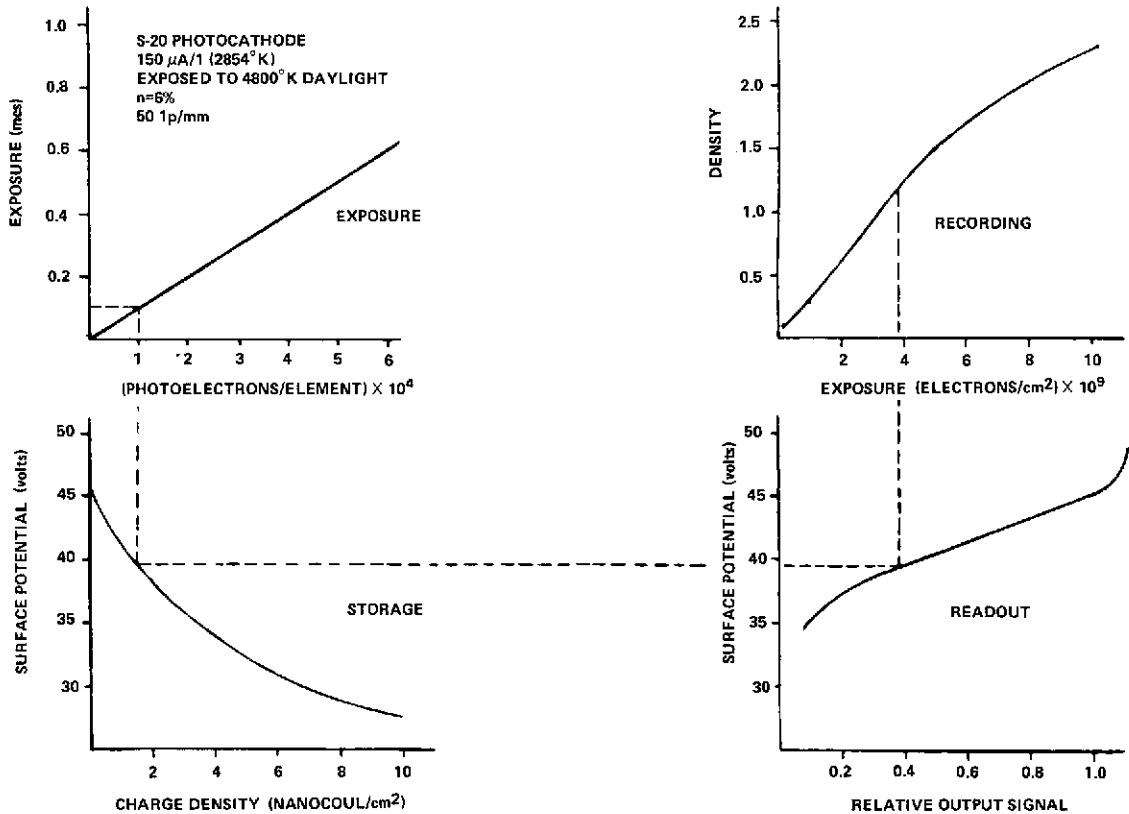


Figure V-3. Camera operation.

Performance of the overall camera is shown in the graphs of Figure V-4. The spectral characteristic depends upon the photoemitter window combination used. The quantum efficiency of the photoemission process is the controlling noise factor (limiting ultimate performance).

The modulation transfer function (MTF) is generally determined by the readout beam size and uncertainty in the landing location because of deflection noise.

Perhaps it should be noted here that the image section could also employ deflection to compensate for image motion. This could improve the overall system MTF by reducing smear on very long exposures.

The threshold modulation and resolving power curves attempt to show the calculated performance of the electrostatic camera compared to other sensors. Threshold modulation perhaps is not used very much in the traditional astronomical evaluation; but, if you look at a question of seeing objects that are adjacent, cameras that have better (lower) threshold modulation values for a given exposure would give you better performance.

The resolution of a single bright object in a dark field is of course a different criteria, and it is hard to say what modulation you would consider equivalent.

The resolving power characteristics generally are controlled by two basic limits; on the upper side you end up against MTF limits, and noise limits come up against you on the low exposure side.

This information to which I am comparing the electrostatic camera comes from Otto Shade's relatively recent work and from the ITEK aerial film data. Tri-X is the silver-halide film, RBV is the return beam vidicon according to Shade's data, SO-206 is a Kodak aerial film, and 3414 is another aerial film. The performance curves are in the context of imaging through a f/5.6 lens, which is one of the limits on all of the transfer functions shown.

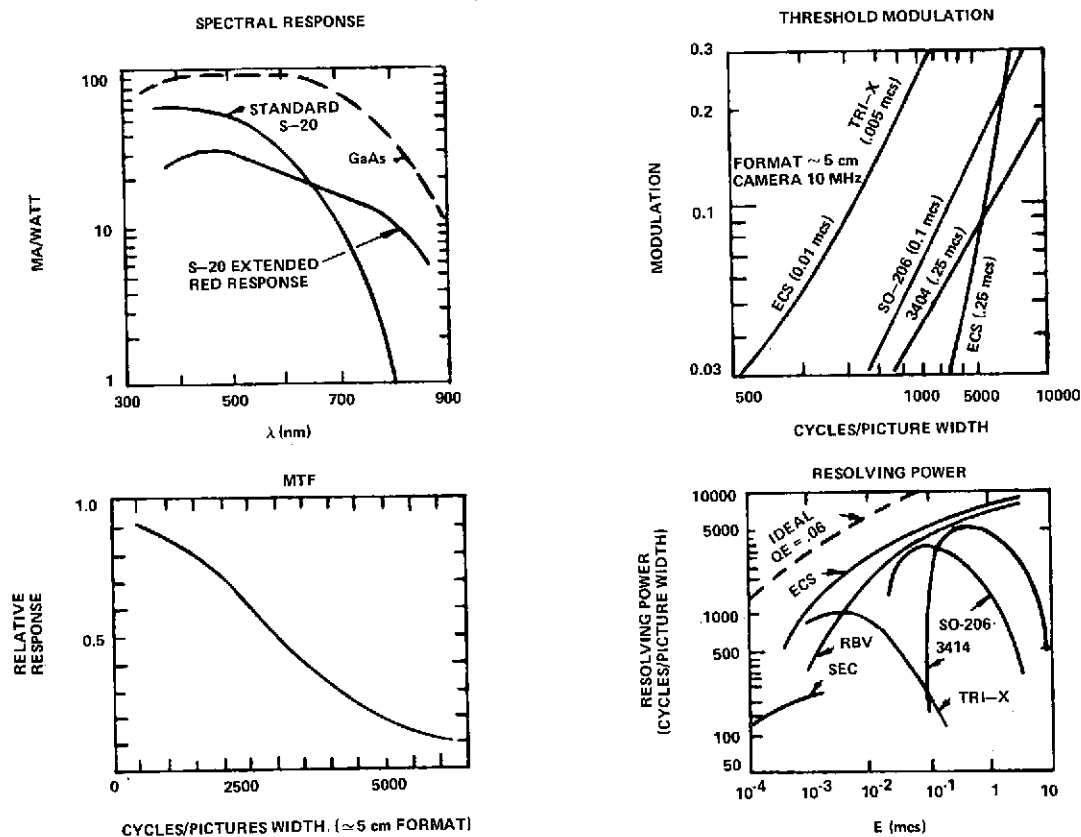


Figure V-4. Camera performance characteristics.

One notes that in comparison to the region of exposure where the resolving power of 3414 film is highest (0.25 mcs), if you look at the threshold modulation characteristic in this exposure range you see that 3414 film is better if you have a sufficiently high modulation.

If you have a lower modulation, or contrast in the image, the electrostatic camera would give you higher resolution. Thus, the contrast range that you are interested in and the class of objects that you're looking for have a significant effect on the interpretation of the resolving power curves.

To apply the electrostatic storage tube to problems which will be treated by the Large Space Telescope, we looked at some of the preliminary data that have been given to us in the past on the expected performance requirements. The data would indicate that we could use a camera having a 5-cm (2-in.) format size, with as a goal, a limiting performance in excess of 100-line pairs/mm. We have sketched up such a design, Figure V-5, based on our general approach.

Figure V-5 is a sketch showing the general configuration of the hardware for the basic camera device. An electromagnetic image section is used for the reasons that have been mentioned earlier. The photocathode in this case is a transmission type. However, this type of technology approach, with the separation of the tube functions, would lend itself to reflective types as well.

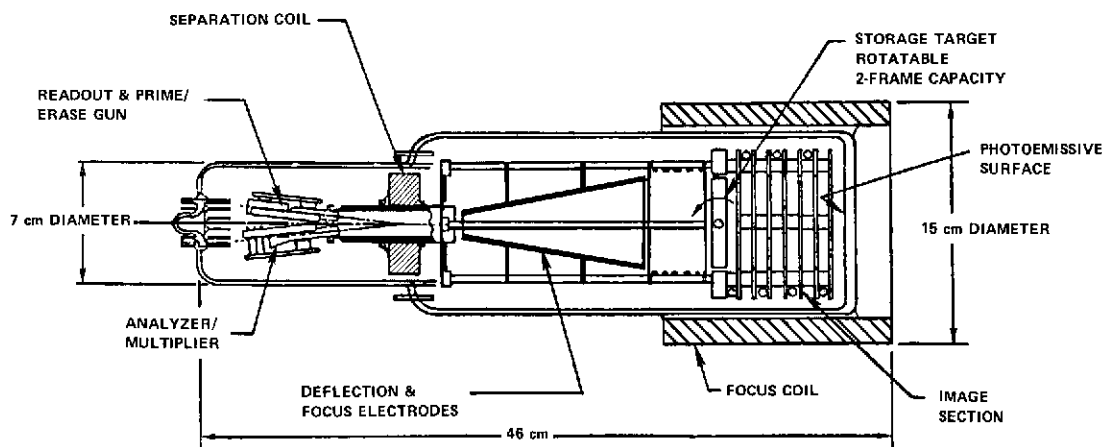


Figure V-5. Electrostatic camera for the Large Space Telescope.

The electronics and the vacuum design aspects involved are usual, and no special problems are expected. The status of this development is that it is a laboratory program at CBS Laboratories; we are building several experimental devices of this type. We have done a fair amount of component study to show that all of these separate processes and separate materials do work. Now we're putting together an experimental device which we should have by late this year or early next.

## DISCUSSION

*A. MEINEL:*

This was 100 lines at what limiting modulation?

*R. E. RUTHERFORD:*

Limiting modulation is usually taken as 5 to 10 percent.

*A. MEINEL:*

What is the time over which you can integrate an exposure; and also, what's the time over which you can hold the image in storage without significant degradation.

*R. E. RUTHERFORD:*

Those times are about the same, that is, the storage mechanism here is primarily a resistance capacity type of storage where the target is a very high resistance dielectric. It could be exposed for hours or days.

Experimentally, we have observed that there is image retention when we did not erase it, which has been for over a weekend without significant degradation.

*A. MEINEL:*

I noted on the intensity scale in Figure V-3 that it is labeled in terms of  $10^4$  photoelectrons. A very large number indeed!

Could this device ever be operated in a photon-counting mode and still maintain very-high resolution?

*R. E. RUTHERFORD:*

Going back to what is the minimum signal one can detect, if one has a very low input (photon) rate, the device will integrate over that period of time until the signal is detectable. Of course, there may be extraneous sources that will add to it.

That minimum photon count signal in turn will probably be limited by our ultimate sensitivity in our potential separator. That is, how many millivolts change this minimum signal makes in the target surface, and can we detect that signal with what certainty is considered acceptable.

The indication is that we can see a 50 mV or so change now in the targets, with fair certainty, and that with better apparatus we could probably go down further.

*A. MEINEL:*

If a multistage image intensifier is placed ahead of it, does the resolution go down significantly?

*R. E. RUTHERFORD:*

Yes. The losses in resolution which occur are associated with that intensifier stage; and we have particularly avoided mosaic structures and things of that sort, such as meshes and transmission films as intermediate stages, to preserve the resolution in the device.

Very low level noise measurements have not been made. In particular, we wish to determine if there is any appreciable noise introduced in the EBIC gain process.

It has been assumed that the noise in the EBIC gain process is that of a secondary emission process; and in our calculations, on which this performance curve is based, we have used that model to calculate performance.

Our early experiments have indicated that this is the case. But at very low currents we don't know, and we're looking at that operating range. We hope to have shortly an experimental resolution of this particular point; but if you go by the calculation, we should be able to get to the performance shown. I should mention that the gain values that we are generally getting are in the order of 50 to 100, which should get us to the quantum noise limit determined by the input statistics from the photocathode.

*E. J. WAMPLER:*

In Figure V-4, if one extrapolates your resolving power sensitivity curve, it apparently crosses over the SEC curve, doesn't it, at the lower light level? Is it true that at the very low light levels the SEC is more sensitive?

*R. E. RUTHERFORD:*

Yes, this curve would show that. In the lower exposure region of the curve we are expected to be limited by the noise sources in the readout process. I don't know if this curve is a true comparison for the SEC in the same context. We think it is approximately so from the literature that we've studied. This is not our measurement in a comparable situation.

And of course, the curve for the SEC is calculated based on our model, which when extrapolated into the low resolution area (I doubt that the design which we used had an appropriate target thickness) would be an optimum design for the exposure resolution range shown for the SEC. By changing certain parameters, such as the size of the target and the thickness of the target, we can generate an optimum design that would operate more advantageously in this range. The SEC for the curve shown was designed to operate over the higher range of exposure and resolution, and the target thickness was chosen for such.

If you want to design for a particularly low-resolution, low-light type of operation, one would go to a slightly different target thickness, which would give you more initial gain but limit the overall signal range.

*M. GREEN:*

It is probably fairer to compare the performance of this high-resolution tube with some of the high-resolution SEC tubes which give significantly better limiting resolution, that is, on the order of 1000 to 2000 TV lines.

*R. E. RUTHERFORD:*

It was difficult to obtain data from catalog sheets regarding this point. Most television tubes are evaluated on the basis of a continuous exposure. We are really talking about a single flash exposure, and obtaining data which corresponds to that condition is not easy.

*K. HALLAM:*

The readout technique here intrigues me. Could you elaborate on it on the basis of whatever hardware you've made? Can you compare it to the RBV technique and to the isocon technique?

*R. E. RUTHERFORD:*

The readout technique has been generated to avoid the problems one sees in the RBV, the isocon, and similar types of camera tubes. What we've tried to do in this approach is to have a modulation process rather than a charge replacement process to generate the signal current. We are modulating the potential of the return beam, so that the current in the return beam is only a carrier of the signal information. With such a process we can repeatedly scan the target to read out the signal, or we can adjust that current to what we think is the optimum for our noise conditions. One can avoid having to compromise the beam current because of recharging the target considerations and similar effects.

Another point is that the readout beam is landing at a relatively high energy: 100 V. This avoids the problems of beam spreading that one encounters with near-zero energy landing conditions. In this way, one minimizes resolution loss, especially for the normal energy spread in the beam that results from the thermionic cathode or some beam distortions.

That we have avoided a beam-spread problem by going to the high-energy landing can be observed because we can use the same device in the charge replacement mode; a considerable improvement in the resolution obtains as a result of landing at high energy.

A secondary emission process is involved, and, according to the literature, secondary emission around one should give rise to infinite noise. Of course, that results from the simplification of the noise equation, where the denominator of the noise factor is allowed to go to zero. It is our experience that, as one approaches this secondary emission value of

unity, something very close to the square root of 2 obtains. We recommend the use of  $\Delta + 1/\Delta$  rather than  $\Delta/\Delta-1$  for noise factor. When we operate with a secondary emission ratio of approximately one, we do get a secondary emission beam that does not significantly change the potential on the surface; and even if we operate at a secondary emission ratio other than unity, the whole surface changes uniformly. Therefore, we are not changing the information on the surface; we are only changing the bias level.

The information then can be read repeatedly, and it isn't necessary to operate around unity, only as a matter of convenience.

*M. GREEN:*

Haven't the previous schemes suffered from microscopic variations that give rise to fixed pattern noise?

*R. E. RUTHERFORD:*

Yes, the problems of that type have occurred, and that is one of the reasons why we have chosen a material that is homogeneous, non-crystalline, and essentially without structure. For this reason, we don't see the problem unless one considers the application where the device is used as an electromicroscope; and of course, then one does begin to see structure.

*A. MEINEL:*

What limits the resolution in this type of tube?

*R. E. RUTHERFORD:*

Depending on the bandwidth required, the resolution limit is usually caused by the read-beam brightness. In attempting to operate at a higher frequency, more beam current is needed to maintain a given noise level, and therefore a higher beam brightness is needed.

However, for the LST case with 10 MHz or so operation, there shouldn't be any problem with current, conventional cathode structures. The read-beam current must be adequate in a temporal resolution sense so that the signal conveyed is not masked by the statistics of the beam noise. The beam current is related to the readout beam current, which is not directly related to the photon current.

Also, the secondary emission ratio varies a little with the potential on the surface, but this is a secondary effect. There will be a change in return-beam current because of the potential difference on the target, but the slope of that curve is very slow, and it is definitely a second-order type effect. It would occur only with very large signals, which are being compressed by a target operation anyway.

Looking at resolution such as in the case where one might try to see a faint object that is near a very bright or near-bright object, this type of target should be particularly good be-

cause it doesn't have the spread that is expected in a silicon-type target. For these targets, diffusion of the carriers is over a significant distance. Improvements, especially against blooming, arise because the target thickness of less than one micron is used in the electrostatic tube.

*R. W. ENGSTROM:*

Does the fall off in resolution at low-light levels indicate the contribution from the photoelectron statistics?

*R. E. RUTHERFORD:*

Yes, the ideal case is given by the line shown dotted as "ideal." This particular calculation is for a target design optimized for higher levels of irradiance. By using a thicker target (in this particular case where you want lower capacity so you get more voltage change per input) higher voltage can be stored on the target with a subsequent increase in the gain.

*J. A. WESTPHAL:*

There must be a line on the graph in Figure V-4 that shows the photon noise limit independent of the equipment. Is it tangent to the top right end of your curve?

*R. E. RUTHERFORD:*

I believe that this is represented through the 6 percent efficiency curve included.

*A. MEINEL:*

What kind of weight is involved in the use of a magnetically focused system?

*R. E. RUTHERFORD:*

The structure would weigh approximately 7 kg (15 lb) using a permanent magnet.

From an earlier discussion on the imaging system it was mentioned that one could use an electrostatic imaging system if one were willing to concede edge resolution. In fact, we have proposed such a system for certain planetary applications where the data is limited anyway, and such an approach would be quite feasible.

*A. MEINEL:*

Preserve the flat field, if at all possible.

*R. E. RUTHERFORD:*

We think for the LST application with a large field and high resolution across the field, a uniform magnetic and electric field type of imaging system offers the best promise. Also, it avoids any type of fiber optics, any type of mosaic structure, and would yield a very high resolution.

N74-17412

PRECEDING PAGE BLANK NOT FILMED

## VI. LARGE SPACE TELESCOPE TELEVISION SENSOR DEVELOPMENT

*J. L. Lowrance  
Princeton University Observatory  
Princeton, New Jersey*

The work at Princeton University Observatory on the development of television sensors for space astronomy has been sponsored by the Supporting Research and Technology program in physics and astronomy at NASA Headquarters. Paul Zucchini accomplished a great deal of the work I will be discussing.

Figure VI-1 is a schematic that shows how the SEC tube works. It has a photocathode, as have most of the devices that have been discussed this morning. The photoelectrons are accelerated to 8000 V. They strike a target that consists of a 70 nm-thick aluminum oxide supporting substrate, a signal plate of aluminum of comparable thickness, and a fluffy layer of 10- $\mu$ m-thick potassium chloride. This KCl layer provides the gain. The 8000-V photoelectrons lose about a kilovolt or so going through the aluminum oxide and the aluminum. When they get into the potassium chloride, the photoelectrons lose the remaining 7000 V and, in the process, generate secondary electrons that migrate through the layer to the signal plate, leaving a positive depletion of somewhere between 70 and 100 electron charges, depending on the particular target and the voltage bias across the KCl layer.

To operate the tube, one turns on the high voltage that accelerates the photoelectrons and the magnetic focus field. After an exposure, which may vary in duration from a few seconds to a few hours, we turn off the high voltage, turn on the electron gun, and scan out the one frame of data. The tube is magnetically focused throughout for maximum resolution. We are currently seeing about 50 percent modulation at 20 line pairs/mm.

Figure VI-2 shows a transfer function of the tube with the input in photoelectrons/pixel. One notes that there is a threshold due to the preamplifier of around 5 photoelectrons/pixel. In a newer target design, the shunt capacitance is lower, and we expect this to drop the threshold to less than 5 photoelectrons/pixel.

At 20 cycles/mm the peak exposure can be as high as 1500 photoelectrons/pixel. So, with the noise threshold of 5 photoelectrons (rms) corresponding to a signal level of 25, the tube has substantial dynamic range and is essentially quantum-noise limited over most of that dynamic range.

Figure VI-3 is a picture of the two SEC-vidicon tubes that we are working with at the moment. We have used the 25-by 25-mm format tube for the last 3 years for ground-based observing and are currently planning to fly it in a sounding rocket payload this winter to obtain UV spectra using an echelle spectrograph.

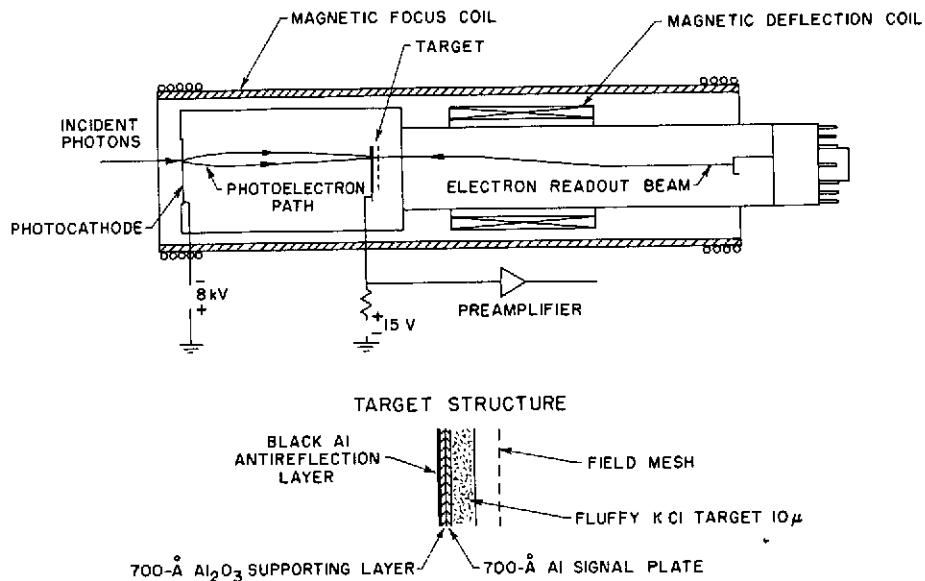


Figure VI-1. The Westinghouse WX 31718 SEC vidicon.

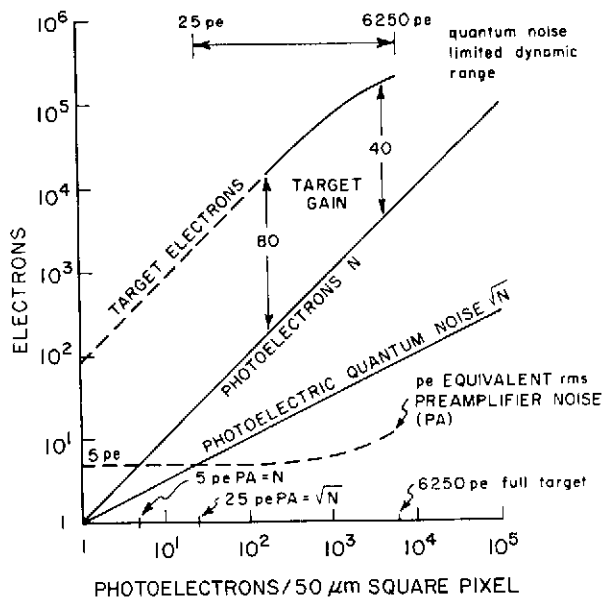


Figure VI-2. SEC vidicon photoelectric transfer function.

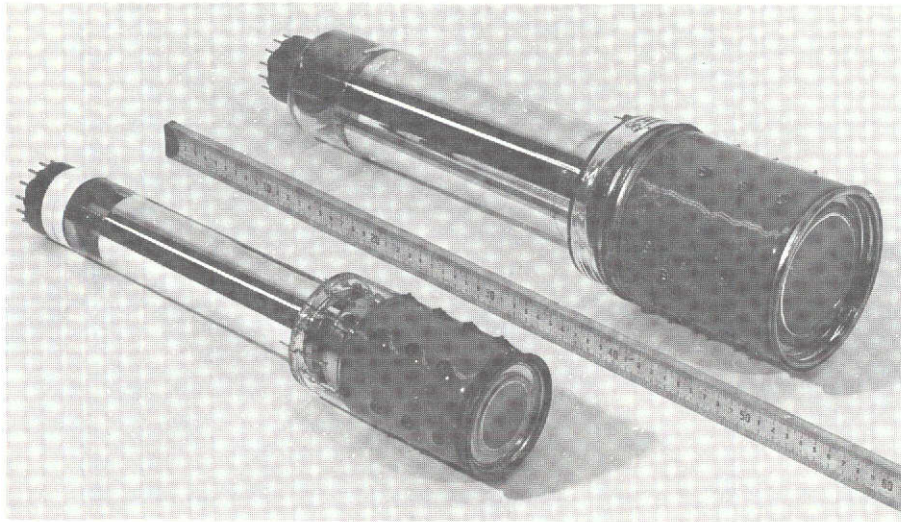


Figure VI-3. Two SEC-vidicon tubes: 25- by 25-mm format and 51- by 56-mm format.

The 51- by 56-mm format tube is a scaled-up version of the smaller tube. The electron optics are a copy of the 11.4-cm (4.5-in.) return beam vidicon; and we expect the resolution of this tube, based on the measurements we have run to date, to certainly be as good (in cycles per millimeter) as the smaller tube. If not limited by the thickness of the KCl target, it may be even better due to the higher resolution that we anticipate from the return beam vidicon electron optics. Our tests to date have been restricted to the resolution in the middle of the tube. We are busy working on this and hope to have much more data in the next few weeks. Table VI-1 gives pertinent characteristics of the family of magnetically focused SEC vidicons.

We have just initiated a program to make the small 20-mm version for the International Ultraviolet Explorer (IUE) satellite. This tube is considerably smaller physically. We expect it to have the same performance in terms of sensitivity and resolving power.

The future work we plan in developing these SEC tubes for space astronomy applications, in particular LST, is to push the resolution even higher, and hopefully, still maintain the capacity of the tube in terms of number of photoelectrons/pixel. One of the limiting factors that determines the overall modulation transfer function (MTF) of the tube is the thickness of the target that stores the photoelectrons. Figure VI-4 shows how the theoretical resolution of just the target varies with the thickness. At 20 cycles/mm an 8- $\mu$ m-thick target has an MTF of 0.4. That is aside from MTF losses in the image section, electron optics, the

Table VI-1  
Comparison of SEC Vidicons

	WX-32192	WX-31718	WX-
	Large SEC vidicon	Medium SEC vidicon	Small SEC vidicon
Photocathode Diameter	76 mm 110 mm	38 mm	25 mm
Target Size	56 × 51 mm	25 × 25 mm	15 × 15 mm
Overall Length	487 mm	432 mm	240 mm
Maximum Diameter	128 mm	80 mm	58 mm
Window	MgF <sub>2</sub> Glass	MgF <sub>2</sub> Glass	MgF <sub>2</sub> Glass
Focus Field	80 gauss	80 gauss	80 gauss
Resolution (50% modulation)	20 cycles/mm	20 cycles/mm	20 cycles/mm
No. Picture Elements	4 × 10 <sup>6</sup>	10 <sup>6</sup>	3.6 × 10 <sup>5</sup>
Photocathodes	NaK Sb S-20 ER	NaK Sb S-20 ER	NaK Sb CsTe S-20 ER

readout beam, and so forth. Figure VI-4 shows where the SEC tube falls with its fluffy thick KCl target. We are looking at other targets that are thinner, and hopefully we will have higher intrinsic resolution. The likely candidates are listed in Table VI-2.

Table VI-2  
Candidate Targets for LST TV Camera Tube

Target	Gain Electrons/ Photoelectron	Capacity μf/mm <sup>2</sup>	Integration Capability
Potassium Chloride	100	5	Excellent
Silicon	1000 – 2000	40	Must be cooled to 213 K
Silicon Dioxide	100 – 200	100	Excellent
Zinc Sulphide	400	100	Under investigation

The potassium chloride is the target that we are now using. The silicon target is quite interesting, but we have essentially dropped it for those LST applications where the tube

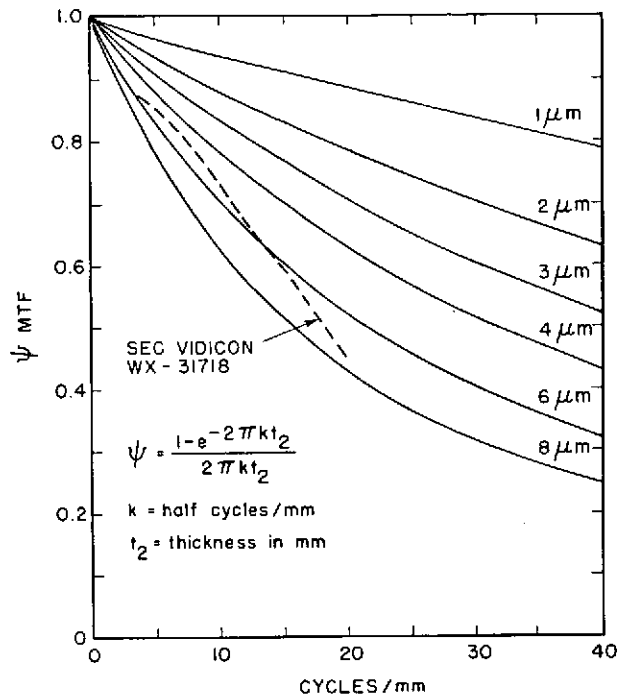


Figure VI-4. Theoretical target resolution variation with thickness.

must integrate the image, rather than integrate the signal in some external digital memory, as was discussed this morning. One would have to cool the silicon target down to 213 K (60°C) in order to integrate for 2 to 3 hours. It has been found during the LST Phase A studies that it is difficult even to cool the tubes down to 263 K (-10°C) to minimize the cathode's dark current.

Silicon dioxide is a potential target material that has promising storage capability for this work. The capacitance is high, which means that at increased resolution, one can maintain the capacity in photoelectron/pixel. Zinc sulphide is another material that we are in the process of evaluating. It has a high gain, which is interesting, and the capacitance is high. The major unknown is the dark current: its temperature coefficient and how this might be modified.

In the next few months we will be refining our evaluation of the possibility of zooming the image section of a magnetically focused tube enabling one to vary the f-number of the system to suit the observing situation. This investigation was prompted by Dr. E. J. Wampler awhile back, and our preliminary measurements were very encouraging. We have just completed the setup of an image intensifier that is the same as the image section of our

television tube. This provides a means for quickly looking at the output image and varying it. A microscope is set up to look at the output image. We will be able to analyze the effects of zooming the tube to vary the magnification from 1:1 up to perhaps 3:1 or 4:1. Figure VI-5 is a picture of our preliminary measurements of zooming. By increasing the magnetic field at the front of the tube, the electrons tend to follow the flux lines; one gets magnification.

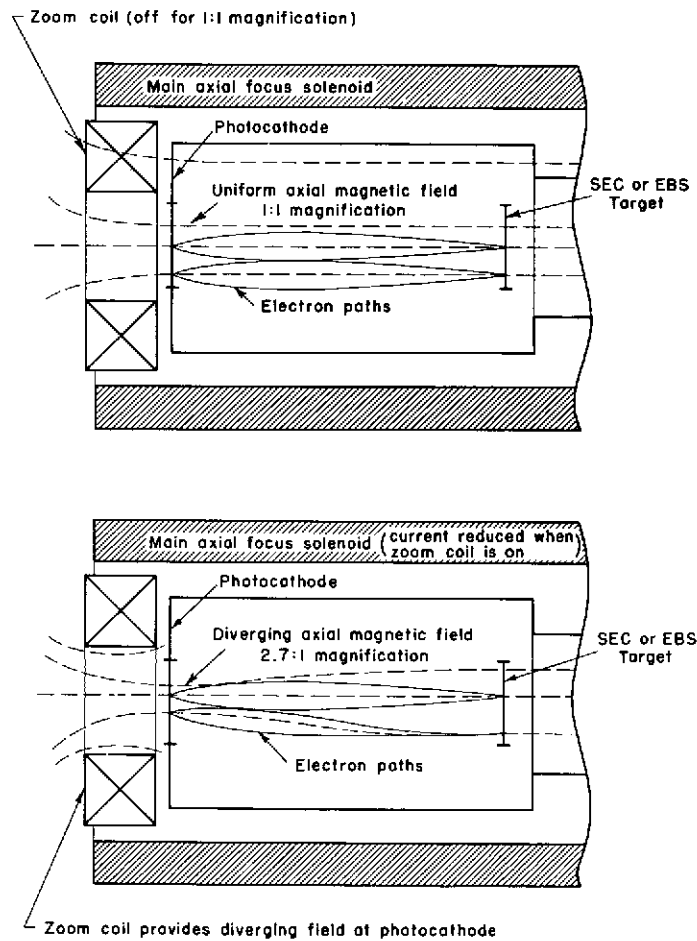
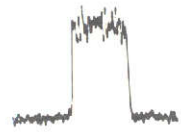


Figure VI-5. Preliminary measurements of zooming.

A quantitative measure of this technique, given in Figure VI-6, is an actual measurement of the MTF. Shown for the unzoomed case, is the response at 10 cycles/mm and 20 cycles/mm, and it is essentially zero at higher spatial frequencies because the frequency response is cut off electrically with a filter.

# SEC SQUARE WAVE MTF

WITHOUT IMAGE SECTION MAGNIFICATION



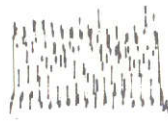
Spatial Frequency on Photocathode

10 C/MM

20 C/MM

30 C/MM

40 C/MM



WITH IMAGE SECTION MAGNIFICATION

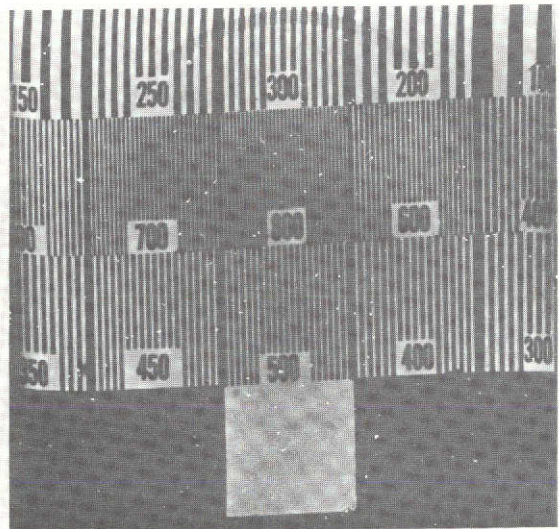
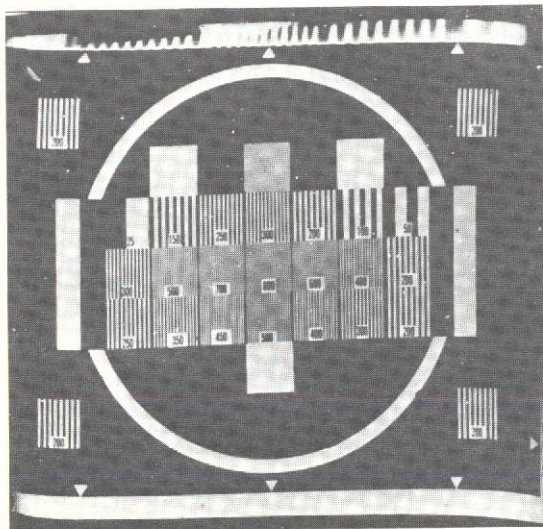


Figure VI-6. Actual measurement of the modulation transfer function.

Zoomed up by a factor of 2.7, the 20-cycles/mm pattern is now almost full amplitude, and the response at 40 cycles/mm is equal to the unzoomed response at 20 cycles/mm. This data was taken near the middle of the tube. We are in the process of trying to obtain that same data off-axis and determining just how large a magnification factor one could achieve.

Figure VI-7 shows how the various background noise levels in the tube vary as a function of spatial frequency. The amplifier noise is independent of spatial frequency. We do have to give it a greater weight at higher spatial frequencies due to the MTF of the tube. The modulation transfer function of the tube filters the signal at higher spatial frequency but does not filter the amplifier noise. To express amplifier noise in terms of photoelectrons we multiply it by the reciprocal of the modulation transfer function of the tube.

The noise background due to dark current from the photocathode and the field emission from the tube walls is also given in Figure VI-7. It is not very great in the tubes that we are currently building. It was a very big problem in the beginning but has been decreased by techniques Westinghouse developed for coating the inside of the image section with chrome oxide and treating parts to minimize field emissions. For a quarter-fold exposure, the performance is limited by the statistical noise in the signal, not by the background components in the tube.

This week, we have been running a radiation measurement, using the cyclotron at Princeton to generate 42-MeV protons, and a Cobalt-60 source to generate gamma rays. We found that there is a tube background, but it is not too discouraging. A 100- $\mu$ Cr Cobalt-60 source was located 25 mm from the front window of the tube, which was Corning 7056 glass, 2.3 mm thick. In a 40-min exposure, we estimate that about 2,500 electrons/s/cm<sup>2</sup> were generated in the window due to the gamma rays. This resulted in  $2.8 \times 10^7$  photoelectrons/cm<sup>2</sup> in this 40-min exposure. At 20 cycles/mm this works out to be about 175 photoelectrons/pixel in background due to the gamma rays. This, correspondingly, would have a noise level of around 13 photoelectrons, which is not much greater than the amplifier noise of 5 photoelectrons. With a magnesium fluoride window 4 mm thick, the background was  $7 \times 10^7$  photoelectrons/cm<sup>2</sup>, which at 20 cycles/mm would be 440 photoelectrons/pixel, with an rms noise of about 21.

These two tubes have different photocathodes with different sensitivities and spectral responses. The glass tube is more sensitive in the red. The magnesium fluoride tube is more sensitive in the ultraviolet because of the magnesium fluoride UV transmission.

Using 42-MeV protons, the glass window tube was given a dose of  $10^5$  protons/cm<sup>2</sup>. That resulted in  $4.2 \times 10^7$  photoelectrons/cm<sup>2</sup>, a yield of 480 photoelectrons per proton, and about 250 photoelectrons/pixel. With the magnesium fluoride window tube, the yield was 56 photoelectrons/proton. This lower yield is probably due to the high purity of the crystalline MgF<sub>2</sub> as compared to glass.

We plan to continue these measurements. There was a gamma-ray background during the energetic proton measurements that we were unable to measure. Another experiment is

Full exposure =  $2.5 \times 10^6$  photoelectrons/mm<sup>2</sup>

Target gain = 70

Target capacitance = 5 pf/mm<sup>2</sup>

Full exposure signal { 6250 pe/half cycle  
1560 pe/half cycle

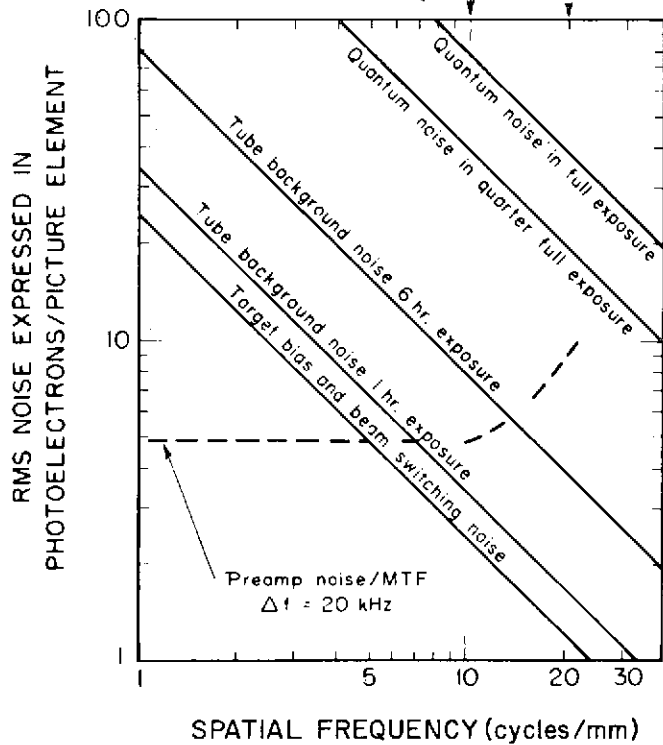


Figure VI-7. Background noise level variations with spatial frequency.

planned to sort out these two effects. We also hope to cool the tube in the gamma ray tests to remove the fraction of the background that is a function of temperature.

We found no delayed effects due to radiation when operating at room temperature or a little warmer. The tube was irradiated with the photocathode voltage turned off. We then removed the Cobalt-60 and turned on the photocathode, integrating for a few minutes to find out if there was an afterglow. We found none in any of these tests.

In a program sponsored by the National Science Foundation we are developing a new television tube that will be of interest to astronomers. This tube is called an I-SIT-isocon. It has an intensifier in the front, coupled to a second intensifier by a phosphor-mica-photocathode sandwich, as in some two-stage image intensifiers. Refer to

Figure VI-8. The second-stage photoelectrons strike a silicon-diode target. This silicon target is scanned by an electron beam that can be operated in the isocon mode, the orthicon mode, or the vidicon mode.

In the vidicon mode, the signal comes directly off the signal plate and goes to a preamplifier. In the orthicon mode, the beam returns into an electron multiplier, and one measures the electrons that were left at the target by the fluctuations in the return beam. The disadvantage of this is that in the dark areas of the scene all of the beam returns to the electron multiplier, and the shot noise in the beam is quite high. In the isocon mode, the beam strikes the target and returns, but only those electrons that have been deflected or scattered by the charge pattern on the target enter the electron multiplier. This decreases the beam shot noise and provides a noise characteristic similar to a photomultiplier where the noise is proportionate to the square root of the signal.

We intend to use this tube for what we call a photon counting camera. This effort is in collaboration with the California Institute of Technology. The scheme is to detect single photoelectrons and count them in an external digital memory that operates in synchronism with the scanning of the tube.

We expect to have a gain of 100,000 electrons stored in the target for each photoelectron that leaves the photocathode. By scanning rapidly enough, no more than one photoelectron

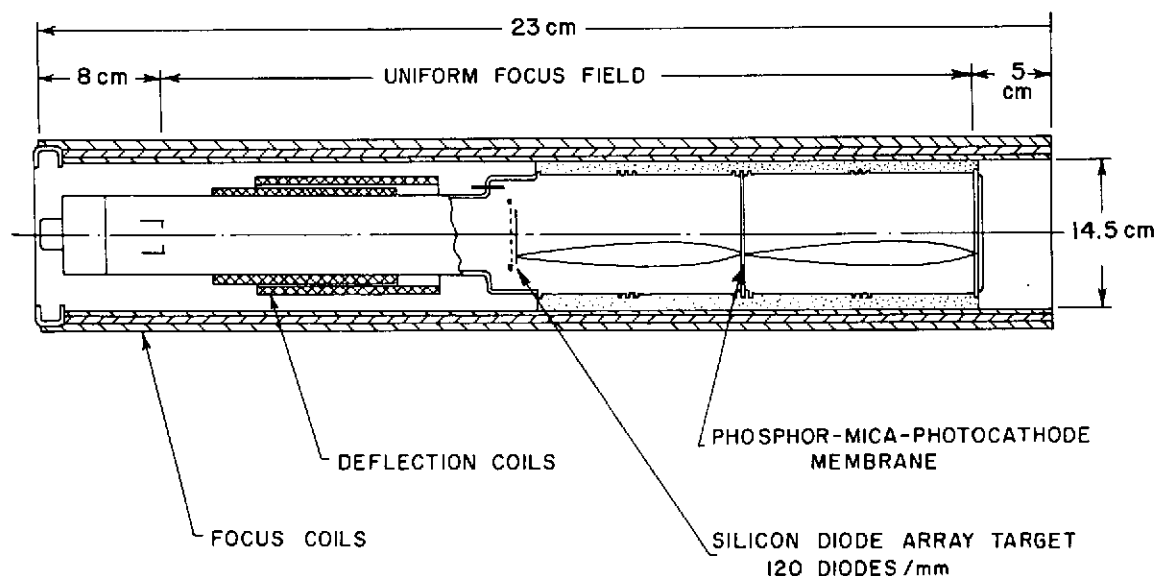


Figure VI-8. RCA-C21180 (32-mm all-magnetic I-SIT-isocon).

arrives per location during one frame period. Each is detected and added to the memory that is running in synchronism with the scanning of the beam.

A next step in this program will be to evaluate the possibility of incorporating the charge-coupled devices that Dr. C Sequin has described. They would be used in place of the silicon target and would be read out without an electron gun.

## DISCUSSION

*G. GILBERT:*

Is there any performance data available on the I-SIT tube with isocon scan?

*J. L. LOWRANCE:*

It hasn't been delivered, but it has been built. P. Zucchini visited RCA Lancaster to see it operate.

*P. ZUCCHINO:*

The tube does function; isocon readout of the silicon target is successful. This was one of the uncertainties in the development. The main problem at that time was cross-talk of the deflection fields into the image section; therefore, we could not fully evaluate the resolution. Just judging by the way that the few defective silicon diodes appeared, the reading resolution was excellent. The single diodes, single shorted diodes, make a very sharp pulse, but the image section performance was limiting; we first thought that resolution was something like 500 lines. There is no fundamental reason to think that the image section will not function classically. RCA is in the process of shielding the deflection field.

*J. L. LOWRANCE:*

You shouldn't draw any conclusions about the resolution for this first tube.

*J. A. WESTPHAL:*

How big is the silicon target in this tube or the tube that is being made?

*J. L. LOWRANCE:*

The one they have in there now is, I think, 25 mm. The reason for the smaller target is that we picked the target that RCA was making that had the lowest capacitance. We wanted to get the maximum voltage swing on the target for the minimum number of electrons.

The primary goal is to count single photoelectrons on as small an area as necessary to prove that we can do it. Then we will work on making the targets larger; the tube can accommodate a target of at least 40 mm.

N74-47413

PRECEDING PAGE BLANK NOT FILMED

## VII. APPLICATION OF SILICON IMAGE TUBES (SIVIT & SIT) TO GROUND-BASED ASTRONOMY

*J. A. Westphal  
California Institute of Technology  
Pasadena, California*

I would like to describe our work at the California Institute of Technology with both ordinary silicon target tubes (SIVIT) and with silicon intensified tubes (SIT).

An SIT is a silicon target tube that has a conventional S-20 photocathode and an electron imaging section where the electrons from the photocathode are accelerated by a voltage, in our case between 2 and 10 kV, and impinge directly on a silicon-diode array target. There is no phosphor involved in an SIT. As the electrons impinge directly on the silicon target, at 10 kV they make about 2800 carriers for each photoelectron, while if they are accelerated by only 2 kV they make about seven carriers. This is a convenient property of the SIT; you can change the internal gain simply by changing the acceleration voltage since these are electrostatic-focused tubes. Commercial tubes are used that are purchased through our local RCA representative. They are not optimum in some ways, but they produce satisfactory results.

One disadvantage of the tube for some applications is that, because of the fiber optic face plate necessary for the electrostatic focus, they have no response short of approximately 370 nm. The wavelength response of the SIT is approximately S-20 discounting the short wavelength cutoff and does not have the advantage of the 850 nm to 1200 nm sensitivity of the SIVIT.

Figure VII-1 shows a contour map of the central region of 47 Tucanae, a star cluster visible from Cerro Tololo, as obtained with an ordinary silicon vidicon (SIVIT). You can see a large number of stars, some of which are overexposed and, in fact, everything you see on the picture is a star—even the single contours. One can appreciate the potential of such a two-dimensional technique for cluster photometry. There are several hundred stars on this frame, and one can measure, down to a percent or so, each of those stars. The potential of being able to do photometry on two stars that are close together in the middle of a cluster I think is also obvious from the figure.

Figure VII-2 shows a picture of Saturn taken just a few days ago, and again, processed at IPL. The streaks you see are due to the SIVIT tube getting warm because it was upside down in the Cassegrain focus of the 200-in. telescope and the dry ice had fallen away from the tube. You can see the crepe ring is quite sharp-edged on the inside.

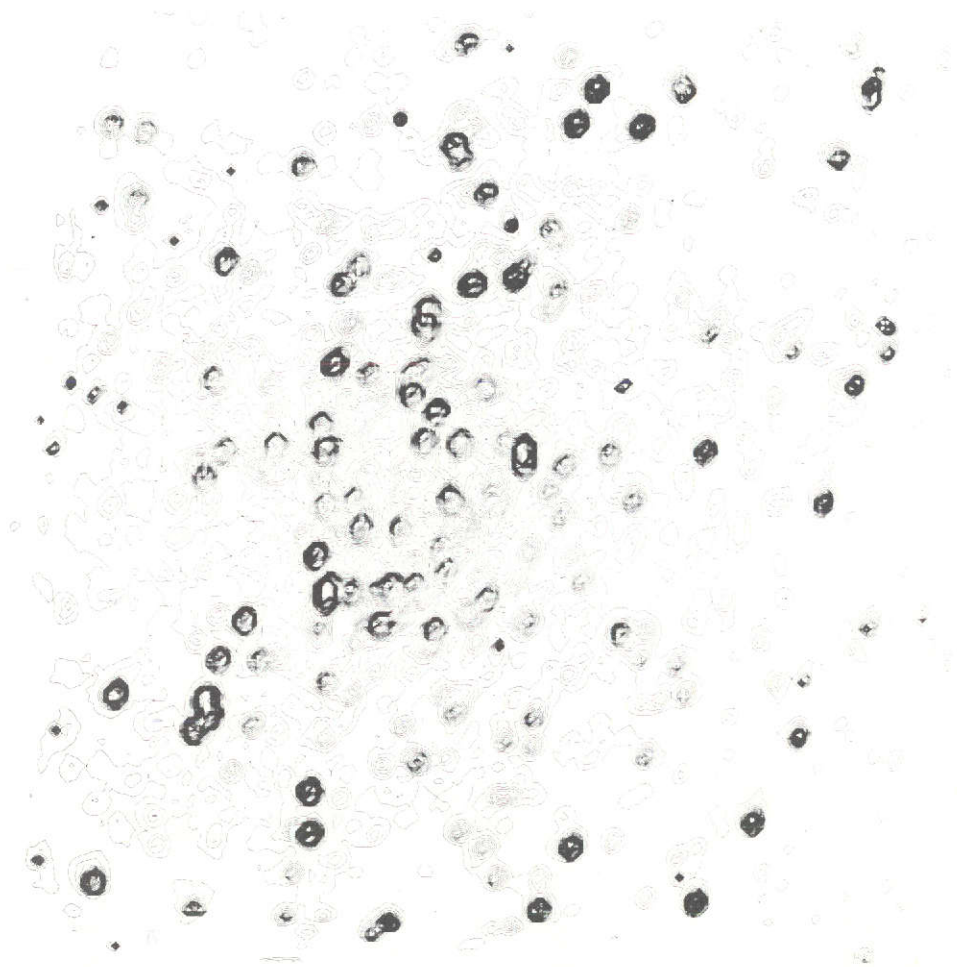


Figure VII-1. Contour map of the central region of 47 Tucanae.

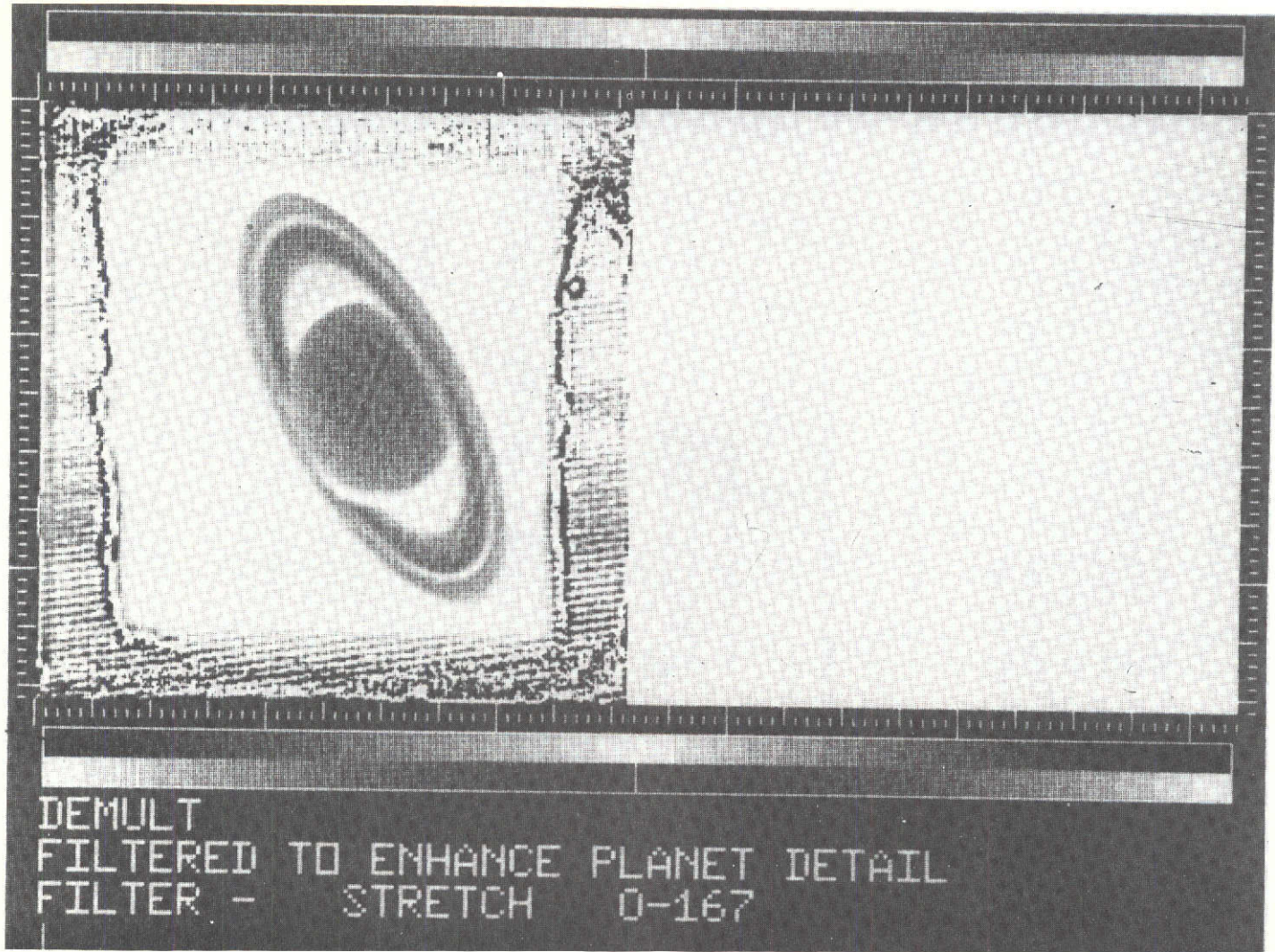


Figure VII-2. SIVIT image of Saturn.

Figure VII-3 is a frame of Jupiter taken in the continuum region at 830 nm. To the first order, it is a map of the albedo of the planet including the limb darkening due to the cosine illumination of the surface.

Figure VII-4 is a frame of Jupiter taken in the methane absorption band at 887 nm, only 50 nm away, and you see again the polar caps and cellular structure that you saw in the photographs earlier. The contour map points out one of the great powers of vidicon, that is, the ability to obtain simultaneous photometric data in two dimensions. In order to analyze the data, the 887 nm frame, which displays the albedo and limb darkening as well as the methane absorption, was unfolded with the 830 nm frame, which contains only the albedo variations and the limb darkening.

Figure VII-5 shows one frame of Jupiter divided by the other. Notice that the limb darkening is gone almost entirely. Since no limb darkening due to methane is observed, the methane must be intimately associated with the scattering region.

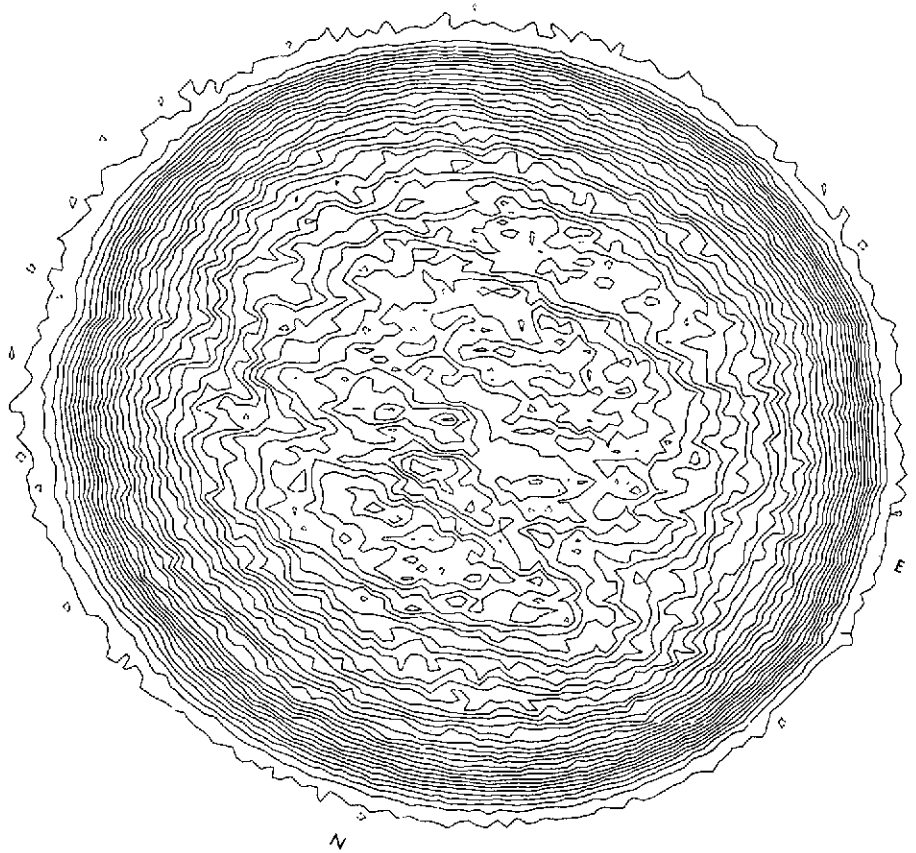
For many uses, a problem with the straight silicon vidicon is its low sensitivity. That is, it takes about 1000 carriers/pixel to exceed the noise in our system, thus making it hopeless to record 22nd-magnitude stars. To solve this problem we are using an SIT vidicon, the advantage being that it has an internal gain within the tube of up to 400. This allows one to reach the sky limit at the prime focus of the 200-in. telescope with a V-filter in about 40 s. At that point one can detect 22nd-magnitude stars in good contrast with the sky on the monitor.

For better statistical accuracy than one obtains with such a short exposure, the high voltage of the SIT intensifier section can be reduced, thereby allowing an exposure up to something on the order of 400 times longer, at which time problems with the electron optics begin to appear.

Figure VII-6 is a frame of an unnamed galaxy, with the flat field unfolded; that is, the spatial variations in sensitivity of the tube are removed. Unfolding the flat field allows one to see more structure in the galaxy. Again the photographic process used in these figures does not convey anything like the dynamic range that is available in the original data.

We have been working mainly to understand the properties of this device. We find that it is linear; that is, the output is a linear function of the input within the photon statistics. Table VII-1 shows some other properties of the SIT and compares them to the SIVIT.

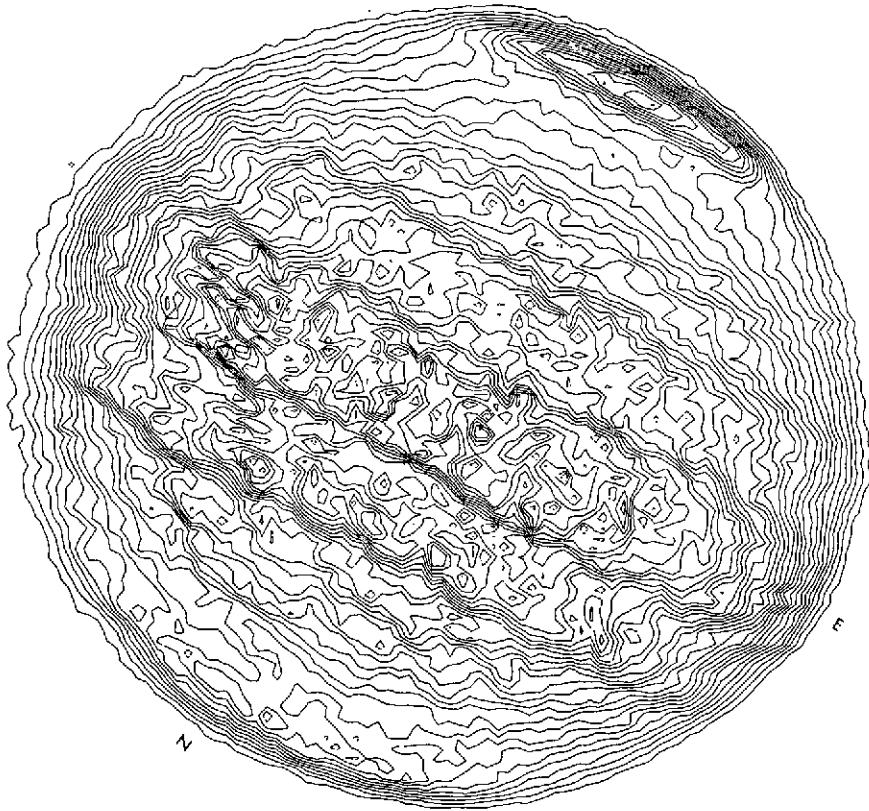
Figure VII-7 is a picture of a field centered near the position of the radio source allegedly associated with Cygnus X-3. The brighter three stars are about 15th magnitude, and the fainter ones are somewhat fainter than 21.5 in this 400-s red exposure. There are 6.5 stellar magnitudes between the brightest and the faintest images. One can see how little the star images grow. A concern has been expressed that overexposed images would bloom all over the picture, but in our experience they are very well behaved.



J1  


00h 09m  
3 June 72  
830 nm  
0.72 arc

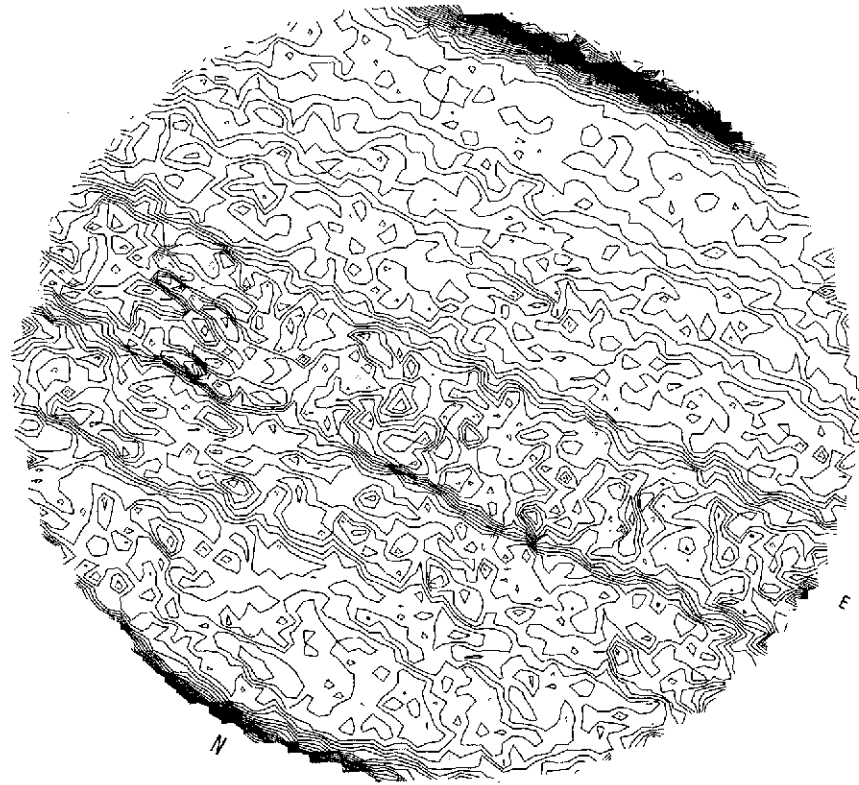
Figure VII-3. Jupiter at 830-nm continuum region.



00h 06m  
3 June 72  
887 nm  
8.01 sec

Figure VII-4. Jupiter at 887-nm methane absorption band.

2-2



N

E

Ratio

Figure VII-5. Ratio of Figures VII-4 and VII-5.

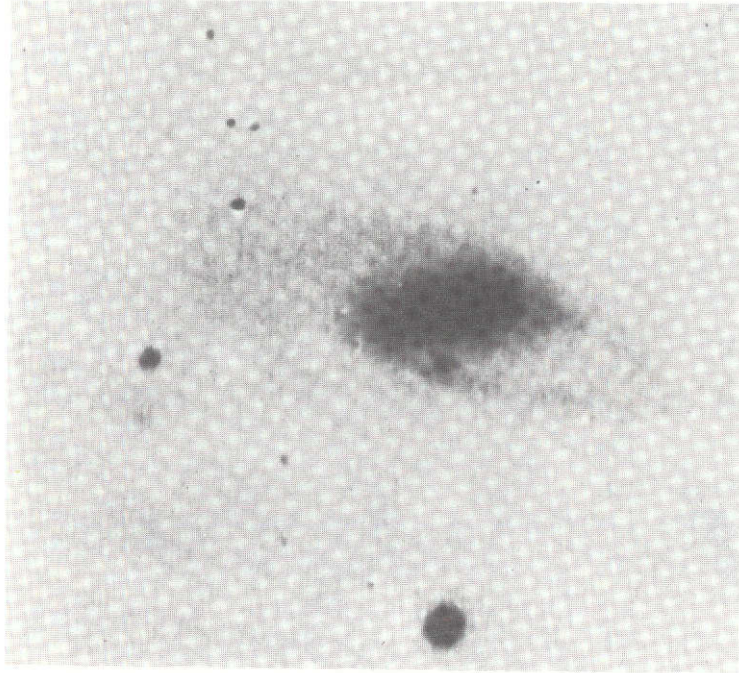


Figure VII-6. Unnamed galaxy with flat field unfolded.

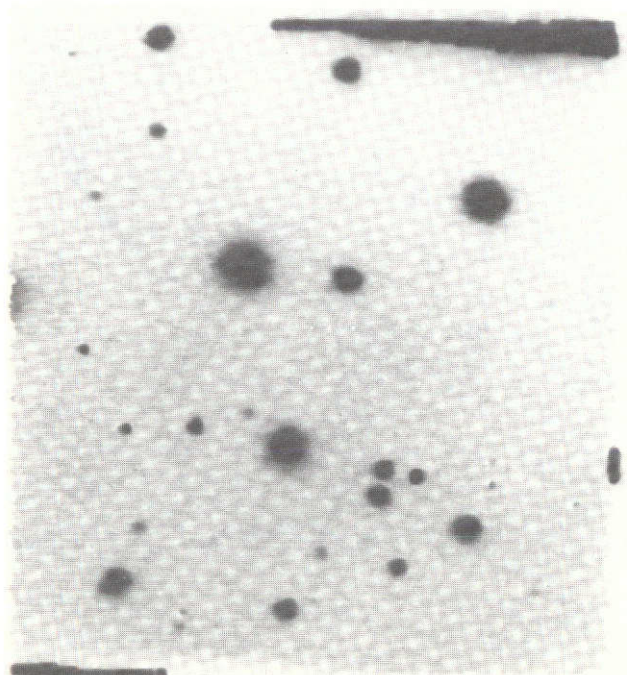


Figure VII-7. Field centered Cygnus X-3 radio source.

Table VII-1  
Comparison of SIT and SIVIT Properties.

	SIVIT	SIT
Linearity	Better than 1%	Better than 1%
Cooling to Dry Ice Temperature	yes	yes
Carriers / pixel for S/N = 1	1000	1.8
Dynamic Range	1000:1	1000:1
Spectral Response	<300 nm – 1300 nm	370 nm – 850 nm
Target Sizes Available	16 mm, 27 mm	16 mm, 27 mm
Relative Speed	1	400 (10 kv)
Tube Cost (Fall 1972)	\$225 (16 mm)	\$1,290 (16 mm)
Format	256 × 256	256 × 256
Total Pixels	65536	65536
Hardware Costs (Fall 1972)	\$15,000	\$16,000
Maximum Exposure Time	> 5 hr	> 5 hr

Figure VII-8 shows the cold box, which holds the tube to cool it to dry-ice temperature, and the base on which it sets on the prime focus pier of the 200-in. telescope. We have plug-in filter wheels that are edge-driven so that we can plug them in like a pizza.

In Figure VII-9 one can see all the electronics for the camera system. The plate in the back fits only a mounting plate in the 200-in. prime focus cage. The tape recorder is at the bottom. The data is recorded in 12-bit binary form on a 9-track, 800-bpi, IBM-compatible tape. At the time that the tape is being written, the data is also read into a Hughes scan converter which then displays the frame on a small TV screen. As a result, we have a monitor picture immediately. In addition, there is a small oscilloscope for watching the video output directly. The system is also arranged in such a way that we can play back the digital tape immediately. We can reverse the tape and move back one frame or as many frames as desired using a frame counter to keep track of the positioning of the tape. The digital tape can be played through a digital-to-analog converter onto the scan converter and be viewed on the screen. This is done to guarantee, while still on the telescope, that the data are actually being written on the tape, and that the picture has been taken corresponding to what was intended. It also is possible to do a first-order sky removal on playback so that one can look to fainter limits than can be seen during the original recording.

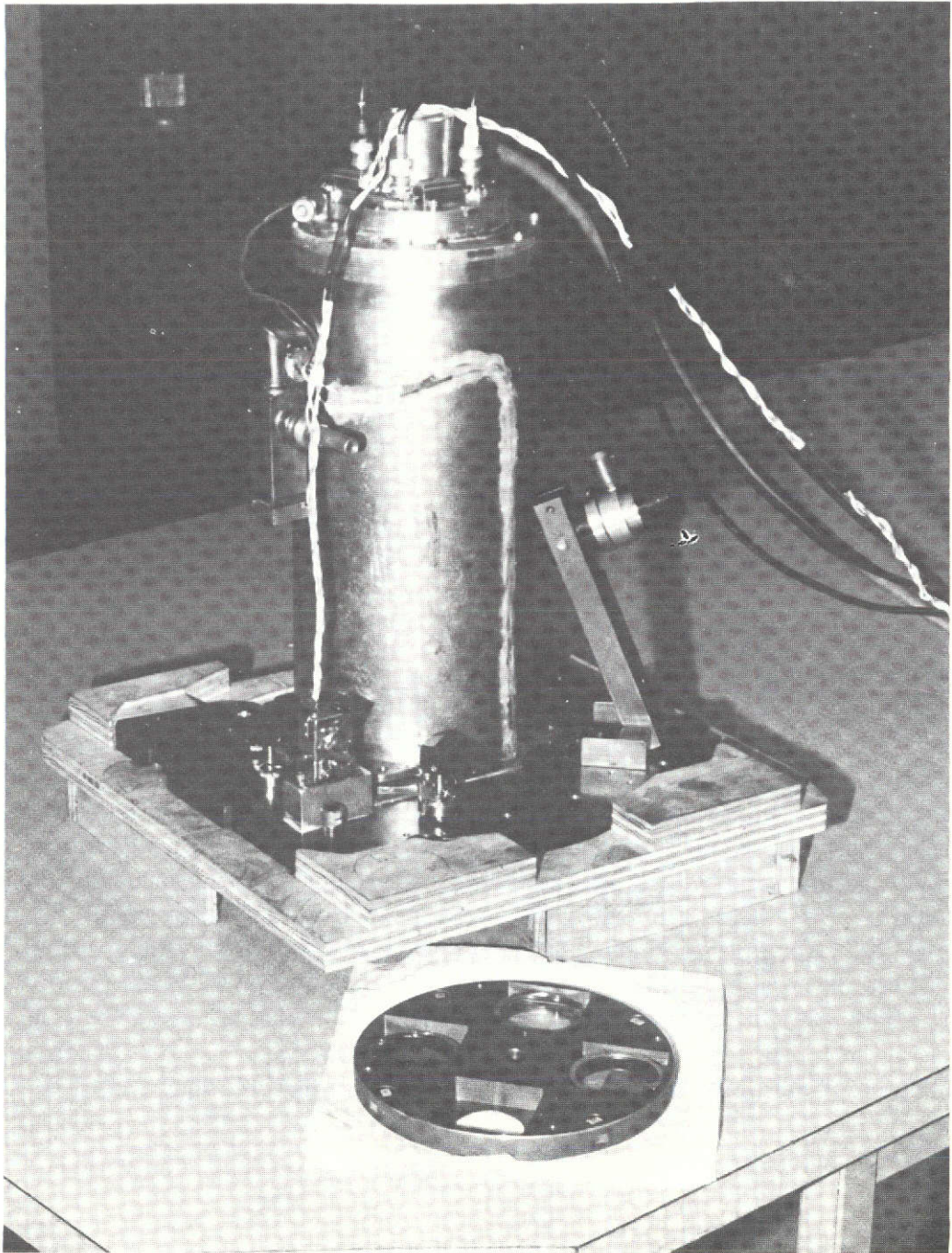


Figure VII-8. Cold box and base.

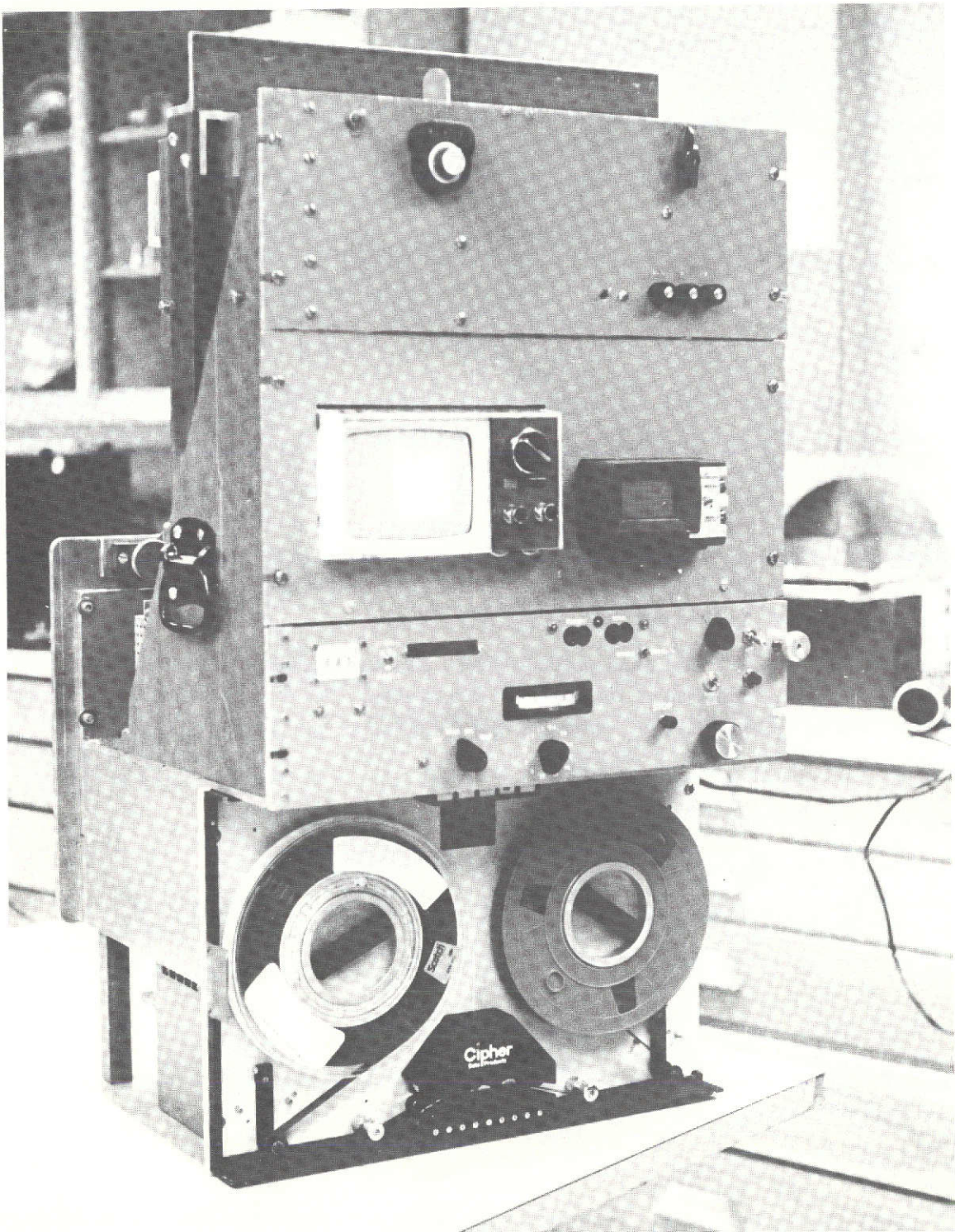


Figure VII-9. System electronics.

## DISCUSSION

*G. GILBERT:*

In the figure showing a stellar region in Cygnus, the brighter stars were somewhat larger in size. Is this effect due to blooming in the target?

*J. A. WESTPHAL:*

I don't know the absolute answer to that, but as best as I can tell, it primarily reflects the scattering in the telescope: the real profile of the star image. Certainly, as the star saturates the target, the carriers must go somewhere, and they do diffuse sideways but apparently not very far.

They seem to be stored in the target because as it is played back, normally one has less than 10 percent residual picture left on after playback; but, a very saturated star will be saturated a second time and the third time. About the fourth play through, it will finally come off the stops, indicating that the carriers are stored somewhere. I don't know the physics of where they are. So, it's very hard to know the answer to your question, because, that is a tremendous overexposure. There certainly is much scattering in the optics and filters and in telescopes; it is hard to know just how much that is. Even in a laboratory, it is very difficult to answer those kinds of questions.

It is very difficult to generate an optical image that is really sharply defined. Fortunately, the SIT is such that one can accomplish that in a real way. One can place a graticule directly on the fiber-optic face plate and generate a sharp edge. That is really the only way I know to do it.

*E. EBERHARDT:*

Is any of that blooming removed in the computer processing?

*J. A. WESTPHAL:*

No.

*J. F. MCNALL:*

You mentioned one percent photometry. How do you calibrate the system to achieve this, and how do you know you have one percent accuracy?

*J. A. WESTPHAL:*

We know we get one percent photometry by taking pictures of the edges of star clusters where a lot of photometry has been done. That is also how we know the linearity is well behaved.

The other part of your question is a serious problem and one that I would address to this group as a matter of concern. That is, the problem of how do you control the flat-field calibration?

We find that dust gets on filters, that things move around, and so forth. At the moment, the main source of our difficulties in our data reduction is that our flat-field calibrations are not taken care of well enough. At present, we tend to take them at the beginning and end of each tape, which means every 80 frames; but it depends on what we are doing exactly.

But to do a good flat field is not a trivial problem. Currently, we are using the inside of the dome. We close the shutter in front of the telescope and illuminate it with the lights inside the dome. It seems to work in that, if you take a series of flat fields one right after the other and divide one by the other, you should get 1.00 everywhere, and you can get some feeling for how well it works. It works almost all the time, but now and again it doesn't. And why, is not at all clear to me. It is probably some procedural problem we have, but I just don't know the answer. There are some subtleties in it, particularly if you are going to do spectra. We have taken some spectra with the SIT, by the way. We have done some work with the 100-in. coudé that might be of some interest to you.

We find we get the whole multiplex advantage over a Fabry-Perot when we observe the same interstellar lines from the same star. That is, we get the same data in a factor of 60 shorter time, which is just what we should have if everything was photon-noise limited. But when calibrating the spectra, the flat-field problem with spectra is a little more subtle than it is for the filter photometry. It is absolutely essential that the system be calibrated with exactly the same f-ratio as the telescope, which means you do it through the telescope.

You can't hang a light bulb out on the front of the slit; that doesn't work.

(Laughter)

*P. ZUCCHINO:*

What is the frame readout rate?

*J. A. WESTPHAL:*

It takes 6.6 s for one readout at the present time.

*E. J. WAMPLER:*

You said that it took about 45 s at prime focus to reach the sky, but you have a pretty large dynamic range. How long does it take to reach 22 magnitude? Does 23 magnitude take 6 min?

*J. A. WESTPHAL:*

Yes, but it's only about 50 percent number at that exposure. Measurements by ordinary diagram photometry give us about the same numbers. So we seem to be photon-noise limited as well as we can tell.

I would like to make a comment as an aside. It disturbs me very much that you are worried about whether you cool a tube or don't, or whether the tube weights 40 pounds or 400.

I believe the data system is the crux of the telescope. It's infinitely more important to put another 90 kg (200 lbs) in the data system than it is to put another 50 cm (20 in.) on the mirror. If you need to cool an SIT because it's a better detector—which I don't know whether it is or not—but if it is, I think that it would be very important to find a way to use it.

## VIII. DIGITAL MULTICHANNEL PHOTOMETRY WITH DIGICONS

*C. E. McIlwain  
University of California  
San Diego, California*

Before discussing the digicon system, I will make a few comments about the basic facts of life that are imposed when measuring optical images and in particular those resulting from the quantum nature of light. I will deal only with the case of one-dimensional images, because that is what my colleagues and I are working with, and because it simplifies the discussion.

A line image consists of some functional dependence of the number of photons per second per unit length. If the image is observed for some particular time with some particular quantum efficiency, one obtains a certain number of counts per unit length. There will be some specific set of positions where the detected photons landed. If one were to measure the exact location of the arrival of each of those detected photons, all of the available information would obviously be recorded. There is absolutely nothing more that can be done. In other words, one would have an ideal detector with that quantum efficiency.

No real image has indefinitely high resolution. There is some finite distance over which one can average without loss of image information. Therefore, the arrival positions generally can be convolved with some resolution function and still retain all of the image information even though this discards much of the information that was collected. If a detector can obtain a result of the same accuracy and resolution as that convolution, it is obviously an equivalent to an ideal detector regardless of how the result was achieved.

In a real detector we find that we cannot simultaneously operate with the full effective quantum efficiency and the full resolution of a system. One must give up one or the other. There is going to be some intermediate regime where the combination is optimized. So the point I want to make is that we should consider systems at that optimization point, not with the accuracy and resolution separately optimized.

At the top of Figure VIII-1 is shown what might be a sample set of detected photon arrival positions. The next three lines show how these photon arrival positions might be weighted by an ideal sensor in forming its output; that is, the convolution of the photon arrival position with a response function. In this example, the response function is a Gaussian with a full width at half maximum of 1 cm. Note that the result is a continuous function; it is no longer discrete.

The next set of three lines show what a real detector with the same resolution would give. To start with, sampling with at least the density shown (each 0.5 cm) is required to avoid

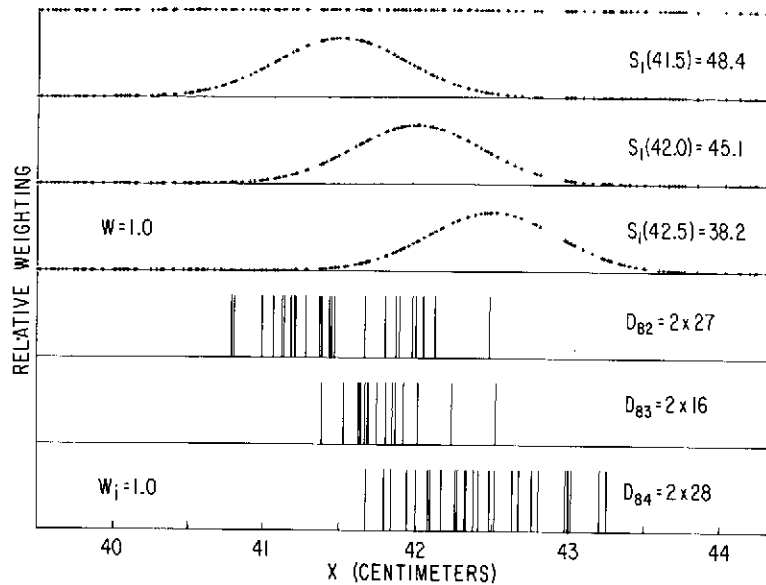


Figure VIII-1. Resolution for ideal and real detectors.

aliasing. If a greater spacing is used, it can be shown that very different images can produce identical outputs. Even though the image is not supposed to have structure that is unresolved by the ideal sensor, this may not be a safe assumption in practice. Note that since the adjacent weighting functions must have at least 50 percent overlap, each detector channel can have at most only a 50 percent chance of being the one registering a given detected photon.

Thus, there is a fundamental difference between the character of an ideal detector and a real detector; the ideal detector takes each detected photon position and adds a fraction of it into a whole succession of samplings. A real detector takes each position and puts it all in one bin. It is a probability weighting as opposed to the weighted sum obtained by the ideal detector.

The weightings are fundamentally different, and the statistics are radically different. Obviously, the raw output of a real detector does not approach the accuracy of an ideal detector of the same resolution and quantum efficiency. Fortunately, something can be done about this difference in accuracy. For example, for a detector that had a response function that was very narrow compared to the desired width, the ideal weighted sums could be computed with little error. But that is obviously throwing away a great number of potential resolution points.

So the question is: How close can the accuracy of an ideal detector be approached without losing most of the instrumental resolution? Specifically, what happens to the accuracy when

the data points are convolved with a weighting function designed to yield a particular resolution? When a probability function is convolved with a weighting function, the spatial response will be broadened. The detector must therefore have a higher resolution than the final filtered response.

Let us assume that a final resolution function that is twice the width of those in Figure VIII-1 is desired. The top half of Figure VIII-2 shows the ideal weighting for this width. In

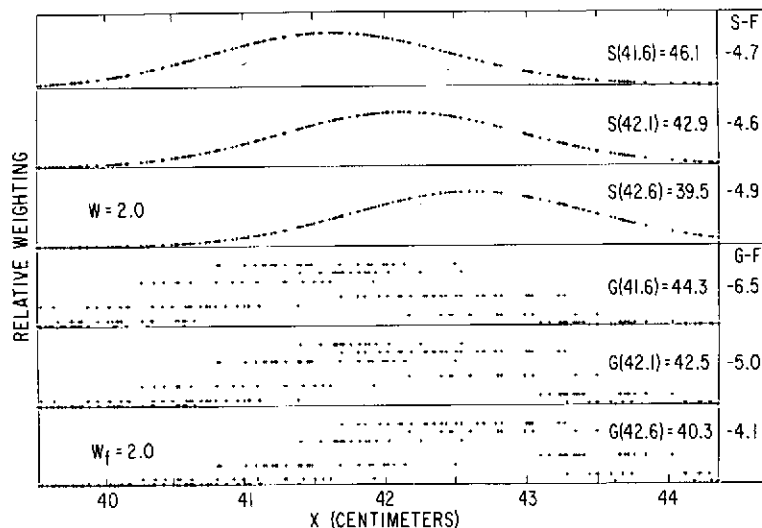


Figure VIII-2. The effect of reduced resolution on detector performance.

the bottom half of this figure is shown the corresponding weighting of the photons contributing to the counts in each filtered data point from a realistic detector. The counts shown in the bottom half of Figure VIII-1 can be easily identified because all of the counts in each data channel receive the same weighting. In common with the ideal output ( $S$ ), the result of taking the weighted sums of the raw data is continuous rather than discrete, and adjacent values correspond to slightly different weightings of the same photons.

Figure VIII-3 shows a larger section of the same image. At the top is the generating function [ $F(x)$ ] which is a constant plus two Gaussians with full widths at half maxima of 7 cm. Next are the discrete data points ( $D_k$ ) that would be obtained by a real detector with a resolution width of 1.0 cm and an effective channel spacing of 0.5 cm. Following this is the result [ $G(x)$ ] of filtering the ( $D_k$ ) values to give a resolution width of 2 cm. Next is the output [ $S(x)$ ] of an ideal sensor measuring the same detected photons with the same resolution.

The statistical errors for the two cases are shown at the bottom of the figure.

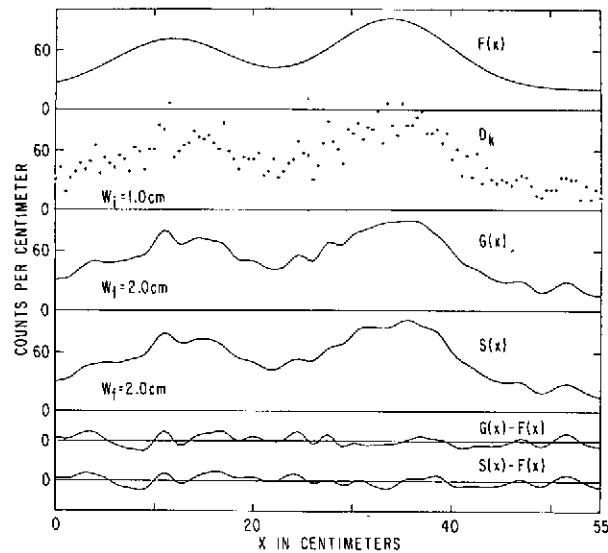


Figure VIII-3. Comparison of signals generated by ideal and real detectors.

The rms error of  $G$  is only 7.2 percent larger than the rms error of  $S$ , but the rms difference between  $G$  and  $S$  is about 36 percent of the error in  $S$ . Thus,  $G$  is almost as good a measure of  $F$  as is  $S$ . At the same time, it is not a very accurate replica of  $S$ . This is to be expected and is not particularly important, because it is  $F$ , not  $S$ , that needs to be determined.

This example has shown that the accuracy obtained from a detector can approach the accuracy expected from its quantum efficiency, if a factor of two reduction in resolution can be tolerated. What is the penalty in accuracy if it cannot? Figure VIII-4 shows that the errors rise rapidly at higher resolutions. These curves are for the particular case where both the instrumental and the desired response functions are Gaussians, but similar results can be expected for other response functions. Figure VIII-5 shows the same results replotted to show the errors in relation to those of an ideal sensor with the same efficiency ( $\epsilon$ ) and with several factors of two lower efficiencies.

How should the filtered resolution be chosen? To answer this, we must consider the relative merits of accuracy and of resolution. Assume for a moment that somehow an optimum response function ( $R$ ) has been found that has a full width at a half maximum of  $W_f$ , so that a detector covering an image length ( $L$ ) contains  $N_f = L/W_f$  resolvable widths. When the raw data are filtered to give this resolution, it can be considered to have effective quantum

efficiency of  $\epsilon_f$ , if the accuracy is the same as that of an ideal sensor with the same resolution and an efficiency of  $\epsilon_f$ . Notice that  $\epsilon_f$  can be further reduced below the actual quantum efficiency by detector background, drift, and by nonlinearities.

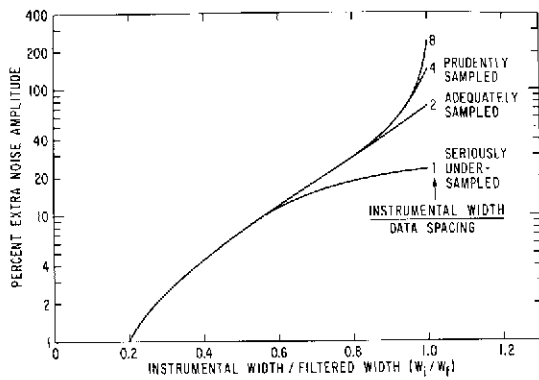


Figure VIII-4. Loss of accuracy as a function of instrumental resolution.

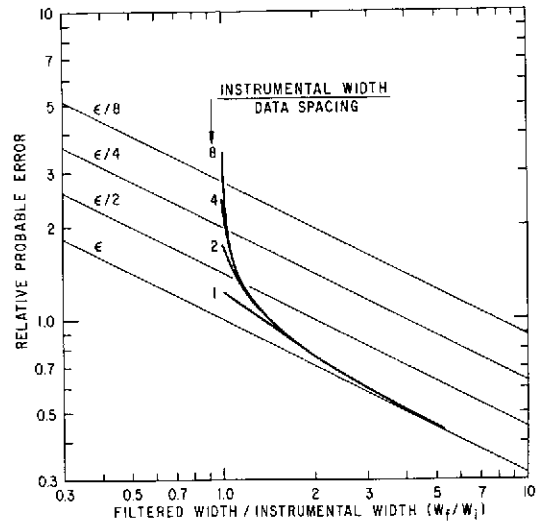


Figure VIII-5. Probable error changes for different detector efficiencies and resolution.

The time required to measure an image to some desired accuracy will usually be inversely proportional to both  $N_f$  and  $\epsilon_f$ , so I define the effective speed product to be  $\bar{Q} = N_f \epsilon_f$ . One way of determining the optimum resolution is to find where  $\bar{Q}$  is maximized. For the gaussian responses used in the previous examples, this occurs when the filtered width is  $\sqrt{2}$  times the instrumental width. At this resolution, the effective efficiency is  $\sqrt{2}$  smaller than the quantum efficiency. The peak speed product is thus a full factor of 2 smaller than it would be if the resolution and accuracy could be separately optimized.

In some cases, the response function,  $\bar{R}$ , is preset by other considerations. It is not unusual that an image has poorer resolution than one would like. For example, there are times when something has blurred an image and you want it to be made sharper. This can be done, but it requires a special type of convolution function. If this type of convolution is needed, it is very important to use it as the final response function when comparing sensors rather than the ones that happen to be ideal for the detectors. In summary, detectors should be compared after filtering: either after the detector's optimal filtering, or after the filtering demanded by the measurements to be made.

With that long preface, I will now describe some aspects of the digicon system we are developing. We have published many details of this system<sup>1,2,3</sup> and I will not go into all of them here. The essential elements are shown in Figure VIII-6.

As with some other sensors described at this symposium, the digicon system starts with a photocathode. It has magnetic focusing of the accelerated photoelectrons, and again the electrons hit an array of solid-state diodes.

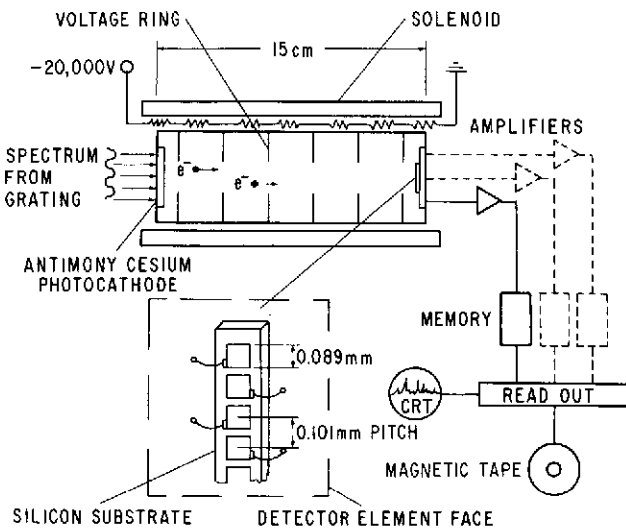


Figure VIII-6. Essential elements of the digicon system.

But there is where it departs from the other systems. Instead of attempting to read the resulting charges on these diodes by probing electrons, or by a charge transfer out, an actual physical wire is connected to each separate diode. This has one huge advantage and that is improved signal-to-noise ratio. In particular, it is sufficiently good that each individual photoelectron arrival can be detected separately, unequivocally, and without background. In other words, the only counts are those due to arriving electrons, and they are detected with about 85 percent efficiency. The other 15 percent are backscattered before they have lost all of their energy. Some background, such as electron bursts due to ions, can be discriminated against because nonstandard pulses are produced.

With the digicon, there is the disadvantage that a separate amplifier, discriminator, and counting system for each diode is required. This disadvantage may largely disappear if integrated circuit technology continues to improve. The preamplifier does require a low noise field effect transistor and may prove difficult to fabricate in integrated form. The present cost of each preamplifier in discrete or hybrid form is less than \$20.

The diode geometry can be almost any shape with individual diode areas anywhere from  $10^{-7}$  cm<sup>2</sup> up to 1 cm<sup>2</sup> if desired. The present system has 40 diodes that are squares of about 90 by 90  $\mu$ m, but this is only because arrays with this geometry were available off the shelf at low cost.

The background is primarily from photocathode thermionic emission. At room temperature, the first tubes have backgrounds of about 100 electrons/cm<sup>2</sup>/s, giving about one count/diode/100 s. In many applications, it can be completely ignored.

The upper end of the dynamic range is set by the speed of the electronics. The present state-of-the-art of electronics is such that it could be as high as  $5 \times 10^7$  counts/s. The minimum cost system we have assembled has a time resolution of several microseconds. So we presently have a dynamic range of approximately 100 million to one, or about 20 magnitudes. At high rates, the current from a diode becomes easy to measure, and an overlapping extension of the dynamic range could be obtained by measuring the average current. This extended range can cover many factors of 10 if desired, but the accuracy of digital operation cannot be expected.

We are presently using this sensor system for spectroscopy of faint objects. Edward Beaver has done most of the work in developing the system and is presently completing 2 weeks of observing with the UCLA telescope at Ojai. In order to facilitate these observations, we have added a number of features. One is a digitally-controlled deflection device. Its primary function is to move the registration of the photocathode relative to the diode array.

As previously mentioned, there must be an overlapping set of detection probability functions or one obtains under-sampled data. We have a system that can move the image of the photocathode relative to the diode array in steps of either eighths or fourths of a diode separation to obtain adequate sampling. We can now do this automatically and rapidly. The deflection system is fairly fast, and we can rapidly alternate between the desired positions. We are presently cycling through eight positions three times a second. A real-time data display system has also been added so we can watch the counts accumulate.

I have made a quick estimate of the speed product of the 40-channel Digicon system and find a  $Q$ -value of about two. In other words, it is equivalent to a perfect detector covering about two resolution elements. By comparison, a single channel photomultiplier tube has a  $Q$ -value of about 0.06 if its quantum efficiency is 10 percent and if its dark rate is small compared to the signal.

Figure VIII-7 is the output obtained using a slit and a lens to project a line image on the photocathode perpendicular to the diode array. This serves as a fairly stringent test of the response off to the side. In other words, the side response would be much less if it were a point source rather than a perpendicular line source.

The side response is not entirely due to the sensor since there are undoubtedly some contributions from the imaging system. Nevertheless, the response goes down by over a factor of  $10^4$  from the peak. Other measurements indicate that the response to a point

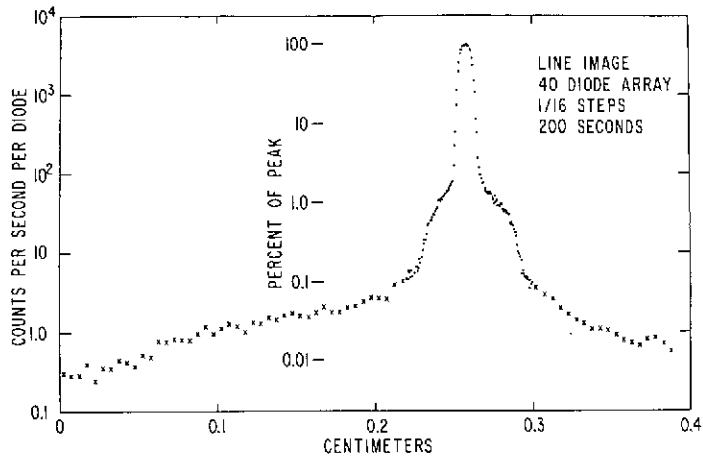


Figure VIII-7. Digicon-system output response.

source decreases roughly as the inverse cube of the distance from the source and reaches one millionth of the peak response near 0.4 cm. A quick integration reveals, however, that about 0.5 percent of the total response is from the region beyond 0.4 cm.

Figure VIII-8 is a spectrum taken with the instrument mounted on a telescope with a

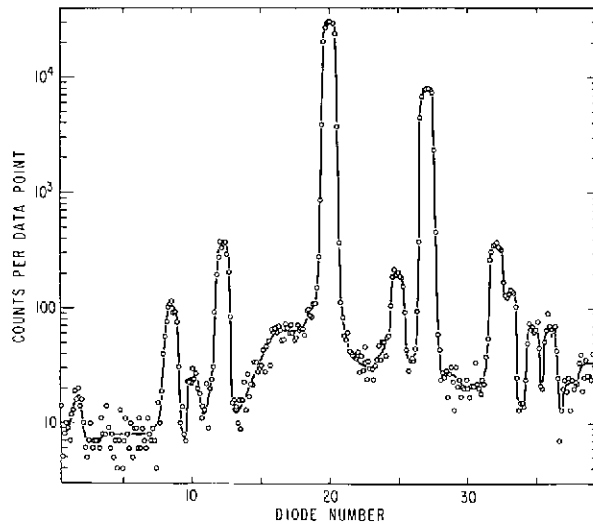


Figure VIII-8. Spectral response of the digicon system.

spectrometer and a calibration source. The response to the spectral lines is almost the shape of the diodes. The steepness of the sides corresponds to a resolution of about 30 lines/mm. If the diodes were smaller, the usual resolution obtainable with a magnetic lens could be obtained. Again, the ability to handle high contrast images is shown by the changes of up to a factor of 500 within one diode spacing (0.01 cm).

Figure VIII-9 shows a portion of the spectrum of PHL-957, which is a sixteenth magnitude

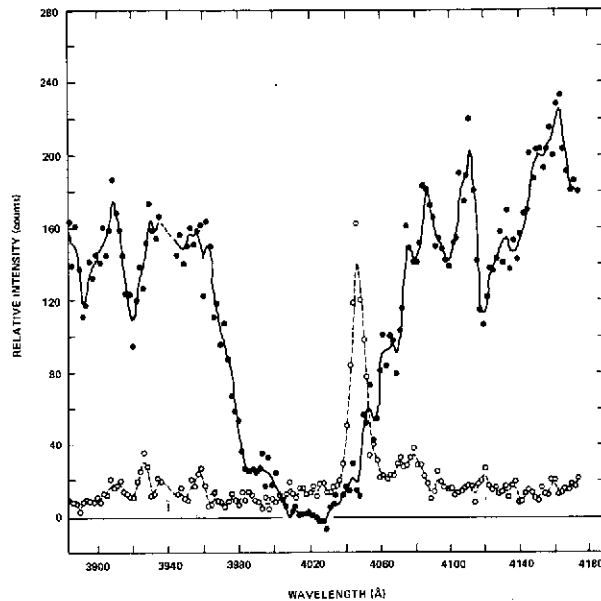


Figure VIII-9. A portion of the PHL-957 spectrum.

quasi-stellar object (QSO). The open circles represent the night-sky spectrum obtained with the object displaced. The full circles are the raw data points obtained after subtracting the night sky spectrum from the QSO data. Note the complete disappearance of the strong mercury line from the San Jose street lights.

Note also how the signal approaches zero, except for statistical scatter, in the middle of the broad absorption band around 402 nm. People in this room have also observed this object and are more familiar with it than I am. But to my knowledge, this measurement gives the lowest upper limit to the intensity in this particular band, and it turns out to be quite low. A three-sigma upper limit is about two percent of the neighboring continuum. I think this performance demonstrates a fundamental capability of this type of system that many others

do not have, that is, the ability to produce differences of two observations which can be believed to within statistical accuracy. As yet, no important systematic errors have been found.

We are now in the process of building an observing system with the diode geometry chosen more appropriately for our specific task of spectroscopy and with more channels. The arrangement of the diodes is shown in Figure VIII-10. We have 200 diodes all in one line for observing the image. The size of each diode is 40 by 300  $\mu\text{m}$ . At each end there are five diodes that are used for alignment. When the perpendicular dimension of the image is confined, such as by a limiting aperture on the spectrometer slit, it can be kept on a particular place on the diode by active control of the alignment using the output of these diodes. Potential systematic effects due to variations of sensitivity across the diodes should become negligible. In addition, there are two large diodes at each end for monitoring the background. With this system we plan to use a small computer to handle the data, monitor the overall operations, and display data while it is being collected.

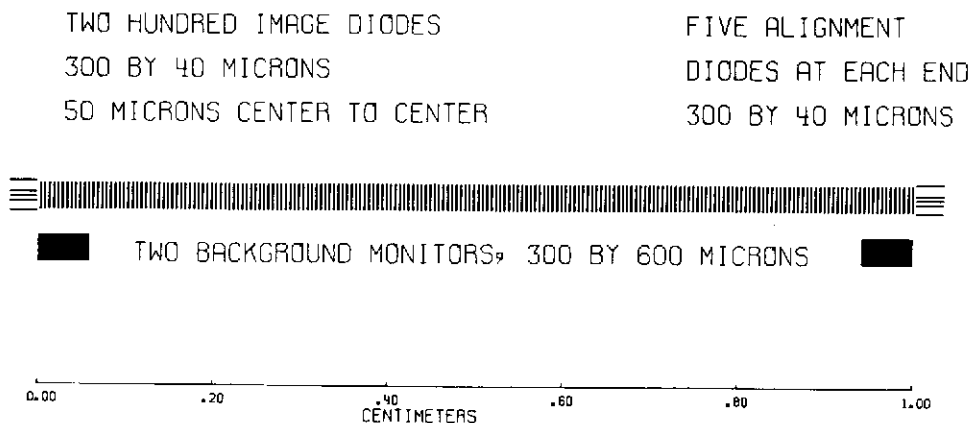


Figure VIII-10. Digicon diode arrangement.

#### ACKNOWLEDGMENTS

The results described here are from a collaborated effort with Edward Beaver, Margaret Burbidge, and Richard Harms. The work has been supported in part by NASA Grants NGL 05-005-007 and NGR 05-009-188.

## DISCUSSION

*E. J. WAMPLER:*

Is a line spectrum presented in Figure VIII-8?

*C. E. MCILWAIN:*

Yes, it was not a broad image. I believe that the entrance slit to the spectrometer limits the image to about one diode width perpendicular to the diode array.

*E. J. WAMPLER:*

This was a comparison spectrum?

*C. E. MCILWAIN:*

He told me it was a neon source.

*N. G. ROMAN:*

What are all those points between lines?

*C. E. MCILWAIN:*

They are the raw data points. They were obtained during calibrations made just last week.

*N. G. ROMAN:*

I am confused. You said that the width of your spectral lines was determined by the width of the detector elements, and yet you have six points or eight points across the width of each element. Does this mean that you are moving the detector by small increments?

*C. E. MCILWAIN:*

We displace it in eight steps: an eighth of a diode space each step. And again, you can see the importance of doing that. For example, what if one only had every eighth point. Obviously, one would not be able to properly interpret it at all. It would be completely hopeless. In fact, if we take every other one, only quarter-stepped, then it would still be difficult to do accurate tracing.

*C. H. SEQUIN:*

Wouldn't it be more advantageous to make the diodes physically smaller?

*C. E. MCILWAIN:*

Yes, if the resolution required to resolve this spectrum at this dispersion is required. As I mentioned, we bought this particular array because it was cheap. If the dispersion were

increased, however, the resolution could be improved with the present diodes. The accuracy would be about the same because the speed product,  $Q$ , is not changed very much by making the diodes smaller.

We have also operated on the 120-in. telescope at the Lick Observatory but with a trial tube that had a damaged diode array. This preprototype tube also had a very low photocathode efficiency. Nevertheless, we were still able to get some useful results.

*J. F. MCNALL:*

What is your estimated cost of the 200-element system, including the data processing required?

*C. E. MCILWAIN:*

It depends on what you include in the cost. Let me make a guess that does not include engineering time, other developmental costs, or any software costs: I would say about \$40,000 for everything up to and including the accumulators. A minimal data handling and recording system also costs about \$40,000. The data system can easily cost five times this amount, but this is true for any detecting system capable of similar performance.

*N. G. ROMAN:*

How long did it take you to get the spectrum of PHL-957? How does that compare with the efficiency of the system Wampler has been using, or the system that Morton has been using?

*C. E. MCILWAIN:*

In that case we observed for an hour on the object and an hour on the background. I believe this compares unfavorably to the others in terms of the time they took to get somewhat equivalent data on this object. The photocathode in this case, however, had a quantum efficiency somewhere around two or three percent, and the spectrometer was apparently giving us fewer photons than we should have been getting. Nevertheless, the comparison might not be unfavorable if only the absorption band measurement is considered.

We have no reason to think that in the future we should not be able to obtain photocathodes with at least a ten percent peak quantum efficiency, in which case, for the limited part of the spectrum that we can cover, I am not aware of any system for which I would expect a higher  $Q$ -factor at low light levels.

*G. GILBERT:*

How do you accomplish the splitting of the detector resolution elements?

*C. E. MCILWAIN:*

Magnetic deflection. It is digitally controlled so deflections as large as a centimeter can also be accurately performed as well as the small 10- to 100- $\mu\text{m}$  deflections used to obtain adequate sampling density. This makes it possible to scan an image that is larger than the diode array. In the case of the 200-element system, however, the photocathode diameter is only about twice the length of the diode array.

Since the deflection is done magnetically, the speed is limited by the inductance of the coils and by eddy currents in the conducting materials used in the construction of the sensor. At the present time, an aluminum coil form limits the response time to several milliseconds, but this will soon be replaced by an insulator.

*J. L. LOWRANCE:*

Could you comment on the relative threshold of your amplifiers versus the charge-coupled device pick-off amplifiers that were discussed earlier today?

*C. E. MCILWAIN:*

I do not know the performance of the Bell Laboratories' amplifiers. Since the charge-coupled scheme seems an attractive way of reading the information out of a system like ours, I have been looking into it, but at the moment nobody seems to be achieving the performance that is required.

*C. H. SEQUIN:*

At the first glance this looks like the ideal task for a charge-coupled device. The device to be used would be a little more sophisticated than the simple line scanner I have shown in Figure VIII-3. It would consist of a charge-coupled channel for the readout and separate storage sites adjacent to one side of that channel. One would integrate the counts in these adjacent storage sites, dump all the information simultaneously into the transfer channel, and read it out in serial form.

You would save the 200 amplifiers, but on the other hand you would not get the same time resolution as in a device with 200-parallel outputs. I do not know if this is an important point. Certainly for counts of less than about 100/s/pixel, the charge-coupled device would be fast enough. But if you go to about  $10^4$  or so, then you probably need the parallel output which you get with the 200 amplifiers.

*C. E. MCILWAIN:*

I think it will be best to have an array of diodes to act as sensing areas and to have a separate system for transferring out the charge. This may be necessary because, in order to have good charge transfer, the exact crystal structure is probably critically important. Bombardment by electrons may lead to a short, useful life, in which case it needs to be separate from the detecting diodes so it can be shielded.

The charge transfer itself seems to be quite good enough for this kind of operation. Eventually, however, the charge must be transferred to an amplifier capable of sensing a charge of only 3000 electrons if reliable detection of single 20-kV photoelectrons is to be achieved. Also, it should give no more than a few false counts per hour.

The present low noise field effect transistors must have a current of over  $10^{-4}$  A going through them in order to achieve this kind of performance. They are also apparently difficult to make in integrated form. Presumably, this technology will improve so that the detecting diodes, the charge transfer devices, and the preamplifiers can all be made on a single substrate. But the potential gain may not be huge. It may be more of a convenience gain than a cost gain. The reason I suggest this is that the data handling system may cost almost as much per channel as the amplifier now being connected to each diode.

The limitations are now primarily just the nuisance of having to deal with so many separate wires in such a small area—200 is already quite a large number. I would start to despair at around 1000; it is not technologically possible to go much higher.

At present, our method of going to a large number is by (1) using a criss-cross arrangement of parallel electrodes going one way on the top and perpendicular on the back and (2) operating the silicon wafer in a totally depleted mode. With an amplifier connected to each line, coincidences between the parallel and perpendicular lines will identify which diode is hit. For an array of 10,000 diodes, only 200 amplifiers are required. It is the kind of coincidence operation that is being commonly used in other applications such as spark chambers and multiple wire proportional counters.

*C. H. SEQUIN:*

Are you still intending to shift the pixel in response to this array?

*C. E. MCILWAIN:*

That is a fundamental necessity. It is not something that is done only if it is convenient. That applies to any device of course, and devices such as charge-coupled ones that do not have the intrinsic capability of doing that shifting may have problems. Either that or accept very much lower resolutions that the device is capable of.

*C. H. SEQUIN:*

Why do you say the charge-coupled device cannot be used in that shifting mode of operation in the same way as the diode line can?

*C. E. MCILWAIN:*

The effective sensing elements must have an overlap of over 50 percent in order to prevent undersampling. There is no discrete device that can avoid it. Either a much lower resolution must be accepted or it must be physically moved relative to the image.

*C. H. SEQUIN:*

The modulation transfer function of a simple element in the charge-coupled device is about the same as one diode in your linear array, so there should be no difference.

*C. E. MCILWAIN:*

I was just using the basic fact that there is no positive function that can be sampled adequately in less than one-half of its full width. And here you have the charge-coupled devices separated by more than their full width. They cannot be any closer and still be separate. The minimum sampling spacing is half that separation.

*N. G. ROMAN:*

Yes, but they can move the image in the same way you do.

*C. E. MCILWAIN:*

Yes, but that would be a mechanical motion.

*C. H. SEQUIN:*

When you integrate in the separate storage areas you can have the storage areas just as close as you have the diodes here, separated by 5  $\mu\text{m}$  or so; and then the potential wells underneath are just as close.

If you integrate in the transfer channel itself, you would be even better off. Now you can electrically shift the potential wells in the device in the following way: You turn on one set of electrodes, generating potential wells underneath. The next time you integrate a line, you turn on another set of electrodes, and now your potential wells are in a different location. In that manner you can increase your sampling density.

*C. E. MCILWAIN:*

But look what the resolution is. It is the width of that particular potential well. That is the available resolution. And those wells need to be nested by less than half their full width.

*C. H. SEQUIN:*

That is comparable to the width of the diodes in your sensor.

*C. E. MCILWAIN:*

But that is an unacceptable situation. You must move the image.

*G. GILBERT:*

Why can't one move the image on the CCD?

*C. E. MCILWAIN:*

I assumed you were putting the optical image directly on the CCD.

*C. H. SEQUIN:*

You would put the CCD right in place of your device. Everything in front of it would be the same.

*C. E. MCILWAIN:*

Then magnetic deflection can be used, but I still believe that there may be no huge advantage to this arrangement.

*C. H. SEQUIN:*

You save 199 amplifiers!

*C. E. MCILWAIN:*

There is also the question of how many elements are needed. If you look in the *Astrophysical Journal*, the information that is actually used to obtain the final results does not always involve a large number of image elements. For spectroscopy, a system with 1000 sensing elements may be preferable to a system with 10,000 elements when the impact on data handling and analysis is taken into account.

*S. DUCKETT:*

What was the voltage that was needed to excite the electrons to obtain the minimum number of electron-hole pairs, and will this device operate indefinitely with that sort of bombardment?

*C. E. MCILWAIN:*

We are presently using 22 kV. The tube will take a higher voltage but no more is needed to obtain an adequate signal-to-noise ratio. Now 22 keV electrons do not have sufficient momentum to displace a silicon atom from a lattice site, so there is no reason to expect any limit to the life of a diode. The pulse mode of operation is unlike most other modes in that it is very tolerant of leakage currents and of charge embedded in the protective layers of insulating material.

*S. DUCKET:*

You have no troubles with interaction with any absorbed gas feeding back to the cathode?

*C. E. MCILWAIN:*

No. Apparently neither with ions on the photocathode or with electron bursts back on the diode array.

#### REFERENCES

1. E. A. Beaver and C. E. McIlwain. *Rev. Sci. Instruments*, **42**. 1971. pp. 1321-1324.
2. E. A. Beaver, C. E. McIlwain, J. P. Choisser, and W. Wysoczanski. *Fifth Symposium on Photo-Electronic Image Devices*. Academic Press, London. 1972.
3. E. A. Beaver, E. M. Burbidge, C. E. McIlwain, H. W. Epps, P. A. Strittmatter. *Ap. J.*, **178**, 1972. p. 95.

## PARTICIPANTS

M. Aucremanne  
NASA Headquarters  
Washington, D. C.

A. S. Baldwin  
Bendix Research Laboratories  
Southfield, Michigan

R. Bless  
University of Wisconsin  
Madison, Wisconsin

A. Bogess  
Goddard Space Flight Center  
Greenbelt, Maryland

W. Brunk  
NASA Headquarters  
Washington, D. C.

E. Chin  
Goddard Space Flight Center  
Greenbelt, Maryland

M. Davis  
National Science Foundation  
Astronomy Section  
Washington, D. C.

E. Dennison  
Hale Observatories  
California Institute of Technology  
Pasadena, California

D. D. Doughty  
Westinghouse  
Elmira, New York

S. Duckett  
EMR Photoelectric  
Princeton, New Jersey

L. Dunkelman  
Goddard Space Flight Center  
Greenbelt, Maryland

E. Eberhardt  
ITT Electron Tube Division  
Fort Wayne, Indiana

R. W. Engstrom  
RCA  
Lancaster, Pennsylvania

G. Gilbert  
Steward Observatory  
Tucson, Arizona

M. Green  
Westinghouse  
Elmira, New York

K. Hallam  
Goddard Space Flight Center  
Greenbelt, Maryland

A. A. Hoag  
Kitt Peak National Observatory  
Tucson, Arizona

F. R. Hughes  
RCA  
Lancaster, Pennsylvania

C. B. Johnson  
Bendix Research Laboratory  
Southfield, Michigan

H. M. Johnson  
Lockheed Missiles & Space Company  
Palo Alto, California

T. Kelsall  
Goddard Space Flight Center  
Greenbelt, Maryland

L. Lewis  
Bendix Aerospace Systems  
Ann Arbor, Michigan

J. L. Lowrance  
Princeton University Observatory  
Princeton, New Jersey

C. E. McIlwain  
University of California  
San Diego, California

J. F. McNall  
University of Wisconsin  
Madison, Wisconsin

W. O. Mansfield  
ITT Electron Tube Division  
Fort Wayne, Indiana

A. Meinel  
University of Arizona  
Tucson, Arizona

C. R. O'Dell  
Marshall Space Flight Center  
Huntsville, Alabama

J. B. Oke  
Hale Observatories  
Pasadena, California

J. R. Olivier  
Marshall Space Flight Center  
Huntsville, Alabama

H. Ostrow  
Goddard Space Flight Center  
Greenbelt, Maryland

R. Predmore  
Goddard Space Flight Center  
Greenbelt, Maryland

N. G. Roman  
NASA Headquarters  
Washington, D. C.

B. Rubin  
NASA Headquarters  
Washington, D. C.

R. E. Rutherford, Jr.  
CBS Laboratories  
Stamford, Connecticut

C. H. Sequin  
Bell Laboratories  
Holmdel, New Jersey

W. Snoddy  
NASA Marshall Space Flight Center  
Huntsville, Alabama

S. Sobieski  
Goddard Space Flight Center  
Greenbelt, Maryland

W. E. Spicer  
Stanford University  
Stanford, California

E. Stuhlinger  
Marshall Space Flight Center  
Huntsville, Alabama

A. Underhill  
Goddard Space Flight Center  
Greenbelt, Maryland

E. J. Wampler  
Lick Observatory  
Santa Cruz, California

O. Weinstein  
Goddard Space Flight Center  
Greenbelt, Maryland

J. A. Westphal  
California Institute of Technology  
Pasadena, California

J. P. Wright  
National Science Foundation  
Washington, D. C.

P. Zucchino  
Princeton University Observatory  
Princeton, New Jersey